Exercise Science - Dissertations   School of Education

12-2011

Skeletal Muscle Function, Morphology, and Biochemistry in Ts65Dn Mice: A Model of Down Syndrome

Patrick Michael Cowley
Syracuse University

ABSTRACT

A common clinical observation of persons with Down syndrome at all developmental stages is hypotonia and generalized muscle weakness. The cause of muscle weakness in Down syndrome is not known and there is an immediate need to establish an acceptable animal model to explore the muscle dysfunction that is widely reported in the human population. Using a combination of functional, histological, and biochemical analyses this dissertation provides the initial characterization of skeletal muscle from the Ts65Dn mouse, a model of Down syndrome.

The experiments revealed that Ts65Dn muscle over-expresses SOD1 protein but this did not lead to oxidative stress. Ts65Dn soleus muscles displayed normal force generation in the unfatigued state, but exhibited muscle weakness following fatiguing contractions. We show that a reduction in cytochrome c oxidase expression may contribute to the impaired muscle performance in Ts65Dn soleus. These findings support the use of the Ts65Dn mouse model of Down syndrome to delineate mechanisms of muscle dysfunction in the human condition.

SKELETAL MUSCLE FUNCTION, MORPHOLOGY, AND BIOCHEMISTRY IN TS65DN MICE: A MODEL OF DOWN SYNDROME

By

Patrick M. Cowley
B.A. Ithaca College, 2002
M.S. Ithaca College, 2005

DISSERTATION

Submitted in partial fulfillment of the requirements of the
degree of Doctor of Philosophy in Exercise Science and Science Education
in the Graduate School of Syracuse University

December 2011

ACKNOWLEDGMENTS

I would like to acknowledge the support and guidance of my committee members: Dr. Keith DeRuisseau, Dr. Stefan Keslacy, Dr. John Tillotson, Dr. Jill Kanaley, and Dr. Bo Fernhall. I have learned a lot throughout this entire process, and much of that is due to their efforts. I would particularly like to thank Keith. He has been supportive throughout the entire process. I've gained a tremendous skill-set working in Keith's lab, and most of it came directly through his instruction. His hands-on approach demonstrates his tremendous commitment to his students. Most of all he has taught me so much about the process of doing science; lessons for which I'm grateful.

I would also like to thank our colloborators: Dr. Lara DeRuisseau for providing the animals for the second set of experiments, and Dr. Frank Middleton for performing the microarray experiment and providing direction for the analysis.

I would also like to acknowledge friends and family members who supported and encouraged me along the way. Most of all I would like to thank my wife, Danielle. She is blessed with such a charming joy of life and positive attitude that no matter how overwhelmed, frustrated, and completely annoyed I was that I couldn't get an assay to work for the nth time, she always assured me that it would indeed work.

TABLE OF CONTENTS

LIST OF ILLUSTRATIVE MATERIALS

Figures

Tables

LIST OF ABBREVIATONS

ADL – Activities of Daily Living

ADP - Adenosine diphosphate

App – Amyloid precursor protein

ATP - Adenosine-5'-triphosphate

CAT – Catalase

cDNA - Complementary DNA

CL - Cluster

COX2 – Cytochrome c oxidase subunit II

CO_2 – Carbon dioxide

CSA – Cross-sectional Area

Cu^+ - Cuprous Copper

DAPI - 4',6-diamidino-2-phenylindole

DAVID - Database for Annotation, Visualization and Integrated Discovery

DMEM - Dulbecco's Modified Eagle Medium

DNA - Deoxyribonucleic Acid

D-PBS - Dulbecco's Phosphate Buffer Solution

DS – Down Syndrome

ES – Enrichment Score

FDR – False Discovery Rate

FE – Fold Enrichment

Fe^{2+} - Ferrous Iron

FDB – Flexor Digitorum Brevis

GAPDH – Glyceraldehyde-3- phosphate dehydrogenase

GO – Gene Ontology

GPX1 – Glutathione peroxidase 1

HEPES - 4-(2-hydroxyethyl)-1-piperazineethanesulfonic acid

Hsa# – Human Chromosome #

H^+ - Hydrogen Ion

H&E – Hematoxylin and Eosin Stain

H_2DCFHDA – 2′,7′-dichlorodihydrofluorescin diacetate

H_2O_2 – Hydrogen Peroxide

KEGG - Kyoto Encyclopedia of Genes and Genomes

K_{ATP} – ATP-sensitive K^+ Channel

ID – Intellectual Disability

L_0 – Optimal Length

Mmu# – Mouse Chromosome #

miRNA – Micro RNA

mRNA – Messenger RNA

NO – Nitric Oxide

NOS – Nitric Oxide Synthase

O.C.T. – Optimal Cutting Temperature Compound

$ONOO^-$ – Peroxynitrite

O_2 – Molecular Oxygen

$O_2\bullet^-$ – Superoxide Anion

$\bullet$OH – Hydroxyl Radical

PCR - Polymerase Chain Reaction

PBS – Phosphate Buffer Solution

P_i – Inorganic Phosphate

P_0 – Peak Tetanic Tension

RNA - Ribonucleic Acid

Rnf160 – Ring finger protein 160

SAM – Significance Analysis of Microarrays

SDS-PAGE - Sodium Dodecyl Sulfate Polyacrylamide Gel Electrophoresis

SEM – Standard Error of the Mean

SOD1 – Superoxide dismutase 1

SOD2 – Superoxide dismutase 2

Ts65Dn - Ts(17^{16})65Dn mouse

VO_2 – Oxygen Consumption

WT – Wild-Type

4-HNE – 4-hydroxy-nonenal

CHAPTER I. INTRODUCTION

John Landon Down published the first clinical description of Down syndrome (DS) in 1866 (1). One hundred years later, Jerome Lejeune discovered that the genetic basis of the syndrome was a third copy of human chromosome 21 (Hsa21) (2). Hsa21 contains over 400 genes, and the altered expression of these genes results in the DS phenotype and associated abnormalities (3, 4). Eighty different clinical characteristics can be attributed to DS, and all individuals born with DS will experience medical problems that will require sustained medical or social care, which can include craniofacial abnormalities, intellectual disability (ID), dementia, hypotonia, low muscle strength, and congenital heart disease (5).

Most persons with DS exhibit some form of physical limitation during the performance of daily tasks, such as walking or rising from a chair (6-9). Persons with DS also have extremely limited physical work capacities (10, 11). Low muscle strength is a predominate factor that explains why persons with Down syndrome exhibit limited physical work capacity and impaired functional ability (12-20). Thus, the outlook for persons with DS is particularly dismal, as further decreases in muscle strength with age will further exacerbate these limitations; resulting in an increased need for medical and social support and services.

The consequences of muscle weakness are potentially far more wide-reaching than just limiting physical function. For example, a reduction in physical function as a result of low muscle strength may lead to more sedentary behavior. In fact, adults with DS are far more sedentary than their non-disabled counterparts (21). Increased sedentary behavior could be partly responsible for a number of other conditions that are prevalent in

this population, such as obesity and low bone mineral density, with the later resulting in a predisposition for bone fractures (22, 23). The development of obesity can also contribute to impairment in mobility. For example, in the general population increased levels of obesity are associated with decreased function on tasks, such as walking and rising from a chair (24). Thus, the development of obesity in persons with Down syndrome could further impair their functional abilities. It's no wonder then, that a lack of mobility is associated with mortality in this population (25, 26).

Low muscle strength also has considerable effects on these individuals' social and economic self-sufficiency. For example, muscle strength and physical work capacity are related to vocational performance in this population (27, 28). As persons with DS are more likely to perform labor-intensive jobs, their ability to complete these tasks may become impaired with further losses in muscle strength that occur with aging. Thus, low muscle strength may have a significant effect on these individuals' vocational opportunity and productivity. This is very discouraging considering employment is an integral part of community integration for persons with ID, and persons with ID removed from competitive employment positions show a decrease in adaptive skill functioning (29, 30).

Thus, there is overwhelming evidence that persons with DS exhibit low levels of muscle strength, physical work capacity, and functional ability. These factors, particularly muscle strength, due to its relation to both functional work capacity and ability are important for independent living, vocational opportunity and productivity, economic self-sufficiency, and quality of life in this population. Thus, understanding factors why persons with Down syndrome have such low muscle strength is an important

area for research that has immense ramifications for these individuals' social and medical care needs.

Since the cause of their muscle weakness is unknown, one potential contributing factor could be oxidative stress, which is thought to be a key factor in the development of DS-related pathologies (31, 32). Described as an imbalance in the production of oxidants and their removal by antioxidants, oxidative stress leads to a disruption in redox signaling and/or cellular damage (33, 34). Oxidants are produced continuously at low but measurable concentrations in skeletal muscle fibers, and are essential for normal muscle function (35-37). In fact, small to moderate changes in muscle cell redox status leading to a slightly oxidized state enhance isometric force generating capacity (38, 39). On the other hand, large and prolonged elevations in oxidant production contribute to impaired muscle function in a number of diseases, such as Myotonic and Duchenne muscular dystrophy, heart failure, cancer, and HIV/AIDS (40). It is currently unknown whether oxidative stress contributes to the development of skeletal muscle weakness in persons with DS.

The cause of oxidative stress in DS may be the result of triplication and altered expression of Hsa21 genes, which includes copper-zinc superoxide dismutase (SOD1). SOD1 is located in the cytosol and inter-membrane space of the mitochondria and functions to dismutate superoxide radicals into hydrogen peroxide and oxygen (41). The over-expression of SOD1 could lead to a disproportionate increase in the production of hydrogen peroxide above the level that can be neutralized by normal antioxidant defenses, specifically catalase (CAT) and glutathione peroxidase (GPX) (32). In fact, cultured neurons from persons with DS exhibit a 3.5-fold increase in the rates of oxidant

production, which is reduced by the administration of antioxidants to the culture (42). The over-production of oxidants can damage various cellular components, and indeed, markers of oxidative injury to proteins, lipids, and DNA are increased in non-muscle tissues from persons with DS (43-45). Therefore, we suspect that the over-expression of SOD1 may lead to oxidative stress and skeletal muscle dysfunction in persons with DS.

Specific Aims and Hypotheses

Persons with DS exhibit severe muscle weakness and the underlying mechanism(s) are not known. To delineate such a mechanism(s), a readily available model must be established. In these experiments we utilized the Ts65Dn mouse to examine the effect of segmental trisomy on skeletal muscle function, morphology, and global gene expression patterns. Furthermore, we examined the effect of segmental trisomy on muscle oxidant production, oxidative injury, protein antioxidant expression, and oxidative capacity.

Ts65Dn mice are segmental trisomic for mouse chromosome 16 (Mmu16), which is homologous to Hsa21 (46, 47). One hundred and thirty-two genes are trisomic in the Ts65Dn mouse, including SOD1 (47). Importantly, Ts65Dn mice display a number of similar phenotypes to persons with DS, including structural and cognitive alterations of the brain, craniofacial abnormalities, and congenital heart defects (48-50).

<u>Specific Aim #1</u>

The first aim was to characterize the effect of segmental trisomy on skeletal muscle function. Ts65Dn mice exhibit reduced running and swimming speeds, and grip strength (51). Therefore, we hypothesized that *soleus muscles from Ts65Dn mice will*

exhibit decreased tetanic specific tension, increased fatigability, and will fail to recover from fatiguing contractile activity compared to wild-type (WT) colony control mice.

Specific Aim #2

The second aim was to characterize the effect of segmental trisomy on skeletal muscle morphology and myosin heavy chain composition. The morphology and myosin heavy chain distribution of skeletal muscle from persons with DS have received little attention in the literature. Biopsies of tongue muscle from persons with DS undergoing partial glossectomy revealed no intramyofiber pathology or changes in cross-sectional area, but exhibited a greater percentage of type II muscle fibers (52). The increased number of type II muscles fibers must be interpreted with caution, as the comparison group in this study was comprised of post-mortem tissue samples from individuals who had died from various diseases known to effect muscle (e.g., cancer). Therefore, we hypothesized that *soleus from Ts65Dn mice will not exhibit changes in cross-sectional area or distribution of myosin heavy chain isoforms compared to soleus from WT mice.*

Specific Aim #3

The third aim was to characterize the effect of segmental trisomy on skeletal muscle gene expression. Transcriptional profiling of trisomic genes in Ts65Dn muscle has been performed previously, however no systematic investigation of global gene expression patterns have been reported (53). Global gene expression profiling of Ts65Dn brain tissues revealed the altered expression of many genes beyond those that were trisomic (54). Therefore, we hypothesized *the gene expression analysis of soleus from Ts65Dn mice will reveal the alteration of numerous cellular pathways.*

<u>Specific Aim #4</u>

The fourth aim was to characterize the effect of segmental trisomy on skeletal muscle oxidant production, oxidative injury, protein antioxidant levels, and oxidative capacity. SOD1 protein is over-expressed without a compensatory increase in the other endogenous antioxidants in non-muscle tissues from persons with DS (55). Therefore, we hypothesized that *protein levels of SOD1 but no other endogenous antioxidants will be elevated in Ts65Dn soleus compared to WT soleus.* Cultured neurons from persons with DS and hematopoietic stem cells from Ts65Dn mice exhibit elevated oxidant production (42, 56). Therefore, we hypothesize that *single adult skeletal muscle fibers isolated from the flexor digitorum brevis of Ts65Dn mice will exhibit increased production of oxidants compared to muscle fibers from WT mice*. Markers of oxidative injury in non-muscle tissues from persons with DS and the Ts65Dn mouse are elevated compared to control samples (43-45, 57).Therefore, we hypothesized that the *expression levels of 4-hydroxy-nonenal (4-HNE) and protein carbonyls, which are markers of lipid peroxidation and protein oxidation will be higher in Ts65Dn soleus compared to WT soleus*. Lower values of basal, whole-body oxygen uptake in Ts65Dn mice are an indication of impaired oxidative phosphorylation (58). Therefore, we hypothesized that *cytochrome c oxidase expression, a marker of muscle oxidative capacity, will be lower in Ts65Dn soleus compared to WT soleus*.

Significance of Study

Understanding the effect of segmental trisomy on skeletal muscle is a critical step to establish a model to explore the muscle dysfunction widely reported in persons with

DS. Future experiments designed to prevent skeletal muscle dysfunction in Ts65Dn mice

may one day lead to therapies for the human population.

CHAPTER II. REVIEW OF THE CURRENT LITERATURE

Preface

This literature review summarizes the research related to muscle weakness in persons with DS. Special attention is given to the impact of oxidative stress on skeletal muscle function, and the vital role SOD1 plays in skeletal muscle homoeostasis. Important background information about the proposed methodology is also reviewed.

Muscle Weakness in Persons with Down syndrome

It is widely reported in the literature that young and old persons with DS exhibit severe reductions in muscle strength. Figure 1 summarizes the findings of 9 different studies comparing voluntary strength output between persons with DS and persons with ID but without DS, and persons without ID and DS. The figure clearly shows that people with DS are significantly weaker than comparison groups. For example, persons with DS produce 40% less force with their knee extensors compared to persons with ID but without DS, and this difference increases up to 70% when compared to persons without ID and DS. Such diminished muscle strength is hard to fathom when considered in light of the fact that it is comparable to the difference seen between healthy persons in their 20s and adults in their 70s (59, 60). It is clear that persons with DS represent a unique population that exhibit severely diminished muscle strength across the lifespan.

Sufficient levels of muscle strength are necessary to perform activities of daily living (ADL), such as rising from a chair and walking (13). It was recently shown by Cowley and colleagues, that muscle strength predicts the ability of young adults with DS to perform ADL (6). These findings are particularly compelling because such associations are typically found in older (> 65 years) but not young adults, suggesting

these individuals are significantly affected by muscle weakness at a surprisingly young age. Thus, muscle weakness may have severe functional consequences for this population, and clearly affects many different areas of daily function (7, 14, 61). Thus, there is a clear need to understand why persons with DS have such diminished muscle strength.
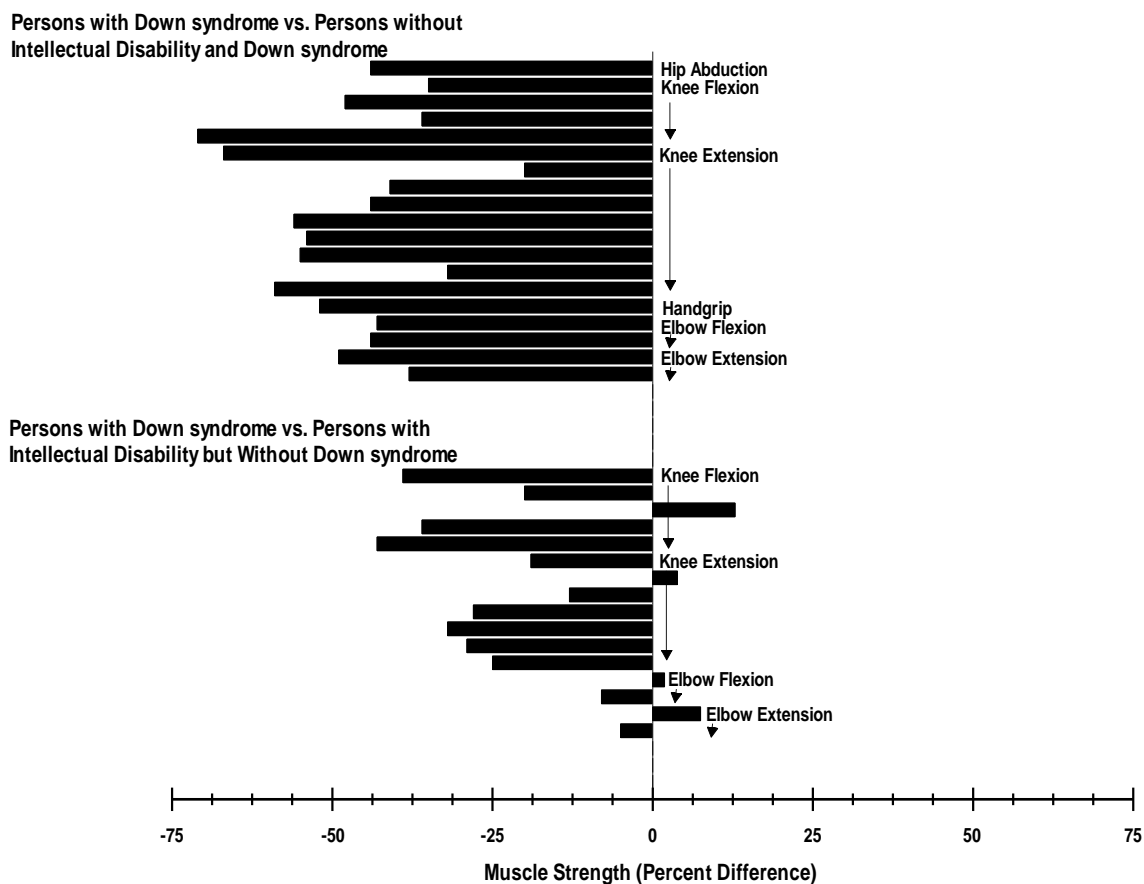
Figure 1. This figure summarizes findings from 9 different studies comparing voluntary strength output between persons with DS and persons with ID but without DS (Bottom), and persons without ID and DS (Top). Each bar represents a study that analyzed muscle strength of a specific muscle group using an isokinetic dynamometer. The participants in these studies included young children to the elderly, and both sexes. The percent difference between groups was calculated using the normalized force values (force per body weight); in this calculation the non-DS group was used as the reference group, and if the value for persons with DS was lower it was expressed as a negative value (i.e., indicating lower strength). References for this figure include (12, 13, 15-20, 62)

Oxidative Stress in Persons with Down syndrome

<u>Introduction to Redox Biology</u>

Redox biology is the process in which one ion or compound is reduced while another is oxidized. Molecular oxygen (O_2) serves as the primary reactant in the production of highly reactive and potentially damaging molecules. These molecules, called reactive oxygen and nitrogen species (herein referred to as oxidants), disrupt normal cell function when in excess, damaging proteins, lipids, and DNA (41). However, oxidants also serve as signaling molecules that are essential for normal cell function (63).

Superoxide radical ($O_2\bullet^-$) is the parent molecule in the oxidant cascade, and is generated by a single electron reduction of molecular oxygen (Reaction 1).

$$O_2 + e^- \rightarrow O_2\bullet^- \qquad\qquad \text{Reaction 1}$$

$O_2\bullet^-$ is highly reactive and initiates the formation of other oxidants. $O_2\bullet^-$ is produced in skeletal muscle cells by complex I and III of the electron transport chain in the mitochondria, phospholipase A_2, xanthine oxidases, and NAD(P)H oxidases (41). $O_2\bullet^-$ can be converted into hydrogen peroxide (H_2O_2) non-enzymatically, and enzymatically by three different isoforms of superoxide dismutase (Reaction 2) (41).

$$O_2\bullet^- + O_2\bullet^- + 2H^+ \rightarrow H_2O_2 + O_2 \qquad\qquad \text{Reaction 2}$$

 SOD1, superoxide dismutase 2 (SOD2), and extracellular superoxide dismutase are located in the cytosol and mitochondria, mitochondria, and extracellular space, respectively (41). H_2O_2 can be converted to H_2O by GPX or CAT (Reaction 3 and 4, respectively) (41).

2 reduced glutathione (GSH) + H_2O_2 $\rightarrow$ oxidized glutathione (GSSG) + 2 H_2O

Reaction 3

$$2\ H_2O_2 \rightarrow 2\ H_2O + 2\ O_2 \hspace{3cm} \text{Reaction 4}$$
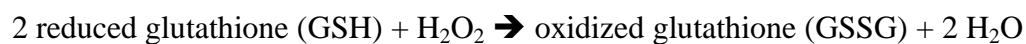
The last biologically important oxidant is hydroxyl radical (•OH), which is formed via the reaction of H_2O_2 with transition metals, such as ferrous (Fe^{2+}) and cuprous (Cu^+) ions through Fenton and Haber-Weiss reaction chemistry, respectively (Reaction 5 and 6) (41).

$$Fe^{2+} + H_2O_2 \rightarrow Fe^{3+} + \bullet OH + OH^- \hspace{2cm} \text{Reaction 5}$$

$$Cu^+ + H_2O_2 \rightarrow Cu^{2+} + \bullet OH + OH^- \hspace{2cm} \text{Reaction 6}$$

$O_2\bullet^-$ can also react with nitric oxide (NO) to form the nitrogen-based oxidant, peroxynitrite ($ONOO^-$) (Reaction 7) (64).

$$O_2\bullet^- + NO \rightarrow ONOO^- \hspace{3cm} \text{Reaction 7}$$

Interestingly, this reaction is nearly three times more efficient than the ability of SOD to scavenge $O_2\bullet^-$; thus, $O_2\bullet^-$ will react preferentially with NO when both molecules are present (64). NO is produced from the reaction of L-arginine with O_2 to form NO and citrulline via three different isoforms of nitric oxide synthase (NOS) (65). Neuronal-type NOS and endothelial-type NOS are associated with the plasma and mitochondrial membranes, respectively (65). Inducible-type NOS expression is stimulated by inflammation (65). Oxidants can also be scavenged by non-enzymatic antioxidants, which includes, but are not limited to: Vitamin E, carotenoids, bilirubin, vitamin C, and uric acid (41).

Collectively, the production of oxidants and their removal by enzymatic and non-enzymatic antioxidants determine cellular redox status. An imbalance in cellular redox status, caused by the accumulation of oxidants due to increased production and/or deficiency in antioxidant defenses causes a shift in redox status to an oxidized state,

13

which is termed oxidative stress. Oxidative stress has been described as an imbalance in the production of oxidants and their removal by antioxidants in favor of the former, that can cause a disruption of redox signaling and/or cellular damage (33, 34, 41). Alternatively, reductive stress occurs due to decreased oxidant production and/or increased activities or quantities of antioxidants.

Powers and Jackson outlined 4 ways that oxidative stress can be monitored in biological systems (41). The first is the measurement of oxidants, which can be increased during periods of oxidative stress. The second is the measurement of non-enzymatic antioxidants (Vitamin C and E) and glutathione, which can decrease during periods of oxidative stress. The third is the measurement of oxidized molecules, like proteins, lipids, and DNA. Oxidized molecules can increase during periods of oxidative stress. The last is the measurement of cellular redox status, which can be assessed by measuring the ratio of GSH to GSSG. Periods of oxidative stress can cause a reduced GSH to GSSG ratio.

Redox Status in Persons with Down syndrome

Oxidative stress is thought to be a key factor in the development of DS-related pathologies, and may be the result of triplication and altered expression of chromosome 21 genes. One gene located on chromosome 21 that may play a prominent role in the development of oxidative stress is SOD1 (31, 32).The over-expression of SOD1 could lead to a disproportionate increase in the production of H_2O_2 above the level that can be neutralized by normal antioxidant defenses (i.e., GPX and CAT) (32).

Figure 2 summarizes the findings from 11 different studies that have examined the expression/activity of SOD1, GPX, and CAT in a variety of tissues from persons with DS and control participants. The figure clearly shows that the expression/activity of

SOD1 in non-muscle tissues from persons with DS is higher compared to control participants by 1.40-fold. The figure also shows there is not an equivalent increase in SOD2 (1.04-fold), CAT (1.10-fold), and GPX (1.18) in DS tissues. These findings suggest that the basal level of oxidant production may be altered in persons with DS. In fact, cultured neurons isolated from brain tissue of persons with DS exhibit a 3.5-fold higher level of oxidant production compared to control neurons (42). In addition, the viability of cultured DS neurons was prolonged by adding a variety of antioxidants (e.g., vitamin E, N-acetyl-$_L$-cysteine, and catalase) to the cell culture media, suggesting oxidative stress played a casual role in neuronal death (42).

Exposure of cells and tissues to elevated and prolonged levels of oxidants can lead to cell damage and altered redox status (66, 67). Table 1 summarizes the evidence showing that markers of oxidative stress are increased in persons with DS compared to control participants. Collectively, these findings suggest non-muscle tissues from persons with DS exhibit oxidative stress
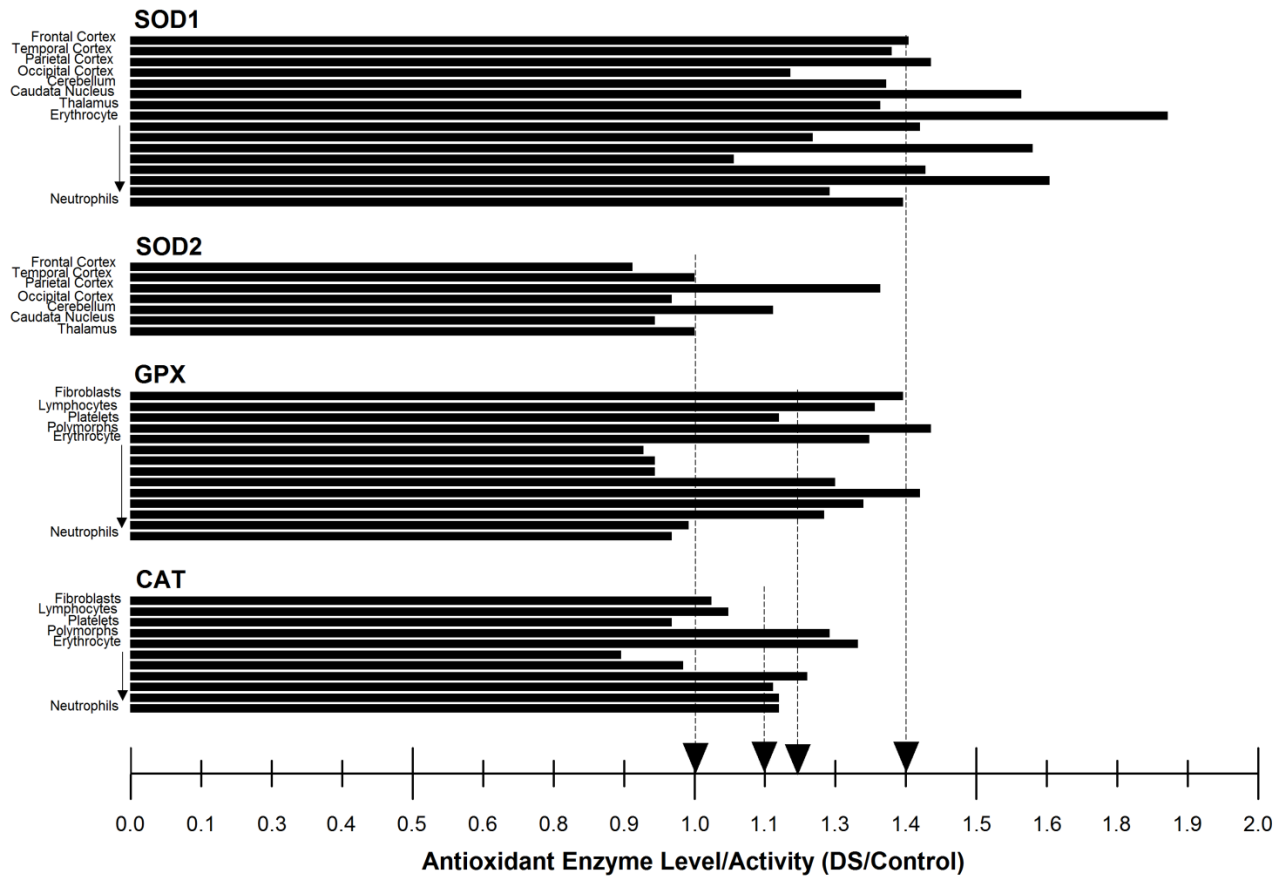
Figure 2. This figure summarizes the findings from 11 different studies examining the expression or activity levels of the major antioxidants in a variety of cells and tissues from persons with DS and control participants. Each bar represents the expression or activity level of a particular antioxidant expressed relative to the DS value. A value of 1 indicates the groups had similar expression/activity values. Values greater than 1 indicate the DS group was higher. The horizontal arrows show the overall mean value. References for this figure include (68-75, 76{Ordonez, 2006 #881, 77, 78)}. Please note this figure is not inclusive, and contains only representative publications from the literature.

Table 1. Markers of oxidative stress in persons with DS compared to control participants.

Tissue/Cell type	Marker of Oxidative Stress	Effect	Reference
Brain	Oxidant Production	↑	(42)
	DNA Oxidation	↑	(79)
	Lipid Oxidation	↑	(42)
	Lipid Oxidation	↑	(44)
	Protein Nitration	↑	(79)
	Protein Oxidation	↑	(44)
Plasma	Reduced/Oxidized Glutathione Ratio	O	(80)
	Lipid Oxidation	↑	(81)
	Lipid Oxidation	↑	(82)
	Lipid Oxidation	O	(45)
	Protein Oxidation	O	(45)
Erythrocyte	Lipid Oxidation	↑	(83)
Urine	DNA Oxidation	↑	(43)
	Lipid Oxidation	↑	(43)

	Lipid Oxidation	↑	(84)
Serum	Oxidant Production	↑	(85)
	Lipid Oxidation	↑	(73)
Leukocyte	DNA Oxidation	↑	(86)
Lymphocytes	DNA Oxidation	↑	(87)

↑ = Increased in DS; ↓ = Decreased in DS; O = No difference

Physiological Mechanisms of Skeletal Muscle Contraction

Our current experimental set-up (i.e., in vitro skeletal muscle contractile function) excludes us from examining events prior to the process of excitation-contraction coupling. Thus, a review of this process is provided [outlined in (88, 89)].

The action potential generated on the muscle fiber membrane travels down the t-tubules, which are deep invaginations in the membrane and are in close proximity to the sarcoplasmic reticulum. Ca^{2+} is released from the sarcoplasmic reticulum via the interaction of the dihydropyridine and ryanodine receptors. The ryanodine receptor acts as a plug and prevents Ca^{2+} release from the sarcoplasmic reticulum. The dihydropyridine receptors respond to the action potential by removing the plug, allowing an efflux of Ca^{2+} from the sarcoplasmic reticulum. Ca^{2+} allows the contractile proteins to interact.

The skeletal muscle fiber is composed of myofibrils that are subsequently composed of sarcomeres, which are the functional unit of skeletal muscle. The sarcomere is composed of thick and thin filaments that overlap; they represent the contractile proteins, which shorten during concentric muscle contractions. The thick filament is composed of a protein called myosin, whereas the thin filaments are composed of actin, and regulator proteins tropomyosin and troponin. Contractile force is produced by the cross bridges, which are formed from the interaction of myosin and actin. The structure of myosin includes a stem and a globular head that protrudes outward. The globular head of myosin contains an ATPase, which hydrolyzes ATP to yield chemical energy. At rest, the globular head of myosin is in a "cocked" position and bound to ADP; in this position the troponin-tropomyosin complex blocks myosin and actin from binding to each other. Ca^{2+} removes the inhibition of the troponin-tropomyosin complex by

binding to the C subunit of troponin, causing a conformational change that pulls tropomyosin off the active binding site.

When myosin and actin bind the myosin head flexes creating a longitudinal force sliding the filaments over one another, which shortens the sarcomere. At this point, myosin and actin detach when another ATP binds to myosin. This cycle continues if Ca^{2+} remains near the contractile proteins and there is available ATP. Ca^{2+} is returned to the sarcoplasmic reticulum mainly by calmodulin and the sarco-endoplasmic reticulum Ca^{2+} ATPase pump. Collectively, the efficiency of these processes determines force-generating potential.

Redox Modulation of Skeletal Muscle Contractile Function

This section will describe the effects of oxidants on skeletal muscle contractile function. Oxidants are produced continuously at low but measurable concentrations in skeletal muscle fibers (35-37, 90). The production of oxidants is activity dependent, as repetitive skeletal muscle contractions increases oxidant production (35, 36, 91, 92). Therefore, in this discussion the contractile history of the muscle must be considered, and the effect of oxidants on unfatigued and fatigued muscle is discussed separately. Findings from studies examining the effects of oxidants on unfatigued and fatigued skeletal muscle will be summarized using Reid's Model (38).

Unfatigued Skeletal Muscle

It is now well established that cellular redox status modulates skeletal muscle contractile function. The first evidence of this came from work by Michael Reid and colleagues at the University of Kentucky. Their work showed that oxidants exhibit biphasic effects on isometric force production using unfatigued rat diaphragm fiber bundles. Specifically, brief incubation of diaphragm fiber bundles with H_2O_2 increases isometric force production, whereas treatment with SOD and CAT decreases isometric force production (39).

Oxidants affect many components of the contractile process, and these effects are both time- and concentration-dependent. For example, incubation of mouse single skeletal muscle fibers with supra-physiological levels of H_2O_2 for short periods of time enhance isometric force production, and these changes do not effect intracellular Ca^{2+} transients (93). These findings indicate that high concentrations of oxidants over a short time period affect the sensitivity of the contractile proteins to Ca^{2+}, but not Ca^{2+} regulation (e. g., sarcoplasmic reticulum function). However, prolonged exposure of muscle fibers to supra-physiological levels of H_2O_2 decrease isometric force and alter Ca^{2+} homeostasis (93). These findings indicate that high concentrations of oxidants over a longer period are required to affect Ca^{2+} regulation (93). Single muscle fibers incubated with physiological levels of H_2O_2 (~ 100 pM) cause an initial increase in isometric force production, but the effect is short-lived, as force slowly decreases back to initial levels (94). These changes are not associated with an effect on intracellular Ca^{2+} transients, indicating a direct effect on the sensitivity of the contractile proteins to Ca^{2+} at physiological levels of oxidants (94). Collectively, these findings suggest both prolonged and acute changes in redox status directly modulate skeletal muscle contractile function.

Less is known about the effects of NO and nitrogen-based oxidants on skeletal muscle contractile function. In a series of experiments, Kobzik and colleagues, showed NO acts to depress contractile function of diaphragm fiber bundles (95). They showed pharmacological blockade of NOS increased the force of submaximal contractions, whereas exposure to NO decreased the force of contractions (95). Exposure of rat diaphragm fiber bundles to $ONOO^-$ decreases isometric force production, which is mediated by a direct effect on the contractile proteins, as the maximum calcium-activated force of single rat diaphragm muscle fibers decreases in response to $ONOO^-$ (96).

<u>Fatigued Skeletal Muscle</u>

The exact sites of fatigue in vivo are categorized into two types: central versus peripheral fatigue. Central fatigue is associated with structures in the brain and spinal cord, where peripheral fatigue occurs at sites in the peripheral nerves, neuromuscular junction, and muscle (97). The discussion to follow will focus on peripheral fatigue mechanisms, specifically those occurring within the muscle, as our current laboratory arrangement excludes examining central mechanisms of fatigue. Skeletal muscle fatigue is defined as the reversible decline in muscle performance due to repetitive muscle activity (97).

The effects of muscle fatigue on performance vary with the type and intensity of contraction. Repetitive near maximal contractions lead to rapid, but reversible decreases in force. Repetitive submaximal contractions, on the other hand, cause metabolic stress, which is characterized by acidosis, accumulation of inorganic phosphate, depletion of phosphocreatine stores, oxidative stress, and delayed recovery from fatigue [reviewed in (97)]. Oxidative stress is considered to play an important role in the development of fatigued caused by repetitive submaximal contractions, as the administration of antioxidants delays fatigue (98-100).

Antioxidants have been shown to delay fatigue in a variety of electrically stimulated muscle preparations in vitro (35, 36, 98, 101). This also holds true in vivo, as Reid and colleagues showed pretreatment with N-acetylcysteine delays fatigue in the human tibialis anterior during a 30-minute bout of electrical stimulation at 10 Hz (100). It is important to note, however that these results were found using submaximal fatigue protocols, whereas contractions at near maximum are unaffected by the administration of antioxidants (36, 99). Collectively, these studies show oxidants plays a casual role in development of muscle fatigue.

The results of studies examining the effects of exogenously administered NO and nitrogen-based oxidants on muscle fatigue have been ambiguous, showing both depressed and enhanced fatigue resistance (102). Studying the effects of NO and nitrogen-based oxidants on muscle fatigue is difficult because NO and nitrogen-based oxidants have effects not only muscle, but also the vasculature and motor nerves (102). Studies using in vitro muscle preparations, which avoids the effects of the vasculature and motor nerves, shows NO and nitrogen-based oxidants have no effect muscle fatigue development. Thus, recent authoritative reviews on this topic exclude NO and nitrogen-based oxidants as substantial contributors to the development of muscle fatigue [reviewed in (102, 103)].

Reid's Model

Based on the findings presented above, a model of how cellular redox status modulates skeletal muscle contractile function has been purposed by Reid and is shown in Figure 3 (38). In Reid's model, resting skeletal muscle exists in a slightly reduced state, which is not optimal for contractile function. However, a moderate increase in oxidants to a slightly more oxidized state is optimal for skeletal muscle contractile function. In this case, the increase in oxidants is not large or prolonged enough to lead to cell damage (i.e., non-pathological) (41). On the other hand, excessive production or exposure of oxidants leads to oxidative stress, and excessive production or exposure to antioxidants leads to reductive stress, with both depressing skeletal muscle contractile function. A shift to a state of oxidative stress could be the result of inflammation, disuse, or diseases states [reviewed in (41, 104, 105)].

Targets of Redox Modulation

The targets of redox modulation of skeletal muscle proteins have been an area of intense research for many years, and the mechanisms have yet to be fully elucidated. A vast array of

important regulator proteins important for sarcolemma function, calcium regulation, and myofilament interaction can be oxidized or nitrated and their function modified. Oxidants can modify protein function by altering tertiary structure, and thereby important regulation sites and reaction kinetics. Cysteine residues, which contain the thiol moiety (-SH) undergo reversible thiol-disulfide interactions with oxidants, and are common sites of modification (106). A number of proteins associated with excitation-contraction coupling undergo reversible thiol-disulfide interactions, such as ion transport pathways [reviewed in (107)], Ca^{2+} release channel/ryanodine receptor (108), sarcoplasmic reticulum Ca^{2+}-ATPase (109-111), troponin (111, 112), tropomyosin (113), myosin (114, 115), and actin (116, 117).
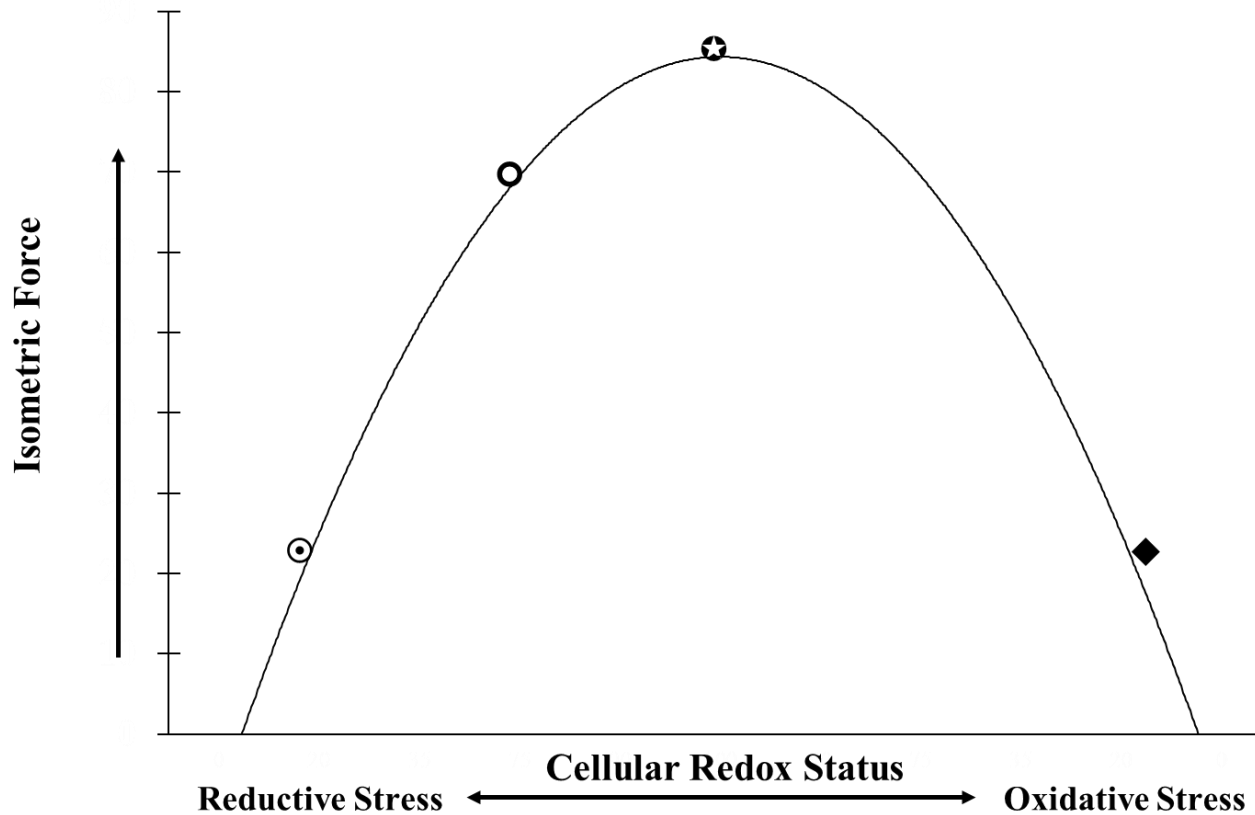
Figure 3. An illustration of the effect of cellular redox status on isometric force production in skeletal muscle. ⊙ An unfatigued muscle in reductive stress due to a reducing agent or antioxidant. O The basal state of unfatigued muscle. This state is not optimal for maximal force production. ✪ Unfatigued muscle exposed to low-levels of oxidants. This state is optimal for maximal force production. ◆ Muscle adversely affected by excessive oxidant production. This could be due to excessive oxidant production in response to disease or muscle atrophy. This figure was redrawn from Reid (38).

The Role of SOD1 in Skeletal Muscle Homeostasis

It is clear that optimal levels of SOD1 are necessary for skeletal muscle homeostasis, as SOD1 transgenic mice display an accelerated skeletal muscle myopathy. The muscle dysfunction in these mice coincides with the presence of oxidative stress, suggesting SOD1 plays a crucial role in mediating skeletal muscle redox status.

SOD1 knockout mice display premature degeneration of their skeletal muscle. For example, at 3-6 and 19-24 months of age mass of the hindlimb musculature is reduced by 21% and 51% compared to age-matched control mice, respectively (118). The loss in muscle mass in aged SOD1 knockout mice is associated with significant decreases in fiber cross-sectional area, the number of type IIb muscle fibers, force-generating capacity, and endurance capacity (119). Both young and old SOD1 knockout mice also exhibit early onset of denervation and motor unit loss (119-123). Importantly, changes in neuromuscular structure are driven by muscle SOD1 expression, because mice with neuron specific knockout of SOD1 do not display muscle denervation (120).

The accelerated age-related loss of skeletal muscle mass and function in SOD1 knockout mice is presumably due to a reduction in scavenging of superoxide radicals (118). Isolated skeletal muscle fibers from SOD1 knockout mice exhibit elevated levels of oxidant production (124). In addition, mitochondria isolated from SOD1 knockout mice produce more superoxide radical than wild-type mice, and they also, surprisingly, produce more hydrogen peroxide (119). As expected, skeletal muscle from SOD1 knockout mice exhibit elevated markers of oxidative injury to proteins, lipids, and DNA (118). In summary, knockout of SOD1 causes muscle dysfunction that is associated with oxidative stress.

Surprisingly, more SOD1 is not necessarily better, as mice over-expressing SOD1 also display premature degeneration of their skeletal muscle. For example, transgenic mice over-expressing a human SOD1 transgene exhibit gross muscle atrophy and elevated levels of serum creatine kinase at 2-5 months of age (125). Inspection of muscle morphology in these mice by hematoxylin and eosin staining revealed infiltration of fat and fibrous tissue, centrally located nuclei, and necrotic muscle fibers (125). Other strains of mice over-expressing human SOD1 exhibit alterations in muscle structure and function. For example, diaphragm muscle of mice over-expressing a human SOD1 transgene exhibits lower specific force, increased non-contractile tissue, and increased percentage of type IIa muscle fibers compared to wild-type mice (126). In another report, 3 different strains of SOD1 over-expressers exhibited neuromuscular dysfunction, which was shown by a higher score on the electromyography pathology index and impaired performance on a rope grip test compared to wild-type mice (127). Analysis of tongue and hindlimb neuromuscular junctions from SOD1 over-expressing transgenic mice are abnormal, displaying significant hyperplasia and altered morphology compared to wild-type mice (128-131). These findings are particularly interesting because tongue skeletal muscle fibers from persons with DS exhibit similar alterations in neuromuscular junction morphology, which includes hyperplasia, along with disorganized, and atrophic neuromuscular junctions (52).

Alterations in skeletal muscle structure and function in these strains is presumably due to an imbalance in the removal of superoxide radical and production of hydrogen peroxide. Experiments conducted using primary muscle cell cultures derived from SOD1 over-expressing mice provide insight into the effect of SOD1 over-expression on oxidant production and removal (132). In this report, myoblast lines were derived from wild-type mice and mice hemi- or homozygous for a human SOD1 transgene with SOD1 activities 3- and 5-fold higher than wild-

type, respectively. The authors were able to demonstrate that as the activity of SOD1 increased, more superoxide radical was scavenged and more hydrogen peroxide was produced. SOD1 over-expression also leads to the production of other oxidants. Muscle extracts from two strains of mice over-expressing a human SOD1 transgene generated significantly more hydroxyl radical compared to wild-type mice (127). Along with producing greater amounts of hydroxyl radical, these mice also display elevated markers of lipid peroxidation (125).

Importantly, the changes in skeletal muscle structure and function in SOD1 over-expressers are likely mediated by a direct effect of SOD1 expression in muscle. For example, transgenic mice with muscle-restricted over-expression of a human SOD1 transgene exhibit similar alterations in muscle structure compared to mice with systemic over-expression (133). For example, these mice exhibit small and irregular shaped muscle fibers with centrally located nuclei, infiltration of loose connective tissue, apoptotic nuclei, denervation, neuromuscular junction abnormalities, and increased markers of muscle protein oxidation and nitration. In summary, similar to SOD1 knockout mice, mice with transgenic over-expression of SOD1 exhibit skeletal muscle dysfunction that is associated with oxidative stress.

Mutations in the SOD1 gene also lead to skeletal muscle dysfunction. Approximately 20% of familial amyotrophic lateral sclerosis cases are due to a mutation in the SOD1 gene (134). Amyotrophic lateral sclerosis is a neurodegenerative disease characterized by death of motor neurons, muscle wasting, and death (135). It is becoming accepted that skeletal muscle has a primary role in initiating amyotrophic lateral sclerosis pathology, as animal models of muscle-restricted SOD1 mutation are sufficient to induce muscle atrophy, dysfunction, and oxidative stress (133, 136).

Collectively, these studies show the essential role that normal levels and normal function of SOD1 have on skeletal muscle homeostasis. SOD1 knockout, over-expression, and mutation all lead to skeletal muscle dysfunction that is associated with oxidative stress. Thus, over-expression of SOD1 could play a role in DS muscle weakness.

Methodological Considerations

Studying the Effects of Trisomy 21

The initial sequencing of Hsa21 in 2000 indicated the chromosome contained over 250 genes (137). This number has grown to over 400 genes in 2005 [see database outlined in (3)]. The altered expression of Hsa21 genes results in the DS phenotype and associated pathology, but how the triplication of Hsa21 actually results in DS phenotypes is not known and is an intense area of research (5).

The "gene dosage effects" hypothesis was the first attempt to explain how triplication of Hsa21 genes results in the development of DS phenotypes. It proposes that increased amounts of normal genes produce increased amounts of gene products, and the increase in protein above normal alters typical development. Theoretically, an extra copy of Hsa21 would lead to a 50% increase in gene expression compared to euploid individuals (i.e., those with 2 Hsa21). However, this is not always the case and the expression of genes on other chromosomes is affected (138-141). Thus, the "gene dosage effects" hypothesis has been continually modified because it does not explain the inter-individual differences observed in people suffering from DS (142).

A modified form of the original "gene dosage effects" hypothesis has been proposed (143). It proposes that the variability in DS phenotypes is a result of a vast and complicated network of altered gene expression caused by the triplication of Hsa21 genes. A discussion of the genetic mechanisms effecting the development of DS phenotypes is beyond the scope of this

review; however it is important to understand that DS-related phenotypes are the result of complex genetic intricacies, and the study of trisomy 21 requires careful consideration of available models. A number of mouse models of DS exist that recapitulate many of the phenotypes observed in the human condition.

Mouse Models of Down syndrome

The mouse has been the model of choice for creating genetic models of human diseases, and has been proven invaluable in understanding the genetic underpinnings of DS. The long arm of Hsa21 is homologous to Mmu16, 17, and 10 (144). Mmu16 contains the largest number of genes homologous to Hsa21, and forms the basis of DS mouse models (144). Many different mouse models of DS have been engineered to over-express single genes, are trisomic for the entire Mmu16, segmental trisomic for Mmu16, segmental trisomic but disomic for individuals genes, and trisomic for Hsa21 [reviewed in (47, 145)].

The simplest way to explore the effect of single genes on DS phenotypes is to create transgenic mice that over-express the specific gene of interest. Mice over-expressing amyloid precursor protein, cystothionine β-synthase, down syndrome critical region 1, dual-specificity tyrosine-(Y)-phosphorylation regulated kinase 1A, S100β, drosophila single-minded, and SOD1 have been used to examine the relative contribution of these genes on DS phenotypes [reviewed in (47)]. However, they are unlikely to capture the full effect of trisomy when examined in isolation.

The most widely studied and well established mouse model of DS is the $Ts(17^{16})65Dn$ (Ts65Dn) mouse developed by Muriel Davisson and colleagues at the Jackson Laboratory using γ-radiation (146, 147). These mice are segmental trisomic for Mmu16, which corresponds to roughly 132 genes (47) (Figure 4). These mice recapitulate many DS phenotypes including,

lower birth weight, increased incidence of obesity, reduced exercise capacity and muscle strength, cognitive and behavioral impairments, hematological abnormalities, craniofacial abnormalities, prenatal lethality, sleep disturbance, cardiovascular malformations, and neurologic structural deficiencies (summarized in Table 2) (48, 49, 51, 147-154). The chief limitation of Ts65Dn mice is they are not trisomic for all Hsa21 orthologs (47). In addition, male Ts65Dn mice are sterile (147).

Many other mouse models of DS have been developed. The Ts[Rb(12.17^{16})]2Cje (Ts2Cje) mouse is segmental trisomic for the same genes as Ts65Dn, but the triplicate segment was fused to Mmu12 and these mice are fertile (155). It remains to be determined whether these mice display similar phenotypes as the Ts65Dn mouse. Other segmental trisomies of Mmu16 include Ts (12; 16)1Cje and Dp (16Cbr1-ORF9) (Ts1Cje and Ts1Rhr, respectively) (Figure 4). Cross breeding the Ts1Cje and Ts1Rhr to Ts65Dn has produced two other DS mouse models: Ms1Cje/Ts65Dn and Ms1Rhr/Ts65Dn, respectively (Figure 4) (156, 157). The newest segmental trisomic mouse model for Mmu16 is the Dp(16)1Yu/+ mouse, which contains all of the Hsa21 orthologs on Mmu16 (much larger segment than the Ts65Dn mouse); however, these mice have yet to be fully characterized (158).

The last two mice are trisomic for the entire regions of Mmu16 and Hsa21 (referred to as Ts16 and Tc1, respectively). The original mouse model of DS, Ts16, is trisomy for the entire Mmu16, which contains some Hsa21 orthologs, but also large segments of non-homologous genetic material as well (contained on Hsa3, 8, 12, 6, and 22) (Figure 4) [reviewed in (46)]. These mice die perinatally and have limited value. The Tc1 mouse carries three copies of about 92% of Hsa21 genes (Figure 4) (159). Tc1 recapitulates many DS phenotypes, however, there is

a high degree of mosaicism because mouse cells eliminate Hsa21 during cell division over time [reviewed in (47, 160)].

Advantage of Using the Ts65Dn Mouse

The expression level of the trisomic genes in 6 different tissues of the Ts65Dn mouse has been determined, and this analysis included skeletal muscle. These studies revealed the expression of SOD1 and GPX1 in skeletal muscle from Ts65Dn mice was 1.45- and 1.02-fold (reference number for euploid is 1), respectively (161). Unfortunately, the expression of CAT was not determined. Kahlem et al. reported similar findings, as SOD1 gene expression was 1.87-fold higher in Ts65Dn mice compared to euploid littermates (53). These findings provide evidence that SOD1 is over-expressed and there is no up-regulation of GPX1 in Ts65Dn skeletal muscle

There is also evidence that non-muscle tissues from the Ts65Dn mice exhibit oxidative stress. Cultured hematopoietic progenitors stem cell populations derived from bone marrow of Ts65Dn mice have a 20-45% higher level of oxidant production compared to wild-type cells (56). These cells also exhibited increased markers of protein oxidative damage, which was shown by an increase in protein carbonyls and 3-nitrotyrosine (56). Levels of lipid peroxidation are elevated in the brain of Ts65Dn mice (162), which further supports that Ts65Dn mice exhibit oxidative stress.

These mice also exhibit neuromuscular dysfunction in vivo. For example, Costa et al. showed 4-8 month old Ts65Dn mice exhibit significant dysfunction in maximum running speed on a treadmill, grip strength, and swimming speeds compared to euploid littermates (51). Klein et al. corroborated these findings, as Ts65Dn mice exhibited a 15% reduction in grip strength compared to euploid littermates, although this was not statistically significant (150).

In summary, Ts65Dn mice exhibit many of the same phenotypes observed in the human condition and are the most studied and established mouse model of DS. The Ts65Dn mouse is a suitable model for the purposes of the present study based on: 1) Gene expression analyses of skeletal muscle from Ts65Dn mice show that SOD1 is up-regulated without any compensation by GPX1; 2) Non-muscle tissues from Ts65Dn mice demonstrate oxidative stress; 3) Ts65Dn mice exhibit signs of muscle weakness in vivo.
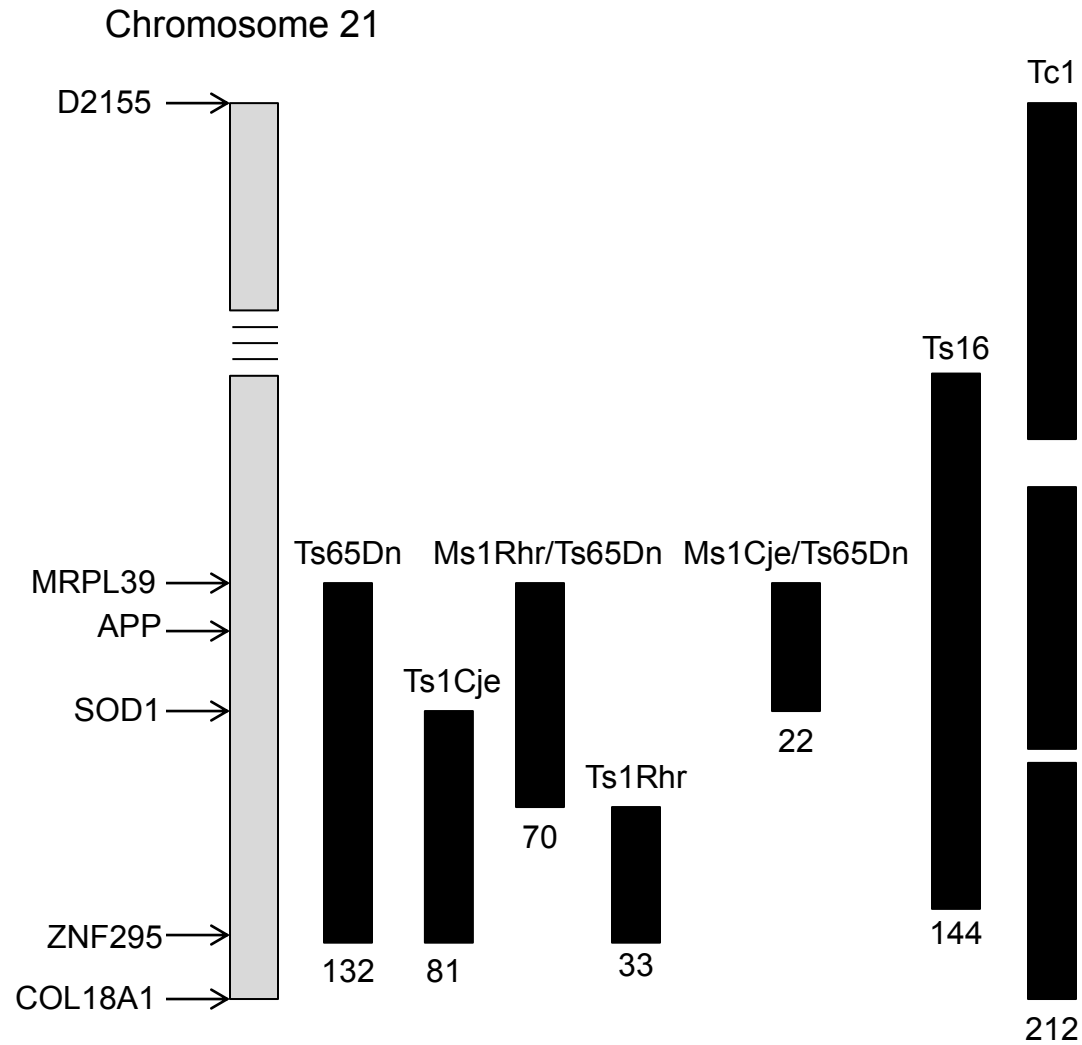
Figure 4. This illustration shows the regions of human chromosome 21 represented in the mouse models of Down syndrome. The number of genes preserved in the models is indicated below each segment (46). This figure was adapted from Salehi et al. and Rachidi and Lopes (47, 163). Chromosome information was attained from Ensembl.

Table 2. Phenotypes present in persons with Down syndrome and Ts65Dn mice. This table was partially redrawn from Patterson and Costa (145). Individual references are embedded in the text.

Feature	Persons with DS	Ts65Dn
Cognitive and behavior impairments	Yes	Yes
Altered brain function and structure	Yes	Yes
Gait abnormalities	Yes	Yes
Growth and development	Slow growth and short stature	Lag in growth and body weight
Obesity	Yes	Yes
Reduced exercise capacity	Yes	Yes
Muscle weakness	Yes	Yes
Craniofacial abnormalities	Yes	Yes
Hematological and/or immunological abnormalities	Yes	Yes
Male sterility	Yes	Yes
Pregnancy	Ovulation difficulties, shorter reproductive life	Small litters, shorter reproductive life
Aging	Shorter life expectancy	Shorter life expectancy
Oxidative stress	Yes	Yes

Prenatal lethality	Yes	Yes
Sleep disturbances	Yes	Yes
Congenital heart defects	Yes	Yes

<u>Assessment of In Vitro Skeletal Muscle Contractile Function</u>

A brief description of the methodology and technical considerations involved in assessing in vitro skeletal muscle contractile function follows, which will include a brief overview of the force-frequency relationship, experimentally induced fatigue, and the effects of bath temperature, muscle bulk, and fiber type.

Force-Frequency Relationship

The force-frequency relationship is often examined in studies of in vitro skeletal muscle contractile function. After excision of a whole muscle or strip of muscle it is placed in an aerated salt solution and electrically stimulated to contract isometrically using two platinum electrodes (Figure 5). The length at which the muscle is positioned determines its force output (i.e., the length-tension relationship of skeletal muscle). Thus, the muscle length at which active tension is maximal must first be determined and is referred to as optimal length (L_o) (164). The force-frequency relationship is determined at L_o by stimulating the muscle at increasing frequencies of electrical stimulation; usually a range is used from 10 to 250-300 Hz (this is to induce fused tetanus) with tetanic train durations of 500 ms [e.g., (165)]. The data generated are expressed in units of force (N) and stress or force per area (N/cm^2). The cross-sectional area of the muscle is calculated according to the equation of Close (166) (Equation 1),

$$\frac{Weight}{[(Length \times 0.71) \times 1.06]} \qquad \text{Equation 1}$$

The length of the muscle is multiplied by 0.71 to correct for fiber length (167), and then multiplied by the density of muscle ($1.06 \ mg/mm^3$).

Experimentally Induced Fatigue

There are two main types of fatigue that can be induced with electrically stimulated contractions, and these include high- and low-frequency fatigue [reviewed in (168)]. High-frequency fatigue is characterized by a rapid loss in force production with a decrease in the amplitude and increase in the duration of the compound muscle fiber action potential (168). These changes are attributed to a failure of impulse propagation across the sarcolemma (likely in the t-tubule system) due to the disruption of ion concentration gradients (particularly K^+). Recovery from high-frequency fatigue occurs within seconds to minutes after the cessation of exercise. High-frequency fatigue is not considered an important cause of fatigue in vivo, as skeletal muscle possesses specific adaptations that prevent its occurrence (e.g., motor unit recruitment patterns, tightly regulated capillary system) (168).

Low-frequency fatigue is elicited using far less intense stimulation (30-40 Hz versus 100 Hz). This type of fatigue is characterized by metabolic stress, which includes depletion of glycogen and phosphocreatine, and increases in H^+ and P_i. Recovery from low-frequency fatigue occurs over hours to days. In addition, ROS play an important role in the development of this type of fatigue (36). There is no established stimulation protocol to induce low-frequency fatigue. This type of fatigue is elicited using repeated short tetani with low stimulus frequencies [e.g., 40 Hz, 0.5 trains/s, 500 ms trains (36, 165)]. These types of protocols continue for a set amount of time (e.g., 5 min) or until force is reduced by a predetermined percentage of the initial force (e.g., 50%).

Effect of Bath Temperature

One common concern when using in vitro skeletal muscle preparations is the stability of the specimen (usually defined as an irreversible decrement in force production over time). The temperature of the bath requires careful consideration. Segal and Faulkner investigated the effect of temperature on specific maximal tetanic isometric force (P_0) of rat soleus and extensor digitorum longus at 20, 25, 30, 35, and 40°C over 60 minutes. They found the stability of the muscles was temperature dependent; higher temperatures resulted in progressively larger decrements in force production over time (169). Most studies examine the force-frequency relationship and fatigue at 37°C because this temperature is physiologically relevant [e.g., (36, 165)]. The literature supports this choice, as oxidants are important contributors to the development of fatigue and the depression of P_0 at 37°C (170, 171). For example, Moonapar and Allen showed that single skeletal muscle fibers fatigued at a faster rate at 37°C compared to 22°C, but this effect was abolished by the addition of Tiron (scavenges superoxide radical and hydroxyl radical) to the bath (171). These results suggest that the production of oxidants is an important mediator of fatigue at 37°C, and it is therefore, appropriate to study the effects of oxidants on fatigue at this temperature.

Effect of Muscle Bulk

The stability of the specimen is also affected by the size of the muscle. Limitations in O_2 diffusion into the depth of the muscle can create an anoxic core. Mouse soleus and extensor digitorum longus muscles are roughly 10 mg, compared to the rat soleus and extensor digitorum longus used by Segal and Faulkner that are 70-90 mg. Segal and Faulkner suggest muscles less than 30 mg are sufficiently small for adequate

oxygenation and nutrient uptake (169). This has been refuted recently, as the development of a hypoxic core does contribute to fatigue induced using stimulation frequencies of 50-70 Hz (172). Thus, the development of anoxic core is a limitation when studying in vitro muscle fatigue.

Fiber Type Effects

The performance characteristics of skeletal muscle are largely influenced by the distribution of the myosin heavy chain isoforms (i.e., fiber types) (89). The mouse soleus is composed predominantly of Type I and Type IIa muscle fibers, whereas the extensor digitorum longus is composed of mostly Type IIa and IIb muscle fibers (173). Muscles composed of Type I and Type IIa fibers are more oxidative and contain larger stores of endogenous antioxidant proteins [reviewed in (41)]. This observation suggests that muscles like the mouse soleus would be more resistance to changes in redox status than the extensor digitorum longus. However, Plant et al. showed that P_0 of mouse soleus and extensor digitorum longus were equally affected by oxidizing agents, suggesting researchers would be justified in choosing either muscle to study the effect of oxidants on skeletal muscle function (174).
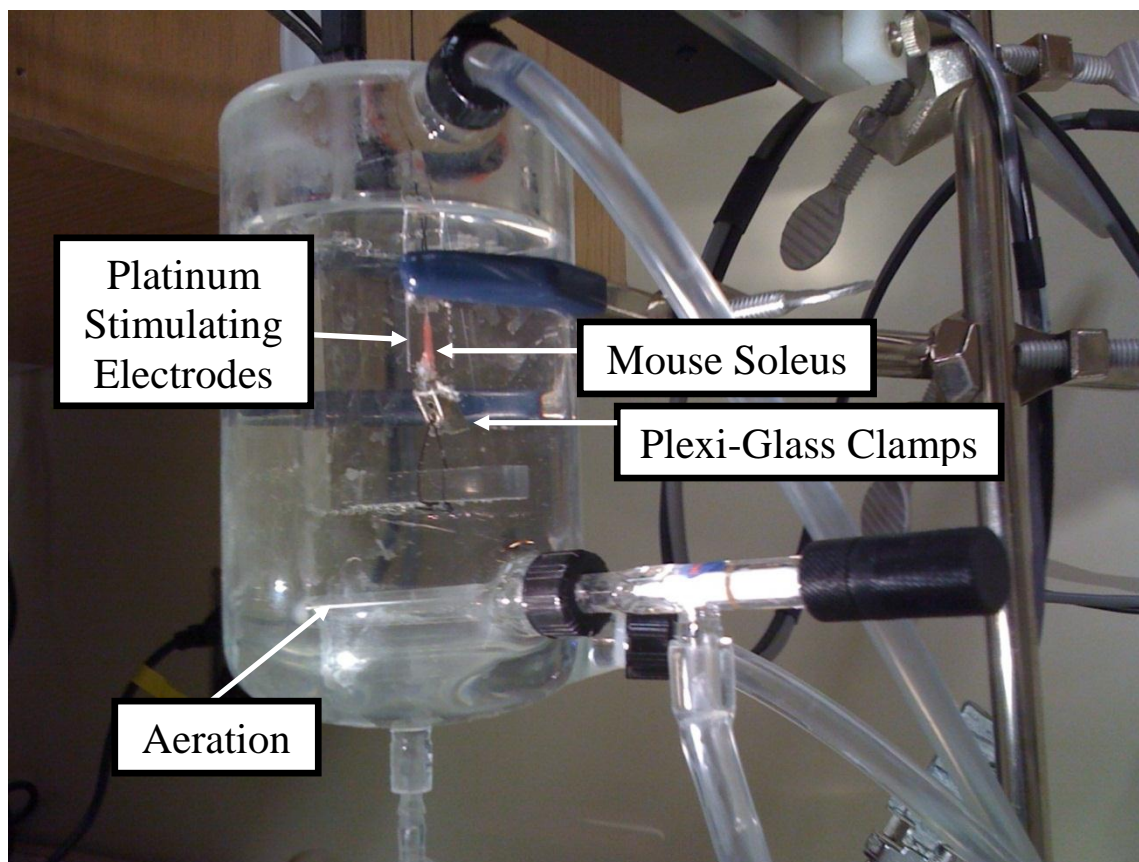
Figure 5. This figure shows the experimental set-up to study skeletal muscle function in vitro.

Affymetrix Microarray Technology

Microarray technology allows for the quantification of mRNA from thousands of genes, and is commonly used to examine the effect of perturbations on skeletal muscle gene expression (e.g., disease or atrophy) (175). The technology is based on the principle of Watson and Crick base pairing, where two complementary strains of DNA form hetero-duplexes. The process is largely automated and performed by specialized microarray core facilities. A number of platforms have been developed, and one of the most common is the Affymetrix platform. Affymetrix microarrays are made using a process called in situ synthesis, where oligonucleotides (short strands of DNA) are synthesized base-by-base on the glass surface of the array (176). Each oligonucleotide or probe is specific for a particular gene. Affymetrix 1.0 ST arrays contain ~4 probes per exon and ~40 probes per gene, which allows for both gene-level and exon-level analyses (177). The Mouse Gene 1.0 ST Array probes for 28,853 genes with 770,317 distinct probes (178). Affymetrix microarrays are a one-color oligonucleotide array, which means there is only one sample per array.

The first step in using the microarray is extracting RNA from the sample (176). Once the RNA is extracted from the sample it is used as a template to produce cDNA and then biotin-labeled (176). At this point the single-stranded cDNA is introduced into the array. This step is where the oligonucleotides on the array form hetero-duplexes with the labeled cDNA; this process is called hybridization (176). Following hybridization the arrays are washed to ensure that only complementary hetero-duplexes remain, which reduces non-specific binding and cross-hybridization (176). The final step is to produce an image of the surface of the array using a scanner (176). The intensity of the

fluorescent probe attached to the hetero-duplexes is proportional to the RNA transcript present in the sample (175). The dataset generated is extremely large and data analysis is tedious and time consuming. The identification of genes that are differentially expressed can be determined using a variety of statistical analyses specifically developed for microarray data. These genes are further analyzed by patterns of expression and identification of their biological meaning.

Affymetrix has developed a number of built-in methods to reduce systematic errors and bias introduced during the experiment. These processes are referred to as normalization, and include data cleaning and transformation, assessing array quality, and between-array normalization (176). Data cleaning involves examining the background and noise signal. The Gene 1.0 ST Array estimates background auto-fluorescence using a set of approximately 17,000 generic background probes (178). Affymetrix has also developed a method to examine signal noise, which is referred to as the Q value (179). The Q value is a measure of the pixel-to-pixel variation of the probe cells on the array (179). There are no guidelines for what background values are acceptable, but arrays from the same experiment should have similar background values (179).

It is common practice that the raw intensities from microarray data are log transformed before data analysis (176). The most common transformation is to use logarithms to base 2 (176). The purpose of transformation is to ensure that there is a broad range of intensities, the variability at each level of intensity is relatively constant, and the distribution of experimental errors and intensities are close to being normally distributed (176).

Affymetrix has developed several methods to assess array quality. These include, poly-A controls, hybridization efficiency, and positive and negative control genes. Poly-A controls are genes of *B. subtilis* that have been modified by the addition of poly-A tails, spiked in the RNA sample, and carried through the sample preparation process (179). They are evaluated like internal control genes, and their signal intensity should increase with the level originally introduced into the sample (179). Hybridization controls are composed of a mixture of biotin-labeled cRNA transcripts with increasing concentrations introduced during hybridization (179). Signal intensity of the hybridization controls should increase with the level originally introduced during hybridization. Actin and GAPDH are used as internal control genes to assess RNA sample and assay quality (179). The signal values of the 3' probe sets for actin and GAPDH are compared to the signal values of the 5' probe sets. The ratio of the 3'/ 5' should be no more than 3 (for a 1-cycle assay). Values higher than 3 are an indication of degraded RNA or inefficient transcription (179). The arrays also contain negative controls genes. The Mouse Gene 1.0 ST array contains 5,222 putative intron-level probes from putative constitutive genes (178).

Between-array normalization is performed using a scaling factor because the intensity of each array varies from one array to the next (178). In order to reliably compare data from multiple arrays, the overall intensity of the arrays must be equalized. The average intensity of each array is multiplied by the scaling factor to bring it to an arbitrary target value (178).

In summary, microarray technology is an extremely useful tool to examine changes in global gene expression. The adoption of standard laboratory practices,

specialized microarray laboratories, and built-in safeguards make microarray a feasible and reliable methodology.

<u>Properties of Single Skeletal Muscle Fibers in Culture</u>

The flexor digitorum brevis (FDB) muscle culture has emerged as a valuable tool to study basic skeletal muscle biology. Methodology to isolate single skeletal muscle fibers was initially developed by Bekoff and Betz, for the purpose of examining the sensitivity of the mammalian motor endplate to acetylcholine in high resolution (180). Bischoff later expanded the method for the purpose of studying the in situ behavior of skeletal muscle satellite cells (181). Since then, a number of modifications have been made to the methodology for the purpose of isolating single fibers from a variety of muscles. The muscle most commonly used is the flexor digitorum brevis (FDB), which is a superficial, multi-pennate, and thin muscle of the foot. It originates from the tendon of the plantaris and converges into long tendons that attach to the digits. The FDB is ideal for isolating fibers because it yields several hundred fibers, whereas larger muscles of the hindlimb yield fewer fibers mainly due to their larger size. The fibers of the FDB are significantly shorter compared to other limb muscles, which prevents them from tangling together and breaking during the isolation procedure.

Rat FDB fibers are roughly ~1 mm in length with a diameter of ~20 μm (181). These fibers contain roughly ~125 myonuclei and ~3 associated satellite cells per fiber (181). The mouse FDB fibers are much shorter with a length of ~350 μm, but they have a slightly larger diameter of ~30 μm (182). Mouse FDB muscles are predominantly fast-twitch, with 80-90% Type IIa/x and 10-20% Type I fibers (183-185).

Importantly, FDB fibers maintain their physiological properties in vitro. Liu et al. showed FDB fibers exhibit no change in resting or peak calcium transients in response to electrical stimulation for up to 8 days in culture (186). Ravenscroft et al. has also reported similar findings that calcium transients are unchanged for up to 8 days in culture, and they also showed fibers maintain the correct spatial resolution of skeletal muscle proteins (185). These findings suggest the components of the excitation-contraction coupling pathway of FDB fibers remain intact in culture. Thus, the FDB provides a unique opportunity to study adult muscle in culture.

Oxidant Detection by 2′,7′-dichlorodihydrofluorescin diacetate

Many compounds have been developed to detect the presence of oxidants. The most common detection agent is 2′,7′-dichlorodihydrofluorescin diacetate (H_2DCFDA). The probe has been recently adapted for use in isolated single skeletal muscle fibers (187). It is a cell permeable, polar, and non-fluorescent molecule that can diffuse into cells. Upon entry the diacetate group is removed by the cell's endogenous esterases leaving H_2DCF, which is retained by the cell. H_2DCF can be oxidized to yield fluorescent DCF that can be monitored by fluorescence microscopy.

A number of chemical species can oxidize H_2DCF to fluorescent DCF. H_2DCF has little or no reactivity to superoxide radical or hydrogen peroxide (188, 189). However, hydrogen peroxide can oxidize DCF through a peroxide-catalyzed reaction (189). Nitric oxide, nitric oxide derivatives, hydroxyl radical, peroxynitrite, oxidized thiols, and metal centers directly oxidize DCF (189, 190). Thus, due to the lack of specificity of DCF, it is considered an indicator of net intracellular oxidant production (188, 189). It must be acknowledged that the conversion of H_2DCF to DCF occurs in

competition with other cellular oxidation reactions, such as those involving the endogenous antioxidants (190)

Three important methodological factors must be considered when using the H_2DCFDA assay, as outlined by Arbogast and Reid (190). These include photo-oxidation, photo-bleaching and dye leak. First, photo-oxidation artifact is controlled by conducting experiments in a darkened laboratory and by standardizing excitation parameters. Second, photo-bleaching is minimized by preloading fibers with excess H_2DCFDA. Last, dye leak is affected by temperature; it is detected at 37° but not at 23° (191). Therefore, careful control of the above factors is essential to produce reliable data using the H_2DCFDA assay.

CHAPTER III. FUNCTIONAL CHARACTERIZATION OF SKELETAL MUSCLE IN DOWN SYNDROME MICE

ABSTRACT

Persons with Down syndrome (DS) suffer from low muscle strength that limits their functional performance. Triplication and altered expression of chromosome 21 genes, including copper-zinc superoxide dismutase (SOD1) could lead to oxidative stress and impaired skeletal muscle function. The purpose of these experiments was to perform a functional characterization of skeletal muscle from Ts65Dn mice with the intent to reveal potential mechanisms responsible for DS-associated muscle weakness. SOD1 expression and protein carbonyls were 26% and 21% higher in Ts65Dn than wild-type (WT) muscle, respectively. However, there was no evidence of increased basal muscle oxidant production in Ts65Dn muscle compared to WT. Ts65Dn muscle exhibited normal force generation in the unfatigued state, but there was a 12% reduction in force generation following fatiguing contractions. The development of muscle weakness in Ts65Dn mice was not explained by myosin heavy chain composition. Limitation in mitochondrial function was postulated to play a role in the development of post-fatigue weakness, which was supported by a 22% reduction in cytochrome c oxidase expression in Ts65Dn muscle. Microarray analysis also revealed the alteration of numerous pathways in Ts65Dn muscle, including: proteolysis, glucose and fat metabolism, neuromuscular transmission, DNA damage, and ATP biosynthesis. Collectively, these findings provide the first insight into the potential mechanisms of muscle dysfunction in DS.

INTRODUCTION

Down syndrome (DS) or trisomy 21 is the most common genetic cause of intellectual disability in the United States and occurs in roughly 1 in 700 live births (192). More than 300 genes are encoded by human chromosome 21 (3), and triplication disrupts normal gene expression resulting in the DS phenotype and associated abnormalities (2). All individuals born with DS will experience some medical issues that will require sustained medical care, which can include craniofacial abnormalities, intellectual disability, Alzheimer's-like characteristics of the brain, obesity, gastrointestinal disorders, hematological disorders, congenital heart disease, and hypotonia and low muscle strength, among many others (4).

Considerable evidence exists in the literature showing that intellectual disability only partially explains the very low muscle strength in persons with DS (12-20). Muscle weakness affects many different areas of daily function in both young and old adults with DS, including limitations in walking, running, rising from a chair, and ascending and descending stairs (6, 7, 14). Furthermore, mobility impairments are predictive of mortality in adults with DS (26). The cause of muscle dysfunction in persons with DS is unknown, and thus, there is a critical need to identify mechanisms underlying their muscle dysfunction.

Oxidative stress is thought to be a key factor in the development of DS-related pathologies, and may be the result of triplication and altered expression of chromosome 21 genes, which includes copper-zinc superoxide dismutase (SOD1) (32, 193). The over-expression of SOD1 could lead to an increase in the production of hydrogen peroxide above the level that can be neutralized by normal antioxidant defenses (32, 193). This

notion is supported by findings that show cortical neurons and astrocytes from fetuses with DS exhibit a higher level of oxidant production (42). Also, non-muscle tissues from persons with DS exhibit elevated markers of oxidative injury to DNA, lipid, and protein (43-45). Large and prolonged elevations in oxidants contribute to impaired muscle function in a number of diseases, such as Myotonic and Duchenne muscular dystrophies, heart failure, cancer, and HIV/AIDS (40). It is currently unknown whether oxidative stress contributes to the development of skeletal muscle weakness in persons with DS.

In these experiments we utilized the Ts65Dn mouse to examine the impact of DS on skeletal muscle contractile properties and characteristics. Skeletal muscle function in the Ts65Dn mouse has not been examined previously and there is an urgent need to establish an animal model to explore the muscle dysfunction that is widely reported in persons with DS. Therefore, the purpose of these experiments was to characterize skeletal muscle function, morphology, myosin heavy chain composition, and global gene expression patterns in Ts65Dn muscle, which is the most widely studied and well-established mouse model of DS (146). We also sought to examine the effect of segmental trisomy on skeletal muscle protein antioxidant expression and oxidant production.

Our data revealed that Ts65Dn muscle over-expresses SOD1 protein but this was not associated with oxidative stress. Ts65Dn soleus muscles displayed normal force generation in the unfatigued state, but exhibited muscle weakness following fatiguing contractions. We show that a reduction in cytochrome c oxidase expression may contribute to the impaired muscle performance in Ts65Dn soleus. These findings support the use of the Ts65Dn mouse model of DS to delineate mechanisms of muscle dysfunction in the human condition.

METHODS

Animals and Experimental Procedures

The Syracuse University Institutional Animal Care and Use Committee approved the use of animals for these experiments, which followed the Guiding Principles for the Care and Use of Vertebrate Animals in Research and Training established by the American Physiological Society. Male B6EiC3Sn a/A-Ts(17[16])65Dn (Ts65Dn) mice and wild-type (WT) colony controls were purchased from the Jackson Laboratory (Bar Harbor, ME) (total n=44; 18 Ts65Dn and 26 WT). Ts65Dn mice are segmental trisomic for mouse chromosome 16 from ZNF295 to MRP139, which corresponds to roughly 132 out of the 230 genes in the human condition (144). These mice display many of the phenotypes observed in the human condition, including structural and cognitive alterations of the brain, craniofacial abnormalities, and congenital heart defects (48-50).

Mice were housed in groups of 3-4 by genotype and maintained on a 12:12 hr light: dark cycle with food and water provided ad libitum. Mice were anesthetized with an intraperitoneal injection of sodium pentobarbital (120 mg/kg) with supplemental dosages provided as needed to maintain a surgical plane of anesthesia. Following a procedure to surgically remove the hindlimb musculature the animals were sacrificed by removal of the heart and diaphragm, followed by the performance of a gross necropsy.

Two groups of Ts65Dn and WT mice were employed in this study. Muscles obtained from the first group of animals were utilized for measurement of in vitro contractile function, global gene expression by microarray, myosin heavy chain composition, hydrogen peroxide content, and protein expression levels (Table 3). These mice were 4-7 months of age at the time of experimentation. Muscles obtained from the

second group of mice were utilized for measurements of oxidant production in isolated skeletal muscle fibers, immunofluorescence labeling of SOD1 in single fibers, and soleus muscle fiber morphology (Table 3). These mice were ~13 months of age at the time of experimentation.

The soleus was the primary muscle under investigation in these experiments. However, the gastrocnemius was included to assess hydrogen peroxide content, and single fibers of the flexor digitorum brevis (FDB) were utilized to assess oxidant production and immunofluorescence labeling of SOD1. The soleus was an appropriate muscle to study in these experiments since it exhibits a similar myosin heavy chain composition to human locomotor muscles (194, 195). Ideally, the soleus would have been utilized for all assays. However, measurements from the gastrocnemius were also included on the basis that the soleus provided a limited amount of tissue, and the isolation of single fibers was performed using the FDB due to the large number of viable fibers that could be obtained.

In vitro muscle contractile function

The soleus muscle was excised and immediately placed in a dissecting dish containing Krebs-Hensleit solution equilibrated with 95% O_2, 5% CO_2 at room temperature. The proximal and distal tendons were clipped with light-weight Plexiglas clamps (Harvard Apparatus, Holliston, MA) and the muscle was suspended vertically in a water-jacketed organ bath equilibrated with 95% O_2, 5% CO_2 gas at 25°C containing Krebs-Hensleit solution and 25 µM d-tubocurarine. The clamp attached to the proximal end of the muscle was secured to a force transducer (301C; Aurora Scientific, Aurora, ON) and the clamp attached to the distal end of the muscle was secured to a fixed

Plexiglas rod; this positioned the muscle directly between platinum wire stimulating electrodes. Following a 15-minute equilibration, optimal contractile length (L_0) was determined by stimulating the muscle with supramaximal voltage and adjusting muscle length in ~0.5 g increments until maximum force was achieved. Force output was continuously monitored using a computerized data acquisition system (Aurora Scientific). Following the determination of L_0, the bath temperature was increased to 37°C and the muscle was allowed to equilibrate for an additional 30 minutes. The force-frequency relationship was determined using contractions evoked at stimulus frequencies of 1, 15, 30, 50, 80, 120, 160, 250, and 300 Hz with train duration of 500 ms with 2 minutes of recovery between contractions (Grass S48 stimulator; West Warwick, RI). Two minutes following the end of the force-frequency protocol the muscles underwent a fatigue protocol (40 Hz, 0.5 trains/s, 500 ms trains) for 5 minutes, followed by a recovery period (40 Hz, 0.5 trains/s, 500 ms trains) with force measurements obtained at 30 seconds, and 1, 2, 5, 10, and 15 minutes. At the end of the contractile protocol, L_0 was measured using a caliper and the muscle was then removed from the bath, trimmed of excess tendon, blotted to remove excess buffer, and weighed. Muscle cross-sectional area was calculated by dividing muscle mass by the product of fiber length and muscle density (166). Fiber length was calculated by multiplying muscle length by the fiber length coefficient of 0.71 (167). A value of 1.06 g/cm^3 was used for muscle density. Force was expressed in absolute values, relative [(% of peak tetanic tension (P_o)], and/or stress, which was calculated by normalizing to muscle cross-sectional area. Area under the curve was calculated using the trapezoidal integral method for the force-frequency, fatigue, and post-exercise datum using Prism 5.0.

Western blot

Soleus muscles were homogenized (1:25, w/v) in phosphate buffer containing EDTA, 1% Triton-X, 5 mM DTT, 0.1% SDS, and protease inhibitor (Sigma, St. Louis, MO) using a micro-tube pestle with a conical tip (Research Products International Corporation, Mt. Prospect, IL). Following complete disruption of the muscle, the homogenate was centrifuged at 10,000 g for 10 min at 4°C. The protein content of the soluble fraction was assessed using the Bradford assay (196). The samples were diluted in Laemmli sample buffer (Bio-Rad Laboratories, Hercules, CA) to yield a final protein contraction of 2.5 µg/µl and placed in boiling water for 5 minutes. Protein samples (10-60 µg) were separated by SDS-PAGE using 12% polyacrylamide gels for 1.25 hr, and then transferred to nitrocellulose membranes at 275 mA for 2-3 hrs. The membranes were stained with Ponceau-S to ensure optimal protein loading and transfer. Membranes were then blocked in 1-5% skim milk protein in PBS containing 0.05% Tween 20, and subsequently incubated with a primary antibody specific for SOD1 (1:1000, Novus Biologicals, Littleton, CO), manganese SOD (SOD2) (1:5000, Cayman Chem, Ann Arbor, MI), CAT (1:1000, Calbiochem, Darmstadt, Germany), GPX1 (1:1500, Abcam Inc., Cambridge, MA), 4-hydroxynonenal (4-HNE) (1:1000, Santa Cruz Biotechnology, Inc., Santa Cruz, CA), cytochrome c oxidase subunit II (COX2) (sc-23984, 1:1000, Santa Cruz Biotechnology, Inc.), or glyceraldehyde-3-phosphate (GAPDH) (1:5000, Sigma) diluted in blocker for 1-12 hr at 4°C. Membranes were subsequently washed with PBS and incubated with a horseradish peroxidase-antibody conjugate (1:1000-5000) diluted in blocker directed against the primary antibody for 1 hr. Membranes were then washed, treated with chemiluminescent reagents (Thermo Scientific, Rockford, IL), and exposed

to light sensitive film. The film was scanned and subsequently analyzed using ImageJ software (197). Bands were quantified and expressed in arbitrary units relative to the GAPDH loading control band. 4-HNE bands were quantified individually and summed to obtain a total value. The 4-HNE membranes were stained with Coomassie G250 (Bio-Rad Laboratories), scanned, and protein per lane was quantified using ImageJ (197). The 4-HNE bands were expressed relative to total protein per lane.

Protein carbonyls

Protein carbonyl formation was measured as an index of protein oxidation using the commercially available OxyBlot assay kit (Millipore, Billerica, MA) according to the manufacturer's instructions. Soluble proteins (15 µg) were reacted with 2, 4-dinitrophenylhydrazone for 15 minutes. Following the reaction process, 10 µg of 2, 4-dinitrophenylhydrazone-derivatized protein was loaded onto 12% polyacrylamide gels, followed by electrophoresis, transfer of protein to nitrocellulose membrane, and visualization of protein according to the procedures described above. Protein bands were quantified individually and summed to obtain a total value. The membranes were subsequently stained with Coomassie G250 (Bio-Rad Laboratories), scanned, and protein per lane was quantified using ImageJ (197). The protein bands were expressed relative to total protein per lane.

Hydrogen peroxide content

Hydrogen peroxide (H_2O_2) content of the gastrocnemius was determined using the Amplex Red Hydrogen Peroxide Kit (Invitrogen, Carlsbad, CA). Roughly 50 mg of gastrocnemius muscle was homogenized in ice-cold phosphate buffer, followed by centrifugation at 10,000 g for 10 min at 4°C. The protein content of the soluble fraction

was assessed using the Bradford assay (196). The Amplex Red reagent (10-acetyl-3,7-dihydroxyphenoxazine) reacts 1:1 with H_2O_2 to produce a fluorescent resorufin, which can be measured spectrophotometrically. A standard curve was prepared from 20 mM H_2O_2 working solution to produce H_2O_2 concentrations of 0, 5, 10, 12.5, 25, 37.5, 50, and 75 μM. Briefly, 50 μL of standard curve samples and unknown samples were loaded into individual wells of a 96-well microplate in duplicate followed by addition of 50 μL of the Amplex Red reaction mixture. The plate was incubated in the dark for 10 minutes followed by an absorbance reading at 560 nm. The concentration of H_2O_2 was calculated by fitting a line of best fit between absorbance and H_2O_2 standards. The H_2O_2 concentration was normalized to grams of protein in the sample.

Histology

Soleus muscles (contracted and non-contracted) were embedded in O.C.T. compound (Sakura Finetek USA, Torrance, CA) and frozen in either liquid nitrogen chilled isopentane or on dry ice. The contracted soleus was fixed at L_o before freezing and was used to determine the distribution of myosin heavy chain isoforms. Non-contracted soleus muscles were frozen at resting length and used for the determination of muscle morphology using the hematoxylin and eosin stain. Sections from frozen muscles were cut at 10-20 μm using a cryostat, mounted on slides, and stored at -80°C until processing.

Myosin heavy chain immunofluorescence

Muscle sections were air dried for 10 minutes followed by incubation in PBS containing 0.5% Triton X-100. Sections were simultaneously exposed to dystrophin (Thermo Fisher Scientific, Fremont, CA), myosin heavy chain type I (A4.840; DSHB,

IA) and myosin heavy chain type IIa (SC-71; DSHB) antibodies in a dark, humid chamber at room temperature for 1 hr. Sections were washed in PBS three times and simultaneously exposed to TRIT-C goat anti-rabbit (Invitrogen), Alexa Fluor 350 goat anti-mouse (Invitrogen), and FITC goat anti-mouse (Invitrogen) antibodies diluted in 10% normal goat serum in PBS in a dark humid chamber at room temperature for 1 hr. Sections were washed three times in PBS and mounted with Vectashield mounting medium (Vector Laboratories Inc., Burlingame, CA). Images were obtained at 10X magnification using a Zeiss AxioImager fluorescence microscope equipped with an AxioCam MRc digital camera and analyzed with AxioVision software (version 4; Carl Zeiss, Germany). The proportions of type I, type IIa, and type IIx myosin heavy chain isoforms was determined by counting all visible fibers.

<u>Hematoxylin & Eosin stain</u>

Muscle sections were air dried for 10 minutes and incubated in Harris hematoxylin for 5 minutes followed by rinsing in running tap water for 5 minutes. Sections were then briefly incubated in acid alcohol, running tap water, ammonia water, and then running tap water for 10 minutes. The sections were subsequently incubated in eosin for 4 minutes, dehydrated in alcohols, cleared, and mounted in permount. Images were obtained at 10X magnification using a Zeiss AxioImager microscope and associated camera and software. The total number of fibers in the mid-belly of the muscle was manually calculated using the cell counter plug-in in ImageJ (197). Single fiber cross-sectional area was calculated in 100 randomly selected fibers using ImageJ and plotted as a histogram to examine the distribution (197).

Myosin heavy chain electrophoresis

Soleus muscles were homogenized using a micro-tube pestle (Research Products International Corporation) in buffer (w/v 1:20) containing v/v 10% SDS, 40 mM DTT, 5 mM EDTA, 0.1 M Tris-HCL, and protease inhibitor (Sigma) (198). Homogenates were boiled in water for 5 minutes to denature the samples and the protein concentration of the soluble homogenate was determined using the RC DC Protein Assay (Bio-Rad Laboratories). The samples were then diluted in Laemmli sample buffer (Bio-Rad Laboratories) to yield a final protein concentration of 0.4 µg/µl. 6 µg of sample were loaded per lane of the gel.

SDS-PAGE was performed according to procedures outlined by Talmadge and Roy with minor modifications (199). The percent of glycerol in the stacking and separating gel was increased from 30% to 35%. The acrylamide:N,N'-methylenebisacrylamide ratio was 37.5:1 for the stacking gel and 99:1 for the separating gel. All gels were 0.75 mm thick, contained 10 wells and were used within 24 hrs after they were made. The Mini-PROTEAN 3 Cell and PowerPac Basic Power Supply (Bio-Rad Laboratories) were used for electrophoresis. The running buffers were made from a 10X stock solution (Bio-Rad Laboratories). The upper running buffer contained 50 mM Tris, 384 mM glycine, and (w/v) 0.1% SDS (pH = 8.3). The lower running buffer contained 25 mM Tris, 384 mM glycine, and (w/v) 0.1% SDS (pH = 8.3). The volume of the upper running buffer was 150 ml and 500 ml for the lower running buffer. ß-mercaptoethanol was added to the upper running buffer to give a final v/v of 0.12% (200). The buffers were made fresh before each run, stirred for 10 minutes, and then cooled to 4°C before electrophoresis. The buffers were not stirred during electrophoresis.

Two gels were used for each run at a constant 7 mA for 24 hrs at 4°C. Following

electrophoresis the gels were stained with a Coomassie G250 (Bio-Rad Laboratories),

scanned, and the bands were quantified using the gel analyzer feature in ImageJ (197).

RNA isolation and microarray hybridization

The isolation of RNA, microarray hybridization, and initial data processing were

performed at the State University of New York Upstate Medical University microarray

core facility. Muscle tissue was disrupted by passage through a 22G needle and

homogenized with a QIAshredder column (Qiagen Inc., Valencia, CA). RNA was

extracted with the RNeasy Mini Kit (Qiagen Inc.). Quality and quantification of RNA

was performed using the Agilent 2100 Bioanalyzer (Agilent Technologies Inc., Santa

Clara, CA). For microarray processing, 9 ng of total RNA was used for each sample. The

samples were processed with the WT-Ovation Pico RNA Amplification System (NuGEN

Technologies Inc.) to produce cDNA. The cDNA was then processed with the WT-

Ovation Exon Module (NuGEN Technologies Inc.) to produce cDNA of the appropriate

strand for the Gene ST arrays. The cDNA was then fragmented and biotin labeled using

the FL-Ovation cDNA Biotin Module V2 (NuGEN Technologies Inc., San Carlos, CA).

A hybridization mix (5 μg of the labeled cDNA, 50 pM Control Oligo B2, 1X Eukaryotic

Hybridization Controls, 1X hybridization buffer and 10% DMSO) was prepared using

Affymetrix GeneChip Expression Hybridization Controls and the Affymetrix GeneChip

Hybridization Wash and Stain Kit (Affymetrix Inc., Santa Clara, CA). The hybridization

mix was incubated at 99°C for 2 minutes, then 45°C for 5 minutes, and each sample was

added to a GeneChip Mouse Gene 1.0 ST array (Affymetrix Inc.). This array contains an

estimated 28,853 genes. Arrays were incubated for 18 hrs in a GeneChip Hybridization

Oven 640 at 45°C with rotation at 60 rpm (Affymetrix Inc.). After 18 hrs, the arrays were washed and stained on the Affymetrix Fluidic Station 450. Arrays were scanned with an Affymetrix GeneChip Scanner 7G Plus.

Microarray gene expression data analysis

For between-group comparison of the gene expression data, the significance analysis of microarrays (SAM) method (two-class, unpaired) was used using the MultiExperiment Viewer in the TM4 suite of software tools (201, 202). An initial SAM analysis was performed with 1000 permutations to view the SAM plot. The plot is interactive and allows the user to select the delta value and examine the effect on the number of genes called significant, but also the false positive rate. After viewing the test statistic distribution (i.e., observed versus the expected d-value) a delta (=1.626) was selected that strictly controlled type I error that greatly limited the number of genes called significant by chance alone. We then performed two additional SAM analyses with 1000 permutations each using the delta established from the initial analysis. The final list of differentially expressed genes was comprised of those that appeared in all three SAM analyses. We performed this process because the test statistic distribution is different each time the analysis is performed, which provides a slightly different list of genes called significant. For our set of analyses there were 16 genes called significant in at least one but not all three analyses. The final gene list contained 161 genes with a false discovery rate of 0.84%. The false discovery rate is defined as the median number of falsely called genes divided by the number of genes called significant. Based on the false discovery rate and the number of genes in our list there are 1.3 false positive genes. Given our false discovery rate is far below what is considered acceptable (< 5%), we feel

this gives us a high degree of confidence that type I error was adequately controlled. Functional categorization was performed using the National Center for Biotechnology Information and Gene Ontology databases (203).

Microarray pathway analysis

The gene expression data analysis explained above was performed using strict criteria to generate a small list of genes with a high degree of confidence. However more subtle differences may have important consequences, particularly if several genes involved in the same pathway are affected. Thus, pathway analysis was performed using the Database for Annotation, Visualization and Integrated Discovery (DAVID) (204). DAVID systematically maps large gene lists against associated biological annotations from a number of sources, including the Gene Ontology, BioCarta, KEGG, etc. The gene list for DAVID pathway analysis was generated by constructing 95% confidence intervals of the fold change of all genes on the array. Genes outside of the 95% confidence intervals were considered genes that are the most differentially expressed (i.e., most interesting). An additional criteria was also applied to this list of genes, the final list of genes included those with a $p<0.01$ using an unpaired t-test. This gene list, which included 803 genes, was imported into DAVID to perform functional annotation clustering. The premise of this analysis is that similar terms are clustered into groups, which can be used to explore their relationship in a network format rather than examining singular terms (204). Clusters with an enrichment score of 1.3 were considered because they are biologically relevant (204). Terms associated with each cluster were considered if they reached statistical significance ($p<0.05$) with a false discovery rate of <5%.

MicroRNA (miRNA) pathway analysis was also conducted. miRNAs are small non-coding RNAs involved in post-transcriptional regulation of gene expression (205). MicroRNAs play a fundamental role in skeletal muscle biology, and their dysregulation has been demonstrated in various disease conditions (205, 206). A number of miRNA were represented in the gene expression and pathway analysis gene lists. To gain novel insight into the regulatory pathways regulated by miRNA in skeletal muscle from Ts65Dn mice, we used a bioinformatics tool to identify potential miRNA-mRNA-protein interactions. Differentially expressed miRNA were uploaded into the DIANA-mirPATH, which is a computational tool to identify molecular pathways regulated by miRNA expression (207). A list of miRNA target genes was identified by TargetScan 5 (208), followed by calculation of an enrichment analysis using Pearson's Chi-squared test to determine which KEGG pathways were associated with the list of target genes (209). Pathways were considered significant if -ln(p-value) < 3 (i.e., $p < 0.05$).

Quantitative real-time PCR

Microarray data were validated by quantitative real-time PCR from the same RNA used for microarray analysis. RNA reverse transcription was performed using the iScript cDNA synthesis kit (Bio-Rad Laboratories) according to the manufacturer's recommendation. PCR was performed using iQ Supermix (Bio-Rad Laboratories) and the iCycler iQ Real-Time PCR Detection System (Bio-Rad Laboratories) using recommended cycling parameters. Pre-designed Taqman primers and probes were purchased from Applied Biosystems (ABI, Foster City, CA), which are designed to have 100% amplification efficiency. The standard curve method was used to quantify the

expression of SOD1, amyloid precursor protein (App), ring finger protein 160 (Rnf160), and GAPDH, which was included to normalize gene expression data.

Isolation and culture of single skeletal muscle fibers

Single skeletal muscle fibers were isolated from the FDB according to the method of Shefer and Yablonka-Reuveni with minor modifications (210). FDB muscles were excised and placed in sterile conical tubes containing Dulbecco's modified eagle medium (DMEM) with L-glutamine and sodium pyruvate (MediaTech Inc., Manassas, VA), 0.4% (w/v) collagenase type I (Worthington Biomedical Corporation, Lakewood, NJ), and 25 μM HEPES, which was incubated for 3 hrs at 37°C. The tube was gently agitated every 30 minutes to facilitate digestion. Following digestion, the muscles were washed twice in 2 ml of isolation media, which contained DMEM, 10% horse serum (Thermo Scientific Inc., Rockford, IL), 100 U/ml penicillin, and 100 μg/ml streptomycin (Thermo Scientific Inc.). The muscles were then placed in individual 35 mm dishes containing 3 ml of isolation media where debris and connective tissue were removed before gently triturated the muscles with fire-polished Pasteur pipette with openings ranging in diameter from < 1 to 3 mm. As the muscle progressively became smaller with increasing loss of fibers, the muscles were moved to another 35 mm dish containing 3 ml of isolation media and triturated with progressively narrower diameter Pasteur pipettes. This process continued until a sufficient number of fibers had been released. Single fibers were separated from debris and tangled or broken fibers by gravity sedimentation through 4 columns of isolation media for 10-15 minutes. The fibers were then bathed in maintenance medium containing DMEM, 10% fetal bovine serum (Thermo Scientific Inc.), 100 U/ml penicillin and 100 μg/ml streptomycin. Fibers were then plated on Matrigel (BD Biosciences, MD)

coated 35 mm dishes. The plates were placed in an incubator with 5% CO_2 at 37°C for 30 minutes to allow the fibers to adhere to the matrix, after which additional maintenance medium was added. Cultures were maintained in 5% CO_2 at 37°C for at least 12 hrs before they were used for experiments.

Oxidant production measurements from single fibers

Prior to the measurement of oxidant production, culture dishes were removed from the incubator and the medium was replaced with Dulbecco's phosphate buffered saline (D-PBS) for 5 minutes. The D-PBS was removed and replaced with D-PBS containing 20 μM 2',7'-dichlorodihydrofluorescein diacetate (H_2DCFDA; Invitrogen) in ethanol, and incubated in the dark for 45 minutes at room temperature. H_2DCFDA diffuses into fibers where intracellular esterases remove the diacetate group leaving H_2DCF, which is retained by the cell. Oxidants react with H_2DCF to yield fluorescent DCF. Following the incubation period the fibers were washed twice with D-PBS and incubated for an additional 20 minutes in D-PBS at room temperature before imaging.

Cells were imaged using a Nikon TE2000E inverted microscope (Nikon Instruments, Inc., Melville, NY) with 10X objectives and the B-2E filter set with excitation and emission wavelengths of 450-490 and 520-560 nm, respectively. Images were acquired using the microscope camera, which was controlled by NIS-Elements free software. DCF fluorescence was measured at time 0 and 15 minutes. Exposure time was limited to 2 seconds to avoid excessive photo-oxidation. Following the last measurement the shutter was opened and the fiber was continuously exposed with light to confirm that the acquired images were not saturated. Image analysis was performed using ImageJ software (197). The gray value of the entire fiber was measured at 0 and 15 minutes. The

gray value of a small area away from the fiber was also measured for background correction. The gray value of the background was subtracted from the gray value of the fiber at each time point. The background-corrected gray value at 15 minutes was expressed relative to the initial value (187).

The viability of each fiber was assessed following the experiment in three ways: 1) morphology, 2) exclusion of trypan blue, and 3) contractility. The morphology of the fibers was closely inspected for the presence of organized striations and absence of severe bending or twisting. Membrane damage was assessed using a solution of PBS containing 0.4% trypan blue. This solution was added to the culture dish and the fiber was visualized to ensure that the fiber excluded the dye (211). Maintenance of contractility was confirmed by stimulating the fiber using platinum electrodes with trains (2 ms pulse, 500 ms train duration, 50 Hz, 30 V, repeated once every 5 s) following the protocol (187). The fiber was considered viable only if it met the above criteria.

Immunofluorescence of single fibers

Single skeletal muscle fibers were assessed for protein content of SOD1. Following the measurement of oxidant production the fibers were fixed in 2% formaldehyde in PBS at room temperature for 15 minutes, and stored at 4°C with PBS until staining. The fibers were permeabilized with 0.2% Triton X-100 in PBS for 20 minutes and then blocked with a solution containing 10% normal goat serum and 1% bovine serum albumin for 30 minutes. The SOD1 primary antibody (1:100, cat# T2767, BioVision, Inc., Mountainview, CA) was applied and incubated in a dark humid chamber at 4°C for 24 hrs. Fibers were washed with PBS for three five-minute periods following the primary antibody incubation period. The fibers were subsequently incubated with a

Texas Red-labeled goat anti-rabbit secondary antibody (cat# T2767, Invitrogen) for 1 hr at room temperature, followed by three fifteen-minute washes in PBS. The fibers were then mounted in Vectashield with DAPI (Vector Laboratories, Burlingame, CA) and viewed with microscopy. Fibers were imaged using a fluorescence Nikon TE2000E inverted microscope with 10X objectives and the Y-2E/C filter set with excitation and emission wavelengths of 540-580 and 600-660, respectively. Images were acquired using the microscope camera controlled by NIS-Elements free software. Exposure time was limited to 2 seconds to avoid excessive photo-oxidation. Image analysis was performed using ImageJ software (197).

Single fiber analyses

Fiber size and myonuclei number were determined for Ts65Dn and WT FDB fibers. Fiber length and diameter were calculated using an image of the unfixed fibers because this avoids the shrinking that occurs following fixation. Fiber diameter was measured at three different locations and the average value was calculated. Myonuclei were stained with DAPI as detailed above. The total number of nuclei from each fiber was calculated using the cell counter plug-in in ImageJ (197). Myonuclear domain was calculated by dividing fiber volume (fiber length $\times \pi\, r^2$) by the total number of nuclei (119).

Statistical Analyses

The Shapiro-Wilk test for normality was used to test whether the data were normally distributed for parametric statistical analysis. If data violated the assumption of normality, a Box-Cox transformation was used so that the assumption of normality was met. All data were analyzed using independent sample t-tests and presented in the form

mean ± standard error (SEM) unless otherwise stated. Data is visually portrayed using box plots. The box plots depict the inter-quartile range and 10th and 90th percentiles with the mean represented by +. Pearson correlation coefficients were calculated to assess the direction and strength of association among selected variables. The alpha was set *a priori* at $p < 0.05$. Stata 10.1 and Prism 5 statistical package was used for data analysis.

Table 3. Summary of the measurements performed.

Group	Muscle	Measure
1	Left soleus	In vitro contractile function
		Myosin heavy chain composition
	Right soleus	Protein expression levels:
		- Antioxidant
		- Oxidative capacity
		- Oxidative injury
		Global gene expression
	Gastronemius	Hydrogen peroxide content
2	Flexor Digitorum Brevis	Oxidant production
		SOD1 expression
		Fiber morphology
	Soleus	Cross-sectional area

RESULTS

Animal and soleus muscle mass characteristics

Age and body mass of animals utilized for these experiments are presented in Table 4. Age and body mass for the first group of animals was similar between groups (p=0.90 and p=0.28, respectively). For the second group of animals, age (p=0.55) was similar between groups but the Ts65Dn mice weighted significantly less than WT (p=0.02).

Soleus muscle characteristics are presented in Table 5. Soleus muscle mass and muscle mass: body weight ratios were similar between groups (p=0.97 and p=0.36, respectively). Optimal length and predicted cross-sectional area of soleus muscles utilized for contractile experiments were similar between groups (p=0.15 and p=0.81, respectively). The total number of fibers in the soleus muscles were also similar between groups (n=3/group; p=0.38).

SOD1 over-expression was not associated with skeletal muscle oxidative stress under basal conditions

The over-expression of SOD1 has been strongly implicated as one of the possible causes of oxidative stress in DS (32, 193). SOD1 can lower superoxide radical levels by catalyzing its conversion to oxygen and hydrogen peroxide (31). Excess production of hydrogen peroxide, however, could potentially lead to reaction with transition metals producing damaging radicals if not fully compensated by the up-regulation of other key antioxidant enzymes, specifically CAT and GPX1. As anticipated, SOD1 protein expression was higher in Ts65Dn soleus by 25% (p=0.01), however CAT (p=0.53) and

GPX1 (p=0.55) protein expression were similar between groups (Figure 6). Furthermore, protein levels of SOD2 were also similar between groups (p=0.96; Figure 6).

Oxidative stress has been associated with an increase in the production of oxidants and increased markers of oxidative injury (41). We assessed two well-known markers of oxidative injury (4-HNE and protein carbonyls); protein carbonyls were 20% higher in Ts65Dn soleus (p=0.02; Figure 7), whereas 4-HNE was similar between groups (p=0.39; Figure 7). We next addressed whether Ts65Dn muscle exhibited a greater level of basal oxidant production. The hypothesis that Ts65Dn muscle would produce more oxidants was based on previous findings demonstrating increased oxidant production in non-muscle tissue from both persons with DS, and the Ts65Dn mouse (42, 56). Thus we chose to assess oxidant production in isolated, adult single skeletal muscle fibers from the FDB using the 2',7'-dichlorodihydrofluorescein assay. The advantages of this technique are that oxidant production is measured in real-time and the measurement avoids the contribution from non-muscle cells. DCF emissions from single skeletal muscle fibers were similar between groups (p=0.38; Figure 8). Likewise, the assessment of hydrogen peroxide levels by Amplex Red in gastrocnemius homogenate was similar between groups (p=0.48; Figure 9).

The relationship between DCF emissions and SOD1 expression was assessed in single skeletal muscle fibers. Fibers were probed for SOD1 following the DCF experiment. As expected, SOD1 expression was higher in Ts65Dn fibers (186%; p=0.00; Figure 10). There was a significant inverse correlation between SOD1 expression and DCF emission in WT fibers (r=-0.72; p=0.01; Figure 11). However, this relationship did not exist in Ts65Dn fibers (r=0.18; p>0.05).

Ts65Dn soleus displays muscle weakness following fatiguing contractions

DS is associated with a number of phenotypic alterations that include hypotonia and low muscle strength, which directly and negatively impacts these individual's ability to perform activities of daily living (6, 7, 14, 19, 20). Thus, we sought to determine whether the Ts65Dn mouse also exhibits evidence of muscle dysfunction. Twitch and tetanus soleus contractile properties are presented in Table 6 and were similar between groups. The force frequency response is presented in Figure 12. The area under the curve for absolute force (p=0.58), relative force (% of P_o) (p=0.45), and stress (p=0.71) were similar between groups.

The response of the soleus muscle to repeated activation and recovery is presented in Figure 13. Fatigue progressively developed in the muscles as evidenced by the progressive drop in the active force generated during the stimulation protocol. The resting force of the muscles gradually increased for both groups, indicating the inability of the muscles to fully relax during the protocol. No difference in the area under the curve for the absolute force (p=0.70), resting absolute force (p=0.49), and percent of initial stress (p=0.58) was observed between groups. Following the fatigue protocol, the muscles gradually recovered as indicated by the increase in the active force, as well as gradual decrease in the resting force. The area under the curve for absolute force was similar between groups (p=0.49), but the area under the curve for resting absolute force was higher in Ts65Dn than WT soleus muscles (p=0.02). Moreover, the area under the curve for the percent of initial stress was significantly greater for the WT compared to Ts65Dn soleus muscles (p=0.04). These findings indicate that the Ts65Dn soleus muscles show

an impaired recovery response following a bout of fatiguing muscle contractions compared to WT mice.

Soleus myosin heavy chain composition does not explain post-fatigue weakness

Myosin heavy chain content is known to have a significant impact on skeletal muscle function (212). Thus, the composition of myosin heavy chain in the soleus was assessed by immunofluorescence and further confirmed by electrophoresis. We were unable to clearly and consistently separate the Type IIa and Type IIx myosin heavy chain isoforms with the electrophoresis technique, thus we provide a composite percentage for Type IIa/x. Myosin heavy chain composition was similar between groups (Figure 14).

Decreased soleus fiber CSA in Ts65Dn mice

Single fiber cross-sectional area of soleus muscles was quantified from H&E stains in a different and older group of Ts65Dn mice than those used for the contractile experiments (group 2). Analysis of fiber area distribution revealed a leftward shift, indicating a tendency for Ts65Dn soleus to have smaller-sized fibers (Figure 15). Overall, the fibers from Ts65Dn were significantly smaller than WT (1761±365 vs. 1939±283 μm, respectively; p=0.00)

Decrease in myonuclear domain in Ts65Dn single fibers

Skeletal muscle cells are multi-nucleated and each nuclei is transcriptionally active for a certain amount of cytoplasmic volume, which is referred to as myonuclear domain (213). Changes in myonuclear domain can occur due to loss of myonuclei or fiber atrophy. FDB fiber diameter, length, volume, and number of myonuclei are presented in Table 7. Fiber length (p=0.54), diameter (p=0.07), volume (p=0.08), and

number of myonuclei (0.31) were similar between groups. Myonuclear domain was significantly smaller in Ts65Dn FDB fibers compared to WT (p=0.04; Figure 16).

Decreased cytochrome c expression in Ts65Dn muscle

We hypothesized that the development of post-fatigue weakness in Ts65Dn muscle could be attributable, at least in part, to a limitation in mitochondrial function. This postulate was based partly on previous findings that showed: 1) the presence of mitochondrial dysfunction in neural tissue derived from persons with DS (214); 2) reduced exercise tolerance in persons with DS and the Ts65Dn mouse (11, 51); and 3) lower values of basal, whole-body oxygen uptake recorded for Ts65Dn mice compared to WT controls (58). Thus, we determined the protein expression of cytochrome c oxidase subunit II (COX2) as an index of oxidative capacity. COX2 is one of three mitochondrial-encoded subunits with catalytic activity of respiratory complex IV, which is the terminal enzyme complex of the electron transport chain (215). The rationale for selecting COX2 as a marker of oxidative capacity is based on two principal findings: 1) COX2 protein expression responds to changes in training status and aerobic capacity; and 2) protein expression of COX2 are directly correlated with its enzymatic activity (216). We found that soleus of Ts65Dn mice displayed a 22% decrease in cytochrome c oxidase expression (Figure 17). This is consistent with the hypothesis that some degree of mitochondrial impairment may contribute to the post-fatigue muscle weakness.

Microarray Analyses and Interpretation

Effects of trisomy on skeletal muscle gene expression

The Ts65Dn mouse is segmental trisomic for mouse chromosome 16 from ZNF295 to MRP139, which corresponds to roughly 132 out of the 230 of genes in the

human condition (144). There were a total of 94 out of the 132 trisomic genes on the array. At nominal $p < 0.05$, 51 genes were differentially expressed. Thirty-five genes were up-regulated with a mean fold change of 1.76 and 16 genes were down-regulated with a mean change of 1.33 (Table 8).

Conservative gene-by-gene analysis

The global effects of trisomy on skeletal muscle gene expression were determined using microarray analysis. Based on the criteria we designed to greatly minimize type I error, a final gene list was generated using SAM analysis that contained 159 genes. Of these genes, 106 were down-regulated with a mean fold change of 1.6 (range 1.35 to 1.85), and 53 were up-regulated with a mean fold change of 2.1 (range 1.41 to 4.58). Functional categorization of these genes was performed using the National Center for Biotechnology Information and Gene Ontology databases (203). Ninety-seven of these genes had a known function and are presented along with their annotation and fold change in Table 9. The genes with no known function are provided in Table 10. The analysis identified genes with roles in metabolism, neuromuscular transmission, inflammation, muscle differentiation, proteolysis and damage stimulus, skeletal muscle structure and function, and iron metabolism, which are discussed in detail below. A summary of these changes and their effects on Ts65Dn soleus is provided in Table 11.

Microarray results were validated using quantitative real-time PCR for 4 genes (SOD1, Rnf160, App, and GAPDH used as the normalizer). Overall, results of the PCR were consistent with the microarray. In agreement with the array, GAPDH was similar between groups ($p=0.27$). Fold change of SOD1 for Ts65Dn relative to WT was +1.1 and +1.3 for microarray and PCR ($p>0.05$ for both), respectively. Fold change for App in

Ts65Dn relative to WT was +2.4 and +2.5 by microarray and PCR (p<0.05 for both), respectively. Fold change for Rnf160 in Ts65Dn relative to WT was +3.7 and +2.2 for microarray and PCR (p<0.05 for both), respectively. These results provide evidence that the microarray data accurately reflect the gene expression changes in Ts65Dn soleus.

Genes with a role in metabolism

The microarray analysis identified seven genes with putative roles in glucose and lipid metabolism. There were four genes with a possible role in glucose uptake and/or metabolism by skeletal muscle cells, which included MLX interacting protein (Mlxip), trans-acting transcription factor 5 (Sp5), adrenergic receptor alpha 1a (Adra1a), and TBC1 domain family member 1 (Tbc1d1). Mlxip and Tbc1d1 were up-regulated, whereas Adra1a and Sp5 were down-regulated in Ts65Dn soleus. The analysis identified a major regulator of lipid metabolism in skeletal muscle known as sterol regulatory element binding transcription factor 1 (Srebf1), which was down-regulated in Ts65Dn soleus. There were two genes that have putative effects on lipid metabolism, and include tankyrase TRF1-interacting ankyrin-related ADP-ribose polymerase (Tnks) and melanin-concentrating hormone receptor 1 (Mchr1). Tnks was up-regulated, whereas Mchr1 was down-regulated in Ts65Dn soleus.

Mlxip ($\uparrow$[1]) is a member of the basic helix-loop-helix leucine zipper family of transcription factors. The gene has been shown to function as a metabolic sensor in C2C12 skeletal muscle cells by monitoring the level of intracellular glucose-6-phosphate. High levels of glucose-6-phosphate cause Mlxip to shuttle from the mitochondria to the nucleus where it is a transcription factor activator of glycolytic genes, including lactate dehydrogenase A, hexokinase II, and 6-phosphofructo-2-kinase/fructose-2,6-

---

[1] The arrow signifies whether each gene is up- or down-regulated.

biphosphatase 3 (217). Sp5 ($\downarrow$) is a transcription factor of the Sp and is a transcriptional repressor of Sp1 activity (218). Increased cytochrome c expression in C2C12 muscle cells following contractile activity has been shown to be mediated in part by Sp1 (219). Therefore, if Sp5 acted as a transcriptional repressor of Sp1 in skeletal muscle, its reduced expression could lessen Sp5 repression on Sp1 transcriptional activity leading to transcription of Sp1 target genes. However, there is no known role of Sp5 in skeletal muscle.

Mlxip, Adra1a, and Tbc1d1 have putative roles in skeletal muscle glucose uptake. Mlxip ($\uparrow$) is a negative regulator of glucose uptake through its regulation of thioredoxin-interacting protein (220). Adra1a ($\downarrow$) belongs to the G-protein-linked family of receptors. Stimulation of Adra1a by receptor agonist or insulin increases glucose uptake in L6 muscle cells (221). Finally, Tbc1d1 ($\uparrow$) is known as a major player in both insulin- and contraction-induced GLUT4 trafficking in skeletal muscle (222). Phosphorylation of Tbc1d1 by Akt leads to an increased binding of 14-3-3 proteins to Tbc1d1, which enhances the activity of Rab-GTPase-activating proteins. The more active form of Rab-GTPase-activating proteins allows GLUT4 translocation to the cell membrane. Collectively, the genes identified indicate an effect on glucose metabolism and trafficking in Ts65Dn soleus.

Srebf1 ($\downarrow$) is a DNA binding protein that plays a major role in both cholesterol and fatty acid metabolism in liver and adipose tissue (223). The gene may have a similar role in skeletal muscle as a regulator of lipogenesis and triglyceride storage (224). Tnks ($\uparrow$) may have an effect on skeletal muscle lipid metabolism. For example, transgenic mice deficient in Tnks are lean, hyperphagic, and hypermetabolic. In addition, these mice

exhibit an increased gene expression of genes involved in β-oxidation in their skeletal muscle (225). Collectively, the effect of Srebf1 and Tnks could mean suppressed fat production, storage, and metabolism in Ts65Dn soleus.

The role of Mchr1 ($\downarrow$) in skeletal muscle metabolism is not known, however it does have systemic effects on metabolism. Mchr1 is the receptor for melanin-concentrating hormone. Chronic infusion or transgenic over-expression of melanin-concentrating hormone stimulates feeding and increases adiposity, whereas deletion of melanin-concentrating hormone or Mchr1 leads to leanness and increased energy expenditure (226, 227).

Genes with a role in neuromuscular transmission

The microarray analysis identified four genes involved in neuromuscular transmission, which included solute carrier family 18 (vesicular monoamine) member 3 (Slc18a3), intersectin 1 (SH3 domain protein 1A) (Itsn1), amyloid precursor protein (App), and syntaphilin (Snph). Itsn1 and App were up-regulated in Ts65Dn soleus, whereas Slc18a3 and Snph were down-regulated. Slc18a3 ($\downarrow$) is a mediator of acetylcholine transport into synaptic vesicles of presynaptic motor neurons. Synaptic vesicles are replenished through the process of endocytosis, and formed vesicles are refilled with acetylcholine through a process that depends on Slc18a3 (228). Another gene involved in the cycling of synaptic vesicles is Istn1 ($\uparrow$). The gene plays an important role in cycling of synaptic vesicles in neurotransmitter release, possibly by regulating the interaction with the actin cytoskeleton (229).

App ($\uparrow$) is one of the well-known genes shown to be over-expressed in persons with DS, as well as the Ts65Dn mouse, and is often associated with ß-amyloid plaques in

the brain (230, 231). Its role in skeletal muscle is less clear, but is suggested to be a regulator of neuromuscular morphology and physiology (232). For example, transgenic mice lacking App and App-like protein 2 exhibit alterations of pre- and post-synaptic morphology and defective neurotransmitter release. Conversely, App accumulation (over-expression) inhibits innervations in cultured human muscle and transgenic mice over-expressing App display impaired Ca^{2+} release and contractility (233, 234). The analysis identified two additional genes, N-terminal EF-hand calcium binding protein 3 (Necab3) and transthyretin (Ttr), which are involved in App metabolism. Necab3 and Ttr were both down-regulated in Ts65Dn soleus. Necab3 ($\downarrow$) inhibits the association of X11L with amyloid precursor protein (235). X11L suppresses the production of β-amyloid peptides from amyloid precursor protein by associating with its cytoplasmic domain. Ttr ($\downarrow$) is a transporter of thyroxine and retinol-binding protein. It is also commonly found in amyloid deposits where it is thought to have anti-amyloidogenic effects (236, 237).

Snph ($\downarrow$) has been shown to play a crucial role in synaptic function by controlling mitochondria mobility in axons. Nerve terminals have high-energy demands and require a large supply of ATP to control Ca^{2+} levels. Snph regulates mitochondria density in axons by acting as a receptor for docking/anchoring mitochondria in the synaptic knob (238).

Genes with a role in inflammation

The microarray analysis identified three genes involved in inflammation, which included, CD276 antigen precursor (Cd276), tumor necrosis factor alpha-induced protein 8-like 2 (Tnfaip8l2), and complement component 3a receptor 1 (C3ar1). Cd276 and Tnfaip8l2 were down-regulated, whereas C3ar1 was up-regulated in Ts65Dn soleus. Cd276 ($\downarrow$) and Tnfaip812 ($\downarrow$) are negative regulators of immune function. Cd276 is

undetectable in normal muscle fibers but is up-regulated in patients with inflammatory myopathies where it serves to blunt CD8+ T cell-specific lysis (239). While the role of Tnfaip8l2 in skeletal muscle is unclear, it does display detectable levels of expression in skeletal muscle (240). The gene is proposed to be a negative regulator of immune function by inhibiting activation of activating protein-1 and nuclear factor-κB (241). Lastly, C3ar1 (↑) is an important receptor in triggering the immune response. Up-regulation of this receptor in skeletal muscle occurs by inducing insulin resistance through high fat feeding (242).

Genes with a role in muscle differentiation/regeneration

The microarray analysis identified six genes involved in muscle differentiation/regeneration, which included netrin 3 (Ntn3), RB1-inducible coiled-coil 1 (Rb1cc1), kinase insert domain protein receptor (Kdr), nephrosis 1 homology nephrin (human) (Nphs1), numb gene homology (Drosophila) (Numb), and avian reticuloendotheliosis viral oncogene related B (RelB). Ntn3, Rb1cc1, Nphs1, and RelB were down-regulated, whereas Kdr and Numb was up-regulated in Ts65Dn soleus.

Five of these genes play a role in the formation of myotubes during muscle cell differentiation. Ntn3 (↓) is a member of the netrin family of proteins that associate with cell membranes and the extracellular matrix (243). Recombinant Ntn3 stimulates the formation of myotubes during C2C12 muscle cell differentiation. Rbc1cc (↓) is also a determinate of differentiation in C2C12 muscle cells, as interference RNA mediated knockdown of Rbc1cc blocks differentiation of C2C12 myoblasts (244). Nphs1 (↓) is a well-known renal protein involved in the maintenance of the kidney filtration barrier; however, it was recently shown that Nphs1 is necessary for myoblast fusion during

differentiation (245). RelB ($\downarrow$) is one of five gene members of the NF-κB family, which is a component of alternative NF- κB signaling (246). The alternative NF-κB pathway may be involved in skeletal myogenesis and regeneration (246). This pathway is dispensable during myotube formation, but is induced in the later stages of differentiation where it functions to promote mitochondrial biogenesis (246). Numb ($\uparrow$) is a negative regulator of Notch signaling in skeletal muscle that plays an important role in skeletal muscle development and regeneration (247). Cessation of Notch activity is correlated with differentiation of cultured myoblasts. Collectively, these genes participate in muscle differentiation but a direct role of these genes in muscle regeneration has yet to be defined. One identified gene that may play a direct role in muscle regeneration is Kdr ($\uparrow$), which is a receptor for vascular endothelial growth factor (VEGF); an important gene involved in angiogenesis. VEGF and it receptors Kdr and Flt-1 are expressed in regenerating skeletal muscle fibers following ischemia-, chemically-induced or freeze-induced muscle damage (248).

Genes with a role in proteolysis and damage stimulus

The microarray analysis identified nine genes involved in proteolysis and response to cellular damage, which included ring finger protein 160 (Rnf160), ariadne homolog 2 (Arih2), serine/threonine kinase 4 (Stk4), replication protein A2 (Rpa2), rap1 interacting factor 1 homology (yeast) (Rif1), NIMA (never in mitosis gene a)-related expressed kinase 1 (Nek1), ectonucleotide pyrophosphatase/phosphodiesterase 7 (Enpp7), fos-like antigen 1 (Fosl1), and transmembrane BAX inhibitor motif containing 6 (Tmbim6). Rnf160, Stk4, Rpa2, Rif1, Nek1, and Tmbim6 were up-regulated, whereas Arih2, Enpp7, and Fosl1 were down-regulated in Ts65Dn soleus.

Rnf160 (↑) and Arih2 (↓) are E3 ubiquitin ligases that label proteins with ubiquitin, which targets them for degradation by the proteasome (249, 250). Stk4 (↑) is a regulator of neuronal cell death. Stk4 mediates oxidative stress induced neuronal cell death by phosphorylating the transcription factor FOXO1 (251). In skeletal muscle FOXO1 can directly up-regulate muscle-specific ubiquitin ligases which leads to muscle atrophy (252).

Rpa2 (↑), Rif1 (↑), and Nek1 (↑) are involved in the response to DNA damage. Rpa2 is involved in the response to DNA damage stimulus and repair (253). Rif1 is also involved in the DNA damage stimulus where it associates with stalled replication forks (254). Nek1 is required for DNA damage checkpoint control and repair (255). In addition, Nek1 has a novel role in apoptosis. Nek1 regulates cell death by closing the voltage dependent anion channel 1, which prevents pre-apoptotic factors from entering the cytoplasm and mediating apoptotic pathways (256).

Enpp7 (↓), Fosl1 (↓), and Tmbim6 (↑) play a role in oxidant production and the response to oxidative stress. Enpp7 has a number of functions in the human digestive system, which includes hydrolyzing sphingomyelin to generate ceramides (257). It has been shown recently that the production of ceramides in skeletal muscle increases oxidant production in muscle cells, depresses specific force of unfatigued muscle, and accelerates the fatigue process (258). If Enpp7 has the same function in skeletal muscle, the decrease in transcript levels and protein expression may lead to a decrease in the processing of sphingomyelin to ceramide, which could lessen the oxidant load on the muscle cell. Fosl1 is a DNA binding protein that acts as an antagonist to NF-E2-related nuclear factor signaling (Nrf1 and Nrf2). Nrf1 and Nrf2 bind to the antioxidant response element (ARE)

and mediate the induction of antioxidant enzymes, while Fosl1 binds to ARE and negatively relates ARE-mediated gene expression (259). Lastly, Tmbim6 is an anti-apoptotic protein located in the endoplasmic reticulum membrane. Tmbim6 is thought to protect cells from endoplasmic reticulum induced oxidative stress by effecting the regulation of heme oxygenase-1 (260)

Genes with a role in skeletal muscle structure and function

The microarray analysis identified nine genes involved in skeletal muscle structure and function, which included tropomodulin 1 (Tmod1), phosphoglucomutase 5 (Pgm5), moesin (Msn), laminin gamma 1 (Lamc1), myosin light polypeptide 6B (Myl6b), leprecan-like 1 (Leprel1), secretogranin V (Scg5), annexin A6 (Anxa6), and tescalcin (Tesc). Tmod1, Pgm5, Lamc1, Myl6b, Anxa6, and Msn were up-regulated, whereas Tesc, Leprel1, and Scg5 were down-regulated in Ts65Dn soleus.

Tmod1 (↑) is one of four isoforms of tropomodulins that function as capping proteins that modulate thin filament length by controlling actin dynamics at pointed ends. It has been shown using transgenic mice that ablation of Tmod1 results in depressed isometric stress production during muscle contraction and a shift to a faster fiber type distribution (261). Anxa6 (↑) has a variety of functions in muscle. For example, in cardiomyocytes, Anxa6 is an important regulator of Ca^{2+} flux (262, 263). Transgenic mice over-expressing Anxa6 have lower basal levels of intracellular free Ca^{2+} and a reduced rise in Ca^{2+} following depolarization, whereas Anxa6 knockout increases shortening velocity and rate of contraction and relaxation in isolated cardiomyocytes (262). Thus, Anxa6 plays an important role in normal Ca^{2+} homeostasis by effecting membrane ion exchange. Another gene that may affect Ca^{2+} homeostasis is Scg5 (↓),

which facilitates the transport and activation of Pkd2. Pkd2 has a role in heart muscle physiology as a negative regulator of ryanodine-sensitive calcium-release. Pkd2 co-immunoprecipitates with the cardiac ryanodine receptor and inhibits its activity in the presence of calcium (264). Tesc ($\downarrow$) is a newly identified gene that inhibits the activity of the Na^+/H^+ exchanger, which plays a crucial role in muscle pH homeostasis (265, 266).

Pgm5 ($\uparrow$) is structurally associated with dystrophin and utrophin at the muscle plasmalemma (267). While its functions are unknown, Pgm5 has been suggested to exhibit a structural, rather an enzymatic role in skeletal muscle. Msn ($\uparrow$) is part of the ERM family and consists of three closely related proteins, erzin, radixin, and Msn. These proteins play a role in organizing membrane domains through their ability to interact with transmembrane proteins and the cytoskeleton (268). In skeletal muscle, these proteins are putatively associated with talin but their functional role in skeletal muscle is unclear. Leprel1 ($\downarrow$) is a gene of the Leprecan family of proteoglycans that is expressed in skeletal muscle (269). Leprel1 is responsible for hydroxylation of collagen IV (270), which is a major component of the basement membrane in skeletal muscle (271). Lamc1 ($\uparrow$) is one of three subunits that comprise laminin 111. Laminin 111 is expressed during embryonic development in human and mice skeletal muscle but not during adulthood. It was shown that injection of laminin-111 protein into the Mdx mouse model of Duchenne muscular dystrophy increased expression of alpha7-integrin which improves muscular pathology in the Mdx mouse (272). Myl6b ($\uparrow$) has a role in smooth muscle contraction, but its role in skeletal muscle physiology is unknown.

Gene with a role in iron metabolism

Transmembrane serine protease 6 (Tmprss6) which was down-regulated in Ts65Dn soleus is a suppressor of hepcidin, which is a key component of systemic iron metabolism (273). Hepcidin is a circulating peptide hormone that regulates the entry of iron into plasma, however its role in skeletal muscle is not fully elucidated (274). Ferroportin, which is an iron exporter, can be bound by hepcidin causing its degradation. Reduced expression of Tmprss6 could facilitate ferroportins degradation via unsuppressed hepcidin leading to increased cytosolic iron (274).

Pathway analysis

The results presented above were based on stringent criteria to greatly limit type I error, however, more subtle differences in gene expression may have important effects, particularly if multiple genes for one pathway are affected. To this end, we performed pathway analysis using DAVID with an expanded list of the most differentially expressed genes (204). This list included a total of 803 genes, 68 of which were down-regulated and 735 were up-regulated. Seven hundred and forty-five of the 803 genes were identified by the DAVID database and were used to perform functional annotation clustering to identify over-represented pathways. Results of this analysis are presented in Table 12 and a brief summary of relevant pathways follows below.

Twenty-eight clusters were formed with enrichment scores ranging from 1.4 to 6.5. Cluster 1 with an enrichment score of 6.5 shows the most prominently affected pathways were those involved in proteolysis. The second most affected pathways represented in clusters 2, 3, 5, 9, and 16 included genes that interact or comprise the cytoskeleton. Cluster 4 included a number of terms that included processes involved in

nucleotide binding and kinase activity. Cellular components not bound by a lipid bi-layer, which include ribosomes, the cytoskeleton, and chromosomes, were represented in cluster 5. Cluster 7 was comprised of genes associated with nuclear content other than the chromosome or nucleolus, and cluster 18 comprised genes involved in structural constituents of the nuclear pore. Cluster 10 is comprised of annexins and associated genes. Annexins are a family of Ca^{2+}- and phospholipid binding proteins, but have a variety of emerging functions (275). Specifically, annexins play an important role in repairing sarcolemma damage (276). DNA repair and cellular response to stress are the terms that comprise cluster 12. Cluster 14 comprises genes involved in protein transport, and transport of substances into the nucleus. Terms associated with skeletal muscle differentiation comprise cluster 15 and 20. Finally, cluster 22 comprised genes involved in the biosynthetic process of nucleotide metabolism. Also included in this cluster was ATP biosynthetic process, which involves chemical process and reactions that result in formation of ATP. Genes contained within this term included the Na^+/K^+ ATPase transporter, H^+ transporter associated with lysosomes, and the predicted gene of the ATPase synthase of complex V in the mitochondria.

MicroRNA pathway analysis

MicroRNA's (miRNAs) are an emerging class of molecules that play a fundamental role in mediating the stress response to changes in contractile activity and disease states in skeletal muscle (205, 206). Thus, we hoped to gain novel insight into the regulatory pathways regulated by miRNA in Ts65Dn muscle. miRNA were identified from both the conservative and pathway gene lists, which included a total of 8 miRNA that are represented in Table 13, along with their chromosome location and fold change.

Seven of the eight miRNAs were down-regulated in Ts65Dn soleus. DIANA-mirPATH was used to collectively map predicted targets of these miRNA using TargetScan 5 to KEGG pathways (207). The results of this analysis are presented in Table 14. Importantly, a number of pathways relevant to skeletal muscle biology were identified that included: the Wnt, mTOR, ErB, and insulin signaling pathways; regulation of actin cytoskeleton; type 2 diabetes mellitus; ubiquitin mediated proteolysis; and the phosphatidylinositol signaling system. The most affected pathway was the Wnt signaling pathway with 39 genes targeted by the list of miRNAs.

DISCUSSION

Muscle weakness contributes to mobility limitations in persons with DS, and impaired mobility is predictive of mortality in this population (14, 26, 61). To date, there have been no systematic efforts to identify potential mechanisms of muscle weakness in persons with DS. The purpose of the current experiments was to perform a functional characterization of skeletal muscle from Ts65Dn mice, with the intent to reveal potential mechanisms of DS-associated muscle weakness. Several key findings emerged from these experiments that include: 1) SOD1 was over-expressed in skeletal muscle of Ts65Dn mice; 2) SOD1 over-expression was not associated with oxidative stress; 3) muscle from Ts65Dn mice failed to recover from fatiguing contraction to the same degree as muscle of wild-type mice, which is an indication of impaired muscle performance; and 4) global gene expression patterns revealed significant alterations in numerous cell signaling pathways, which provide insight into the potential mechanisms of muscle dysfunction in DS. A discussion of these key findings is presented in the following sections.

Skeletal muscles from Ts65Dn mice over-express SOD1

SOD1 is located in the cytosol and inter-membrane space of the mitochondria and functions to dismutate superoxide radicals to hydrogen peroxide (41). Persons with DS, and the Ts65Dn mouse, could over-express SOD1 because the gene is present in triplicate (137, 144). The "gene dosage effects" hypothesis predicts that the increased gene copy number leads to an increase in gene products. At the cellular level, this signifies that over-expression of SOD1 may lead to increased production of hydrogen peroxide. If hydrogen peroxide production outpaced its removal by CAT and GPX, this could

contribute to the development of oxidative stress. This notion is supported by findings showing over-expression of SOD1 without a comparable increase in the levels of CAT and GPX in non-muscle tissues from persons with DS (69, 71). In addition, neurons and astrocytes isolated from persons with DS and hematopoietic stem cells from Ts65Dn mice exhibit elevated oxidant production (42, 56). Thus, we hypothesized that skeletal muscle of Ts65Dn mice would over-express SOD1 and demonstrate oxidative stress.

As anticipated, SOD1 expression was higher in Ts65Dn soleus by 1.3-fold, but below what is predicted by gene dosage (i.e., 1.5-fold). Conversely, SOD1 expression in Ts65Dn FDB fibers was 3-fold higher than WT fibers, which is much higher than what is predicted by gene dosage. The differing expression levels between the two muscles could be explained by the method used to examine SOD1 (Western blot vs. immunofluorescence), the muscle analyzed [slow-twitch (soleus) vs. fast-twitch (FDB)], and part of the muscle analyzed (soluble fraction of muscle homogenate vs. single whole fibers). This said, variability in the over-expression of SOD1 in various tissues has been reported in persons with DS and Ts65Dn mice. For example, the level of SOD1 over-expression varies within different brain regions in persons with DS (71). Similar findings have been reported in Ts65Dn mice, as the level of SOD1 over-expression varies between tissues (161). Also, only 37% of genes across 5 different tissues in Ts65Dn mice were expressed at the theoretical value of 1.5 fold (161).

There was also no change in the expression levels of CAT, GPX1, or SOD2. This finding is consistent with results showing transgenic over-expression of SOD1 does not affect CAT or SOD2 expression in the mouse diaphragm, and that over-expression of a human SOD1 transgene in myoblasts does not affect GPX or CAT activities (126, 132).

Overall, these findings are consistent with other studies showing over-expression of SOD1 and normal levels of CAT and GPX1 in non-muscle tissues from persons with DS (69, 71).

Skeletal muscle from Ts65Dn mice does not exhibit oxidative stress

Several non-muscle tissues from humans and mice with DS have demonstrated the presence of oxidative stress (42-45, 56). However, our findings indicated skeletal muscle oxidant production was similar between the Ts65Dn and WT mice. Although this is surprising, one possible explanation may be the level of SOD1 over-expression was not of sufficient magnitude to elevate oxidant production beyond what was observed in WT fibers. Experiments conducted using primary muscle cell cultures derived from SOD1 over-expressing mice support this hypothesis (132). Myoblast lines were derived from WT mice and mice hemi- or homozygous for a human SOD1 transgene with SOD1 activities 3- and 5-fold higher than WT, respectively. These authors were able to demonstrate that a 3-fold increase in SOD1 activity only modestly modulated superoxide radical and hydrogen peroxide levels, and it required a 5-fold change to significantly alter levels within the muscle cells. The level of SOD1 expression was 3-fold higher in Ts65Dn FDB fibers compared to WT fibers, which is similar to the expression of SOD1 in hemizygous myoblasts, which likely explains why Ts65Dn FDB fibers did not exhibit elevated oxidant production. In support of these findings, we showed that hydrogen peroxide content measured using the Amplex Red assay of gastrocnemius muscles was similar between groups. In summary, SOD1 over-expression does not affect basal oxidant production in Ts65Dn muscle. However, since both muscle contraction and temperature

affect oxidant production, future studies could examine the effect of these variables on oxidant production in Ts65Dn muscle (187).

To further assess the impact of SOD1 over-expression on the development of oxidative stress in Ts65Dn muscle, we examined the expression levels of 4-HNE and protein carbonyls, which are markers of lipid peroxidation and protein oxidation, respectively. Levels of 4-HNE were similar between groups, but protein carbonyls were elevated in Ts65Dn soleus by 20%. A possible explanation for the selective accumulation of protein carbonyls is two-fold. First, in spite of the fact that components of proteolytic pathways were up-regulated, as indicated by the microarray analyses, the efficiency of these processes may be compromised in DS tissue. For example, the chymotrypsin-like proteolytic activity of the proteasome is reduced in the cerebellum of Ts65Dn mice (277). Thus, the signal for protein degradation is active in Ts65Dn muscle, but the efficiency of the process may be compromised. The net effect would be the accumulation of oxidized proteins, since the proteasome is primarily responsible for degrading oxidized proteins (278). If proteasome activity is lower in Ts65Dn muscle, this bears the question why wasn't 4-HNE higher in Ts65Dn soleus? One possible reason is that 4-HNE is preferentially degraded by the lysosomal pathway (279). Therefore, if proteasome activity is indeed depressed in Ts65Dn muscle, the lysosomal pathway could selectively degrade 4-HNE. Collectively, our results do not support the hypothesis that over-expression of SOD1 leads to oxidative stress in Ts65Dn muscle. Furthermore, increased levels of protein carbonyls may be the result of a decrease in the degradation of oxidized proteins.

SOD1 expression is associated with oxidant production in wild-type mice

A strong inverse relationship between SOD1 expression and oxidant production was observed in the FDB fibers of WT mice (p=-0.72). The relationship between SOD1 and oxidant production in Ts65Dn fibers was weak (p=0.18), suggesting oxidant production was independent of SOD1 expression. The theoretical model proposed by Xing and colleagues can be used to explain the observed relationships (Figure 18) (132). The model proposes that WT muscle falls on the downward slope of the inverted bell-shaped curve, which means that increases in SOD activity reduces cellular susceptibility to oxidative stress by decreasing oxidant production. Thus, a negative, inverse relationship between SOD1 expression and oxidant production would be expected in WT FDB fibers. The model can also be used to explain the lack of a relationship in Ts65Dn FDB fibers. For example, the model proposes that smaller increases in SOD1 activity cause both an increase in dismutation of superoxide radical and production of hydrogen peroxide. Thus, Ts65Dn FDB fibers could be near the nadir of the curve, and if this were the case, a lack of relationship between oxidant production and SOD1 expression would not be surprising. Collectively, these studies suggest that the expression of SOD1 is tightly coupled to oxidant production in WT FDB fibers.

Ts65Dn soleus does not exhibit impaired isometric force

Persons with DS exhibit severe reductions in muscle strength (15, 20). Thus, we hypothesized that Ts65Dn muscle would exhibit deficits in force-generating capacity in the non-fatigued state. However, isometric contractile properties were similar between groups. This finding is consistent with the similarities in soleus muscle mass, myosin heavy chain composition, predicted cross-sectional area, and the total number of fibers

between groups. However, quantification of single fiber CSA of the soleus revealed a leftward shift in the fiber area distributions, which indicated a greater number of smaller-sized fibers in Ts65Dn muscle. It is important to draw attention to the difference in age between the animals that were assessed for force, which were younger than those used to assess muscle morphology (6 vs. 13 months). Due to limitations in tissue availability, CSA was originally assessed on the contracted soleus. However inspection of the muscle sections showed evidence of fiber damage from the contractile protocol (e.g., presence of very large fibers) that was independent of genotype. Thus, we chose to assess soleus CSA in the second group of animals that were not subjected to the contractile protocol. Therefore, the discrepancy between force and fiber size could be explained by age. It is possible that changes in myofiber CSA occur at a younger age in Ts65Dn than WT mice. We believe it is unlikely that CSA was different in the group of animals subjected to the contractile protocol given that soleus muscle mass, predicted muscle cross-sectional area, force output, and myosin heavy chain composition were all similar between groups. Further study of the effects of age on skeletal muscle function and morphology in Ts65Dn mice is warranted.

There are other factors that could explain the lack of a force deficit in Ts65Dn muscle. In particular, our in vitro muscle preparation eliminated factors related to neuromuscular transmission that are important in vivo. The microarray analysis identified a number of differentially regulated genes that are involved in neuromuscular transmission. Thus, it is possible that a principal defect in Ts65Dn muscle lies at the neuromuscular junction. In support of this hypothesis, the morphology of neuromuscular junctions from tongue skeletal muscle fibers are abnormal in persons with DS (280).

Thus, using a muscle preparation where the nerve supply is intact and directly stimulated is of clear interest and could potentially reveal alterations in neuromuscular transmission in Ts65Dn muscle.

Ts65Dn soleus exhibits post-fatigue muscle weakness

Muscle fatigue is characterized by impairment in muscle force production that results from continuous muscle activity. Ts65Dn soleus muscles did not exhibit greater fatigability as hypothesized; however, following the exercise stress there was evidence of post-fatigue weakness. Ts65Dn soleus muscles recovered to only 54% of the initial stress at the end of the recovery period compared to 61% for WT. In addition, examination of the resting absolute force values (measured between contractions) during the recovery period indicated that the Ts65Dn soleus did not exhibit similar decreases in resting absolute force compared to WT, which indicates an impaired ability of the muscle to relax.

Muscle fatigue is associated with a number of biochemical changes, such as depletion of ATP and phosphocreatine, increases in H^+, inorganic phosphate, and lactate that can subsequently effect muscle force recovery following fatigue (97). We hypothesized that a limitation in mitochondrial function may underlie the failure of Ts65Dn soleus to recover to the extent of WT muscle following fatiguing contractions. In support of our hypothesis, cytochrome c oxidase expression levels were 22% lower in Ts65Dn soleus. This finding suggests that an impairment of oxidative phosphorylation may underlie the muscle dysfunction observed in the Ts65Dn mouse, which is consistent with their lower basal VO_2 (58). This is particularly relevant because mitochondrial dysfunction has been reported in persons with DS (214). Moreover, microarray analyses

identified alterations in pathways involved in glucose and fat metabolism, and ATP biosynthesis that could also be indicative of an underlying mitochondrial limitation. For example, impaired glucose uptake, utilization, and storage, and enhanced fat storage in skeletal muscle are associated with mitochondrial dysfunction (281, 282).

We report a 30% reduction in the myonuclear domain of FDB fibers from Ts65Dn mice, which could also be related to a limitation in mitochondrial function. The reason for this can be explained by findings from SOD1 knockout mice, which is considered an accelerated model of skeletal muscle aging (119). These mice exhibit significant impairments in muscle mitochondrial function as well as a reduction in total myonuclei and volume in single skeletal muscle fibers. The authors of this work proposed that a reduction in myonuclei significantly limits the cell's ability to synthesize proteins, which leads to mitochondrial dysfunction and reduced energy production. The muscle cell, in an attempt to return to homeostasis, responds by increasing proteolytic activity to reduce cell size. This is also consistent with our observation that proteolytic pathways were significantly up-regulated in Ts65Dn muscle.

Further insight in support of the notion that a limitation in mitochondrial function underlies post-fatigue weakness in Ts65Dn soleus can be explained by the fatigue and recovery response of soleus from mice with knockout of ATP-sensitive K^+ channel (K_{ATP}). K_{ATP} channels are energy sensing channels that are activated at low ATP/ADP ratios, and have been shown to govern the rate and extent of force recovery following fatigue (283). Activation of these channels is considered a protective mechanism to maintain contractile capacity following fatiguing contractile activity by maintaining membrane excitability, decreasing voltage-dependent calcium entry, and the rise in

resting force (283). Soleus muscles from knockout K_{ATP} mice or inhibition of K_{ATP} with glibenclamide, fail to recover to the same extent as WT following fatiguing contractile activity. This is explained in part by the inability to reduce resting force during fatigue and recovery (284, 285). We propose that during the development of fatigue in Ts65Dn soleus, K_{ATP} channels open at an earlier time due to a reduction in ATP/ADP ratio, which would explain the lower resting force during the fatiguing protocol in Ts65Dn soleus (non-significant). However, as the muscle was stressed further towards the later part of fatigue development, resting force gradually increased because all available K_{ATP} channels were activated and this mechanism could no longer compensate for reduced energy production. This resulted in decreased tetanic force and increased resting force during the recovery period.

Our hypothesis that a limitation in mitochondrial function contributes to the impaired recovery response in Ts65Dn soleus bears the question why Ts65Dn soleus was not more fatigable? If in fact Ts65Dn muscle exhibits mitochondrial dysfunction, we would anticipate a decrease in ATP production from oxidative phosphorylation and a greater reliance on glycolysis. The reduced ATP production could impair muscle performance, and this should become particularly evident when the muscle is continually activated.

One possible explanation why Ts65Dn soleus did not exhibit greater fatigability could be the intensity of the stimulation protocol. Repeated activation of muscle can cause impairment in membrane excitability due to alterations in K^+ ion gradients (97). Decreased membrane excitability is a contributing factor to the reduction in force output (~30%) during fatiguing contractions, particularly for in vitro muscle preparations (97).

Thus, excitation failure could mask an underlying metabolic defect during fatigue. This rationale has been proposed previously to explain the similar rates of fatigue in knockout α-actinin-3 and WT muscles, but greater recovery from fatigue in α-actinin-3 deficient muscles (286). Deficiency in α-actinin-3 leads to the development of a more oxidative muscle phenotype that is characterized by enhanced enzyme activity of citrate synthase, succinate dehydrogenase, and cytochrome c oxidase. The α-actinin-3 deficient muscles, however, do not display fatigue resistance compared to WT muscles as expected, but they do exhibit a faster rate of recovery following fatigue. These authors proposed, as we do, that the intensity of the fatigue protocol masked the expected fatigue differences between groups.

Limitations

We acknowledge the following limitations: *First*, we were unable to account for the possibility that congenital heart defects, which are known to occur in the Ts65Dn mouse model of DS, affected skeletal muscle structure and function (153). *Second*, all functional measurements were performed using the soleus, and the results presented cannot be generalized to other muscles, such as fast-muscles, which can be affected differently by myopathy. Moreover, the functional assessment of the soleus was performed in vitro, which excludes factors that are relevant in vivo, such as neuromuscular transmission and blood flow. *Third*, protein content but not enzyme activity was quantified, thus we provide no information on protein function. *Fourth*, due to the limited available tissue, CSA of the soleus was assessed in an older group of animals than those used for contractile measurements. Thus, we provide no data on fiber size in the younger group of animals used for those experiments and can only speculate

that fiber size was similar between groups. *Finally*, while we suggest that a limitation in mitochondrial function could explain post-fatigue weakness in Ts65Dn soleus, we did not provide a direct measure of mitochondrial function.

Significance of findings

Skeletal muscle function in the Ts65Dn mouse model of DS has not been examined previously and there has been no systematic effort made to establish an animal model to explore the muscle dysfunction that is widely reported in persons with DS (18, 20). To our knowledge this is the first functional characterization of skeletal muscle from Ts65Dn mouse. We demonstrated that muscle from Ts65Dn mice exhibits post-fatigue weakness, which may be the result of a limitation in mitochondrial function. Further delineation of muscle dysfunction in the Ts65Dn mouse is warranted, which may ultimately lead to therapies for persons with DS in an effort to improve muscle function and mobility for this population of individuals.

Table 4. Animal characteristics.

Group of animals	Variable	Wild-type	Ts65Dn
1	Number of animals	16	14
	Age (months)	5.6 ± 0.2	5.6 ± 0.2
	Body mass (g)	34.5 ± 1.2	32.6 ± 1.3
2	Number of animals	7	4
	Age (months)	12.9 ± 0.3	12.7 ± 0.3
	Body mass (g)	38.3 ± 1.7	$32.0 \pm 0.2*$

* $p < 0.05$

Table 5. Soleus muscle characteristics.

Variable	Wild-type	Ts65Dn
Mass* (mg)	10.2 ± 0.4	10.2 ± 0.4
Muscle mass: body mass ratio	0.30 ± 0.01	0.32 ± 0.02
L_0 (cm)	1.25 ± 0.02	1.21 ± 0.02
Predicted cross-section area (mm^2)	1.09 ± 0.05	1.11 ± 0.04
Total fiber number	582.6 ± 28.8	550.7 ± 14.2

*Average of the right and left soleus muscles.
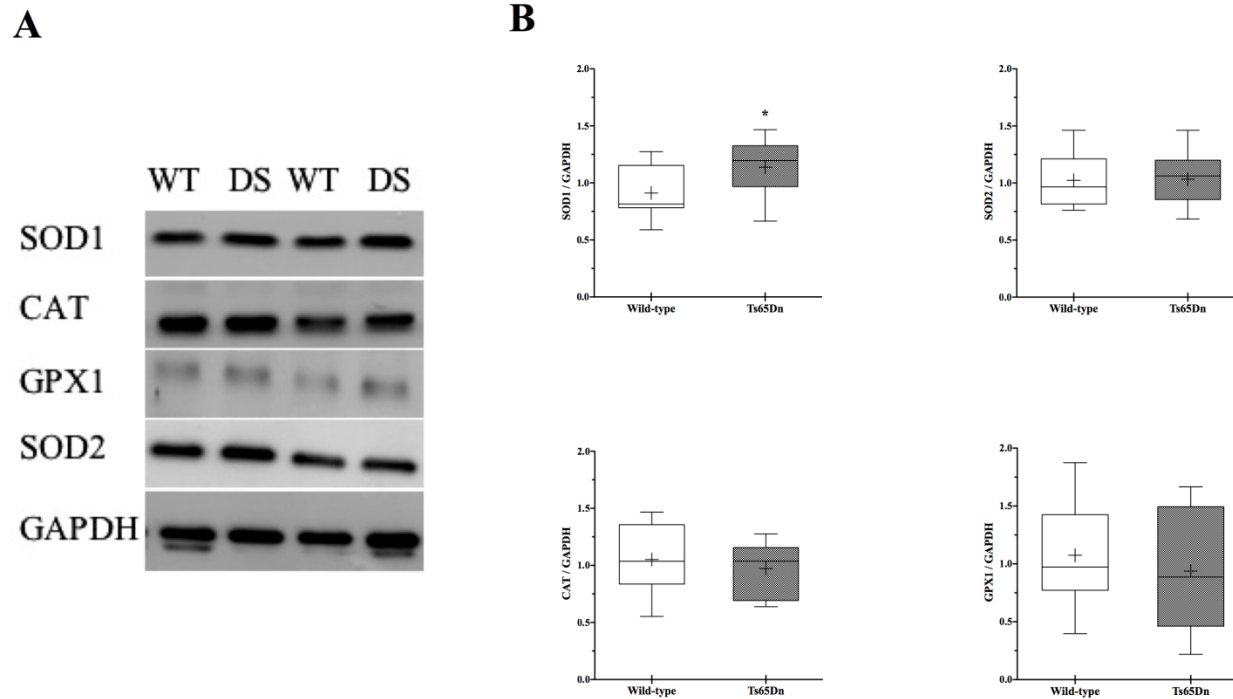
Figure 6. Soleus protein expression of SOD1, CAT, GPX1, and SOD2. Representative Western Blot images of SOD1 (~18 kDa), CAT (~ 62 kDa), GPX1 (22 kDa), and SOD2 (~ 25 kDa) are shown in A. SOD1, CAT, and GPX1 protein bands were normalized to the GAPDH bands shown. SOD2 protein bands were also normalized to GAPDH (bands not shown). In this figure DS refers to Ts65Dn. The arbitrary optical density of SOD1, CAT, GPX1, and SOD2 relative to GAPDH are shown in B. N = 10 animals/group. * Significantly different from WT ($p < 0.05$).
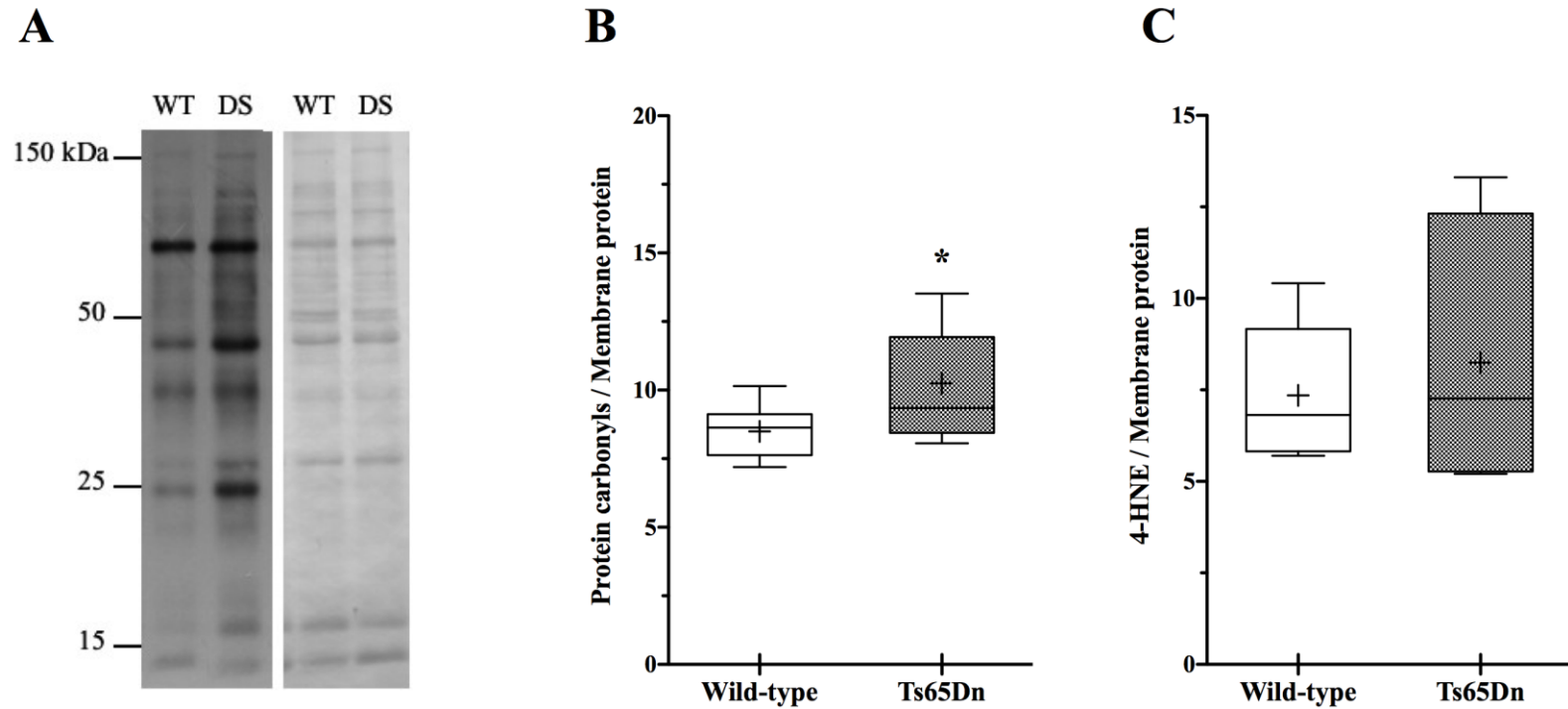
Figure 7. Oxidative injury assessed by protein carbonyl and 4-HNE in soleus. Representative Western Blot of protein carbonyls (A, left) and Coomassie stained membrane (A, right). In this figure DS refers to Ts65Dn. Arbitrary optical density of protein carbonyl (B) and 4-HNE (C) relative to membrane protein. N=10 animals/group for WT for protein carbonyls and 4-HNE. N=9 Ts65Dn animals for protein carbonyls and n=8 for 4-HNE. * Significantly different from WT ($p < 0.05$).
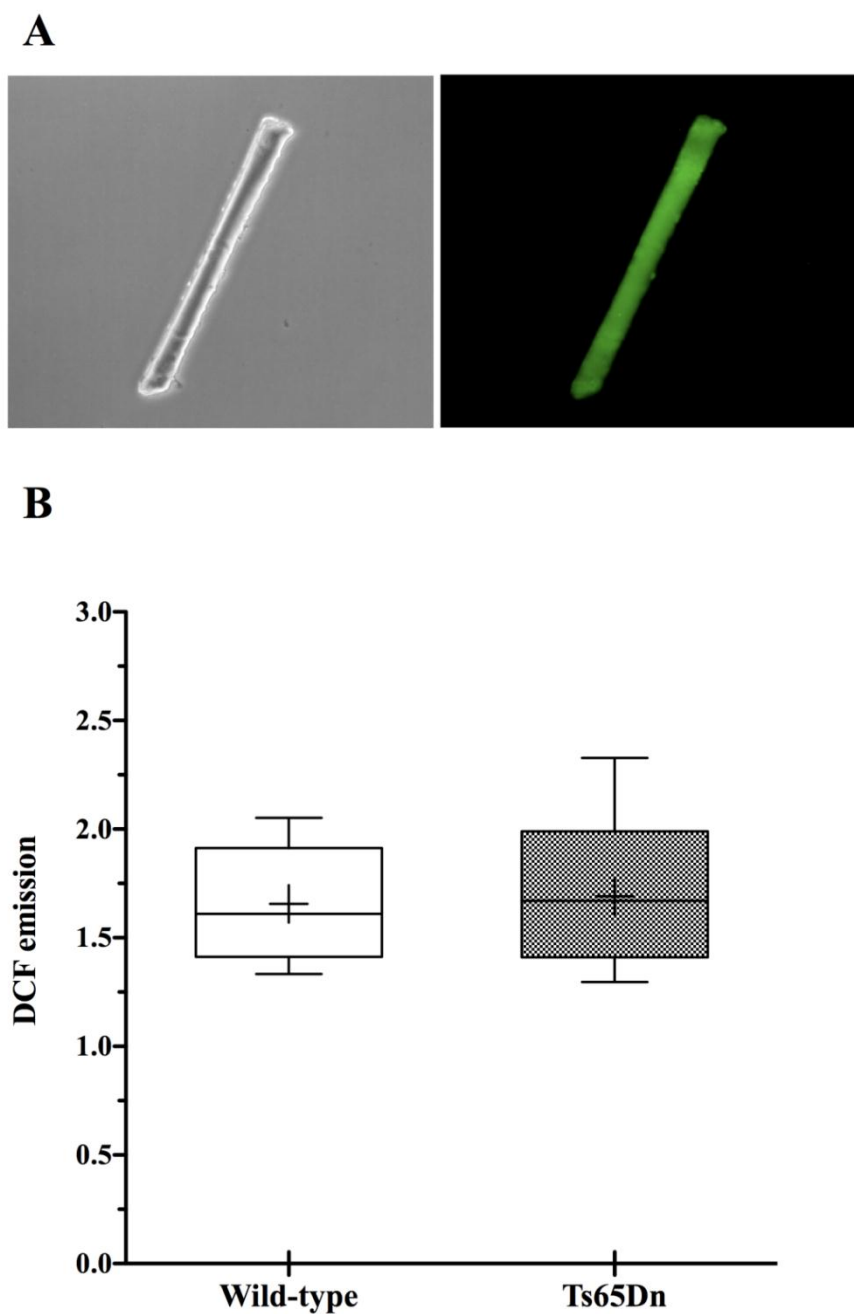
Figure 8. Oxidant production assessed in isolated adult skeletal muscle fibers. Representative bright field (A, left) and DCF emission (A, right) images are shown. DCF emission at 15 minutes expressed relative to time 0 (B). N=4 animals/group and n=2-6 fibers/animal. 16 total fibers from Ts65Dn and 18 from WT.
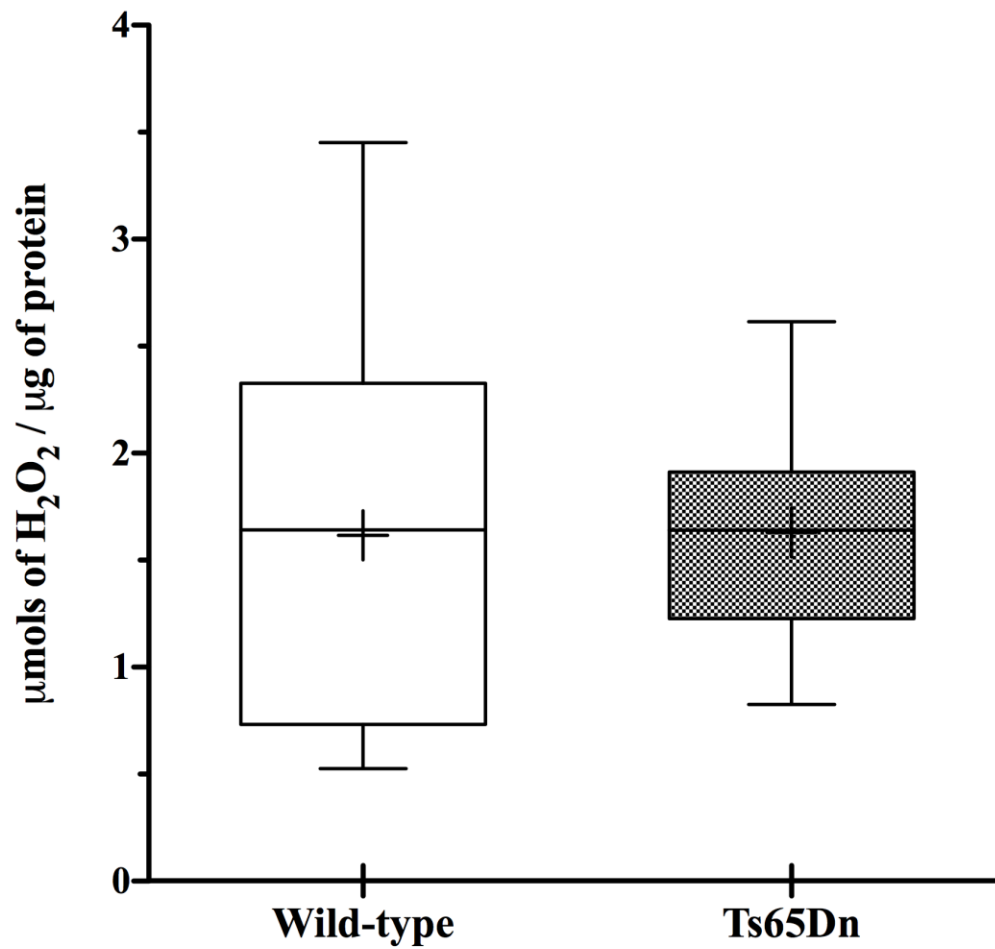
Figure 9. Hydrogen peroxide content of gastrocnemius assessed using Amplex Red. N=10 animals/group.
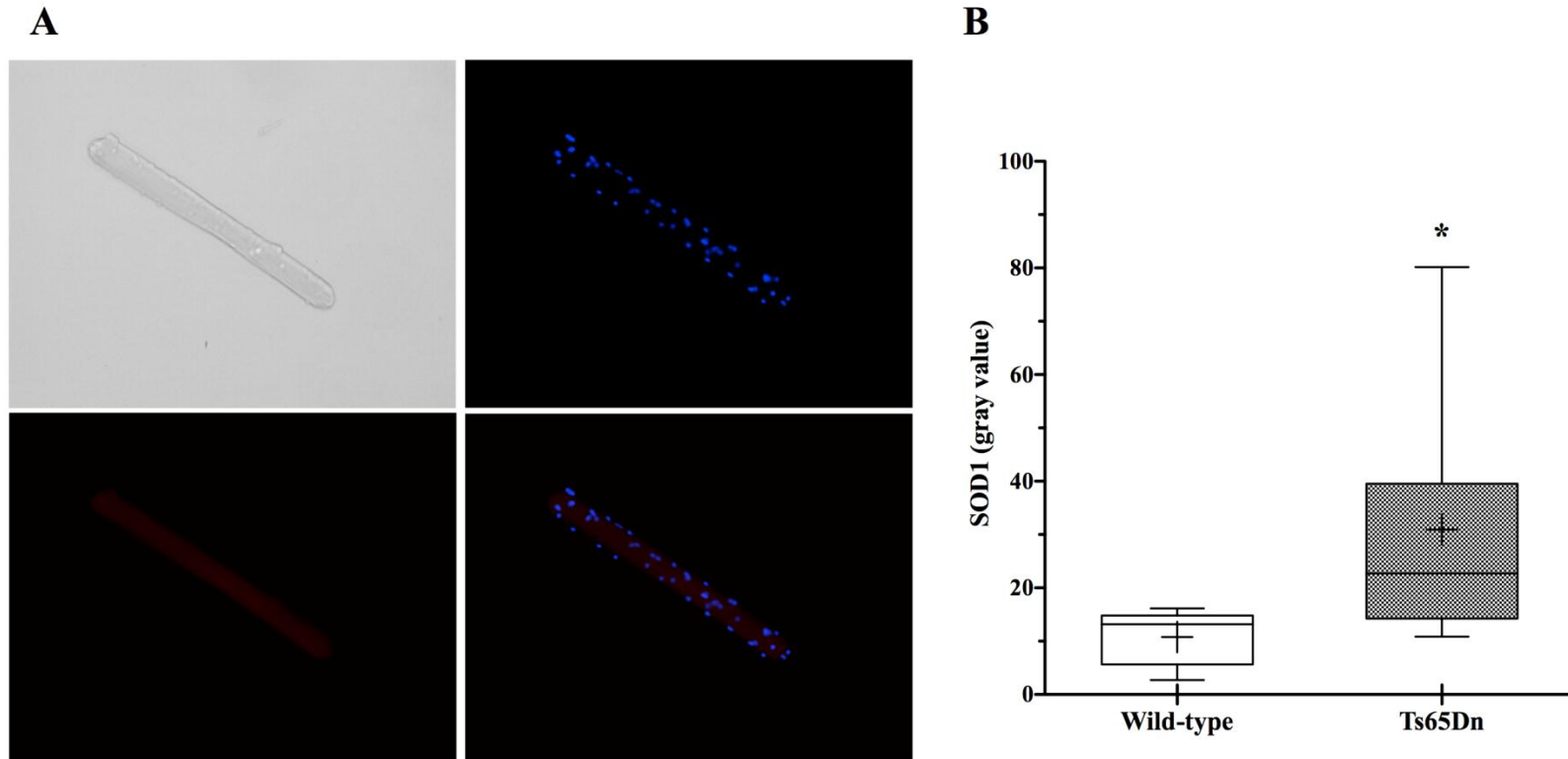
Figure 10. Immunofluorescence labeling of isolated adult single skeletal muscle fibers for SOD1. Representative bright field (A, upper left), DAPI (A, upper right), SOD1 (A, lower left), and DAPI and SOD1 composite (A, lower right) images of an isolated myofiber are shown. The arbitrary optical density of SOD1 are shown in B. N=4 animals/group and n=1-5 fibers/animal. 14 total fibers were analyzed from Ts65Dn and 12 fibers from WT.* Significantly different from WT ($p < 0.05$)
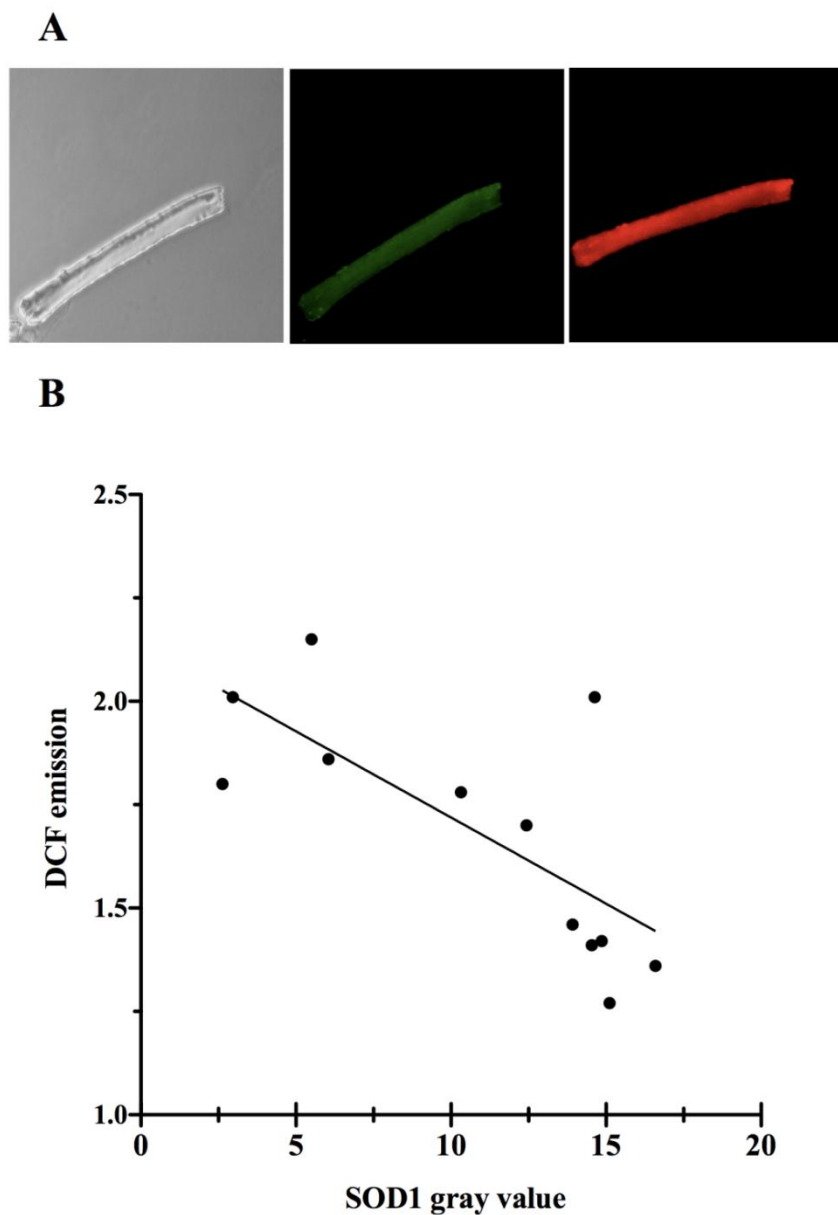
Figure 11. Relationship between DCF emission and SOD1 expression. Representation bright field (A, left), DCF (A, middle), and SOD1 (A, right) images of an isolated myofiber are shown. The SOD1 image was brightened to visually enhance the image for this figure. The correlation between DCF and SOD1 for WT fibers (r=-0.71, p < 0.05) is shown in B. The correlation for Ts65Dn fibers was not significant and data is not shown (r=0.18, p > 0.05). N=4 animals/group and n=1-5 fibers/animal. 14 total fibers were analyzed from Ts65Dn and 12 fibers from WT.

Table 6. Soleus contractile properties.

Variable	Wild-type (n=11)	Ts65Dn (n=12)
Twitch		
Peak tension (mN)	46.2 ± 1.8	44.5 ± 2.7
Specific peak tension (N/cm^2)	4.3 ± 0.2	4.0 ± 0.2
Time to peak tension (ms)	19.1 ± 1.2	19.3 ± 1.0
Half-relaxation time (ms)	22.6 ± 6.3	24.8 ± 4.1
Tetanus		
Peak tension (mN)	230.7 ± 10.3	239.7 ± 11.1
Specific peak tension (N/cm^2)	21.2 ± 0.6	21.6 ± 0.6
Twitch: tetanus ratio	0.20 ± 0.01	0.19 ± 0.01
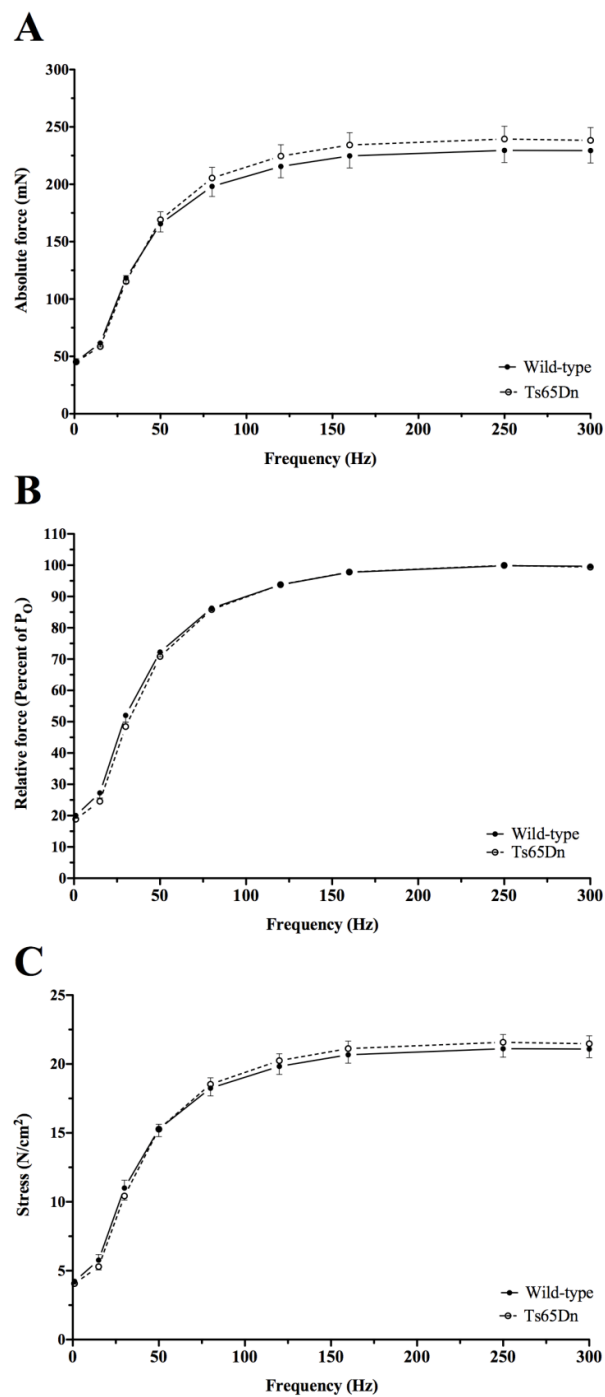
Figure 12. Force-frequency relationship of soleus determined in vitro. A) Absolute force. B) Relative force (% P_0). C) Stress. N=11 for WT and n=12 for Ts65Dn.
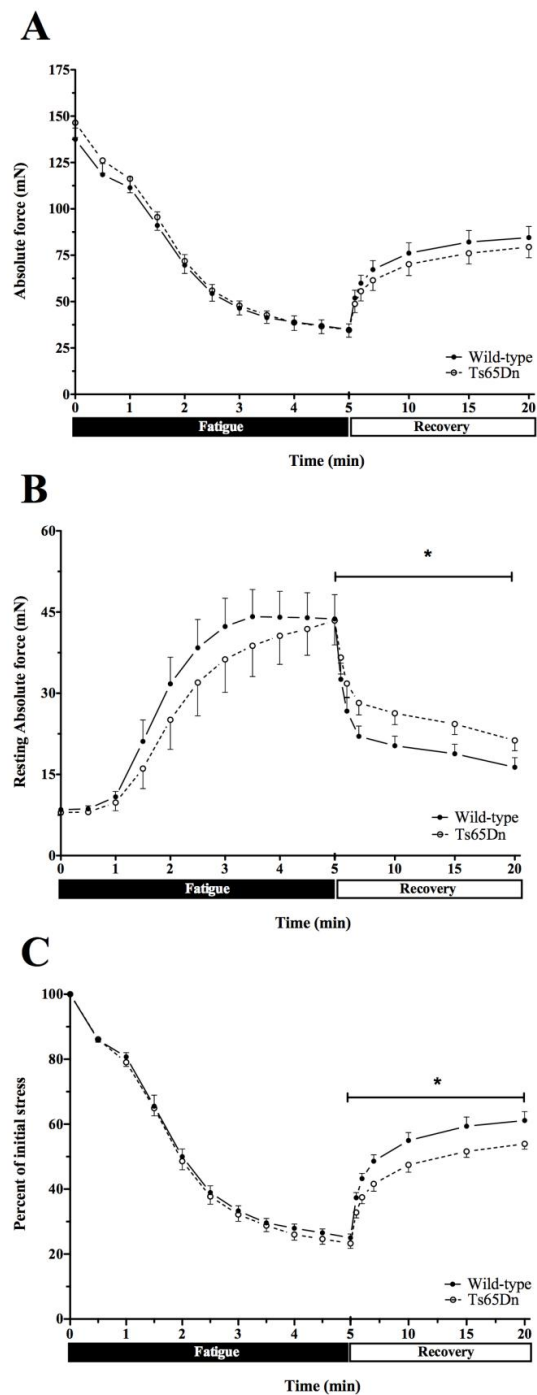
Figure 13. Fatigue and recovery response of soleus determined in vitro. A) Absolute force. B) Resting absolute force. C) Percent of initial stress. N=11 for WT and n=9 for Ts65Dn. * Significantly different from WT (p < 0.05).
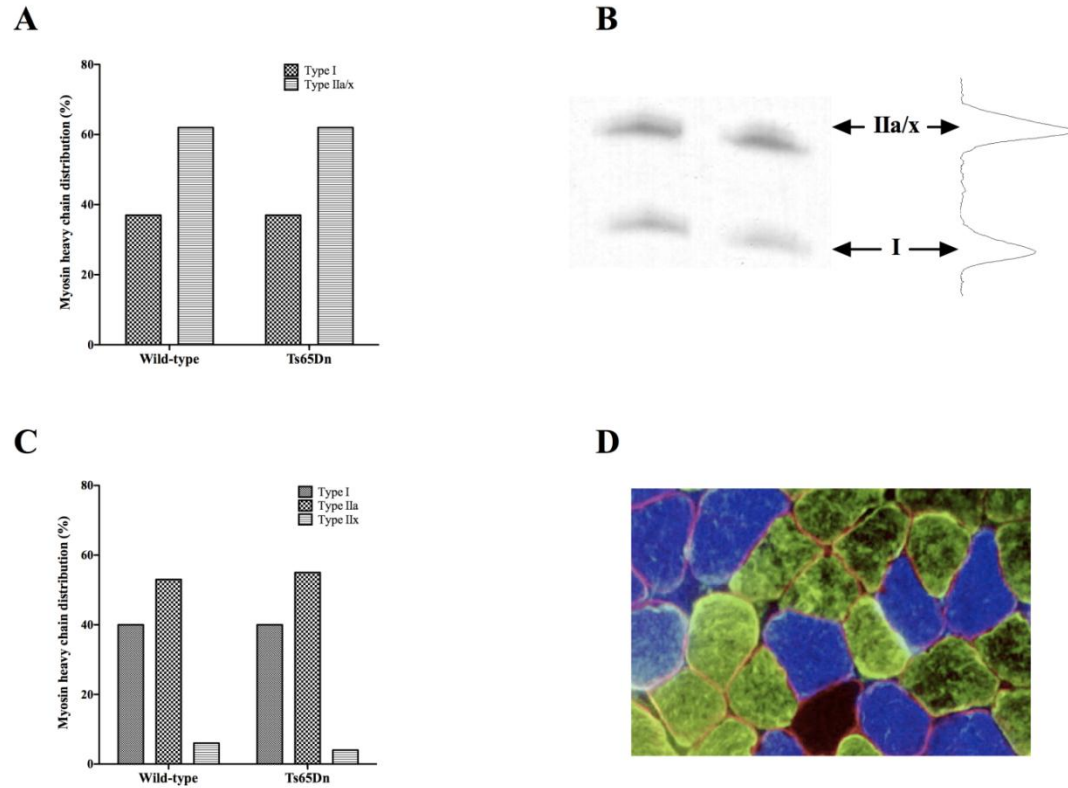
Figure 14. Soleus myosin heavy chain isoform composition determined by electrophoresis (A) and immunofluorescence (C) are shown. Representative images of electrophoresis separation of myosin heavy chain isoforms and labeling by immunofluorescence are shown in B and D, respectively. N=6 animals/group for electrophoresis. For immunofluorescence, n=6 for WT and n=5 for Ts65Dn.
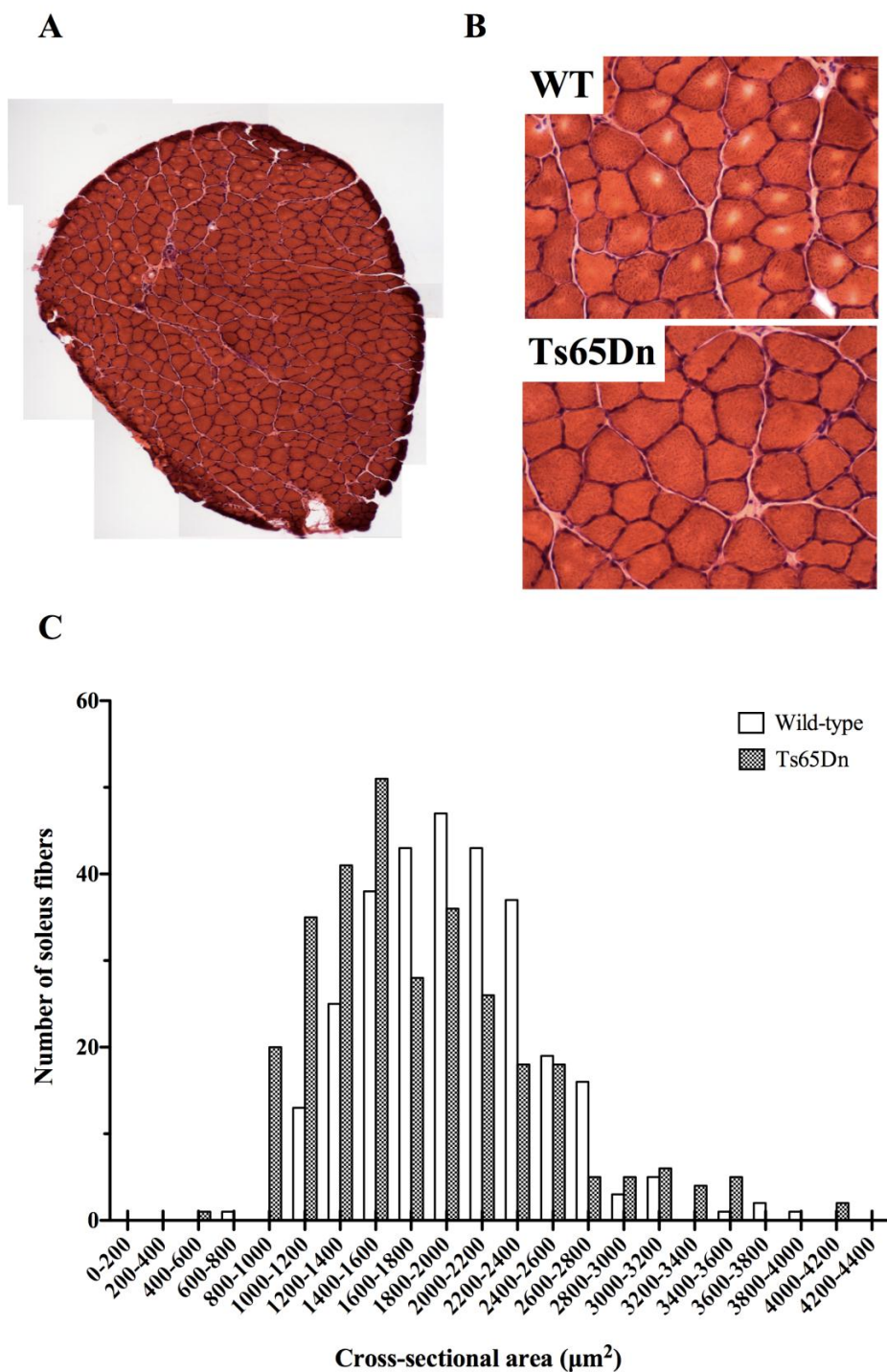
Figure 15. Soleus morphology assessed using H&E staining. Representative image of a complete soleus cross-section (A, left) and morphology of soleus for WT (A, right top) and Ts65Dn (A, right, bottom) at 20X magnification are shown. Cross-sectional area distribution is shown in B. N=3 animals/group.

Table 7. Flexor digitorum brevis (FDB) fiber characteristics (n=4 animals/group).

Variable	Wild-type	Ts65Dn
Number of fibers	8	12
Fiber length (μm)	297.0±10.2	285.4±13.3
Fiber diameter (μm)	31.8±2.2	26.8±1.5
Fiber volume (mm^3)	0.00024±0.0003	0.00017±0.0002
Number of myonuclei	44.5±2.1	40.8±2.6
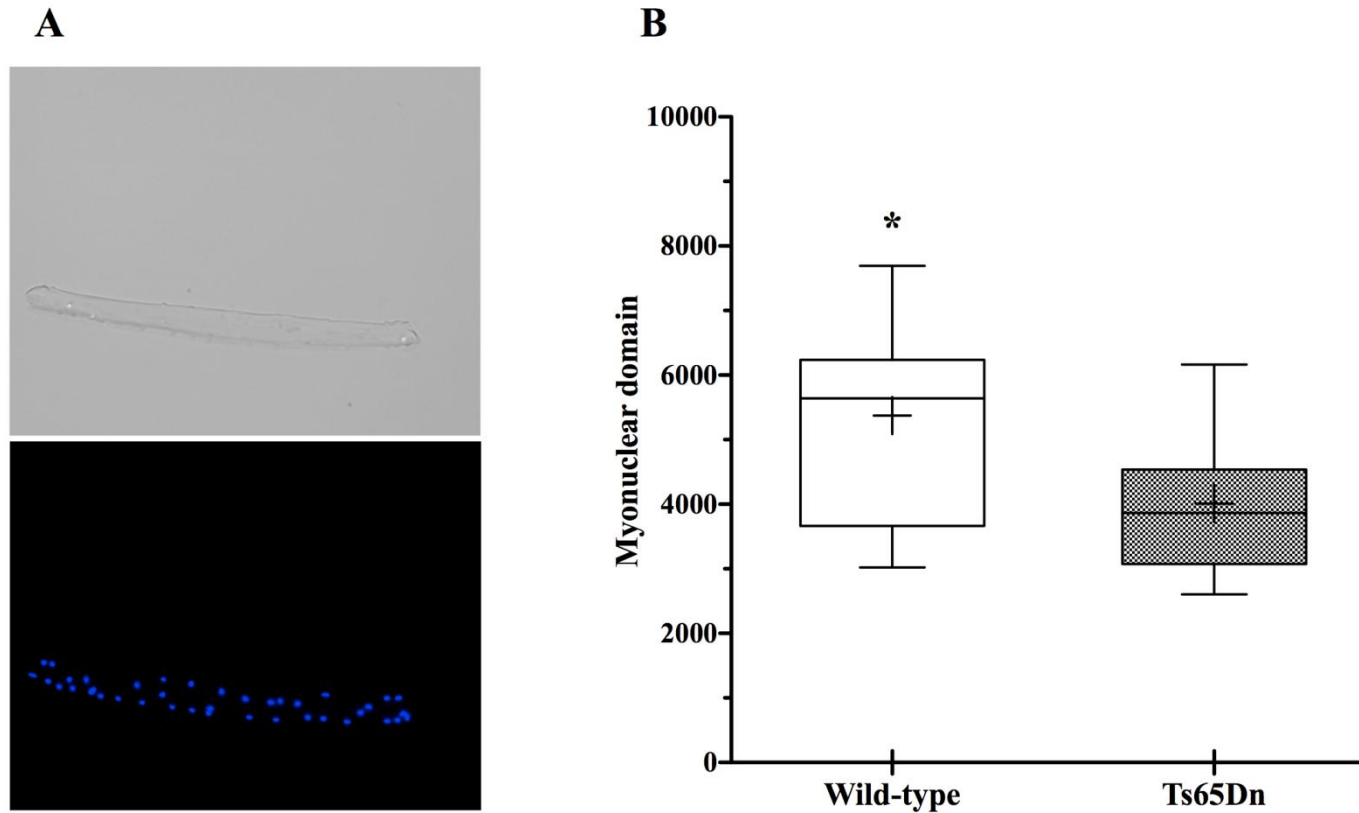
Figure 16. Myonuclear domain of isolated adult skeletal muscle fibers. Representative bright field (A, top) and DAPI (A, bottom) images of an isolated myofiber are shown. The DAPI image was visually enhanced to highlight the nuclei. Myonuclear domain is shown for WT and Ts65Dn FDB fibers in B. N=4 animals/group and n=1-4 fibers/animal. N=8 fibers for WT and n=12 fibers for Ts65Dn. * Significantly different from Ts65Dn (p < 0.05)
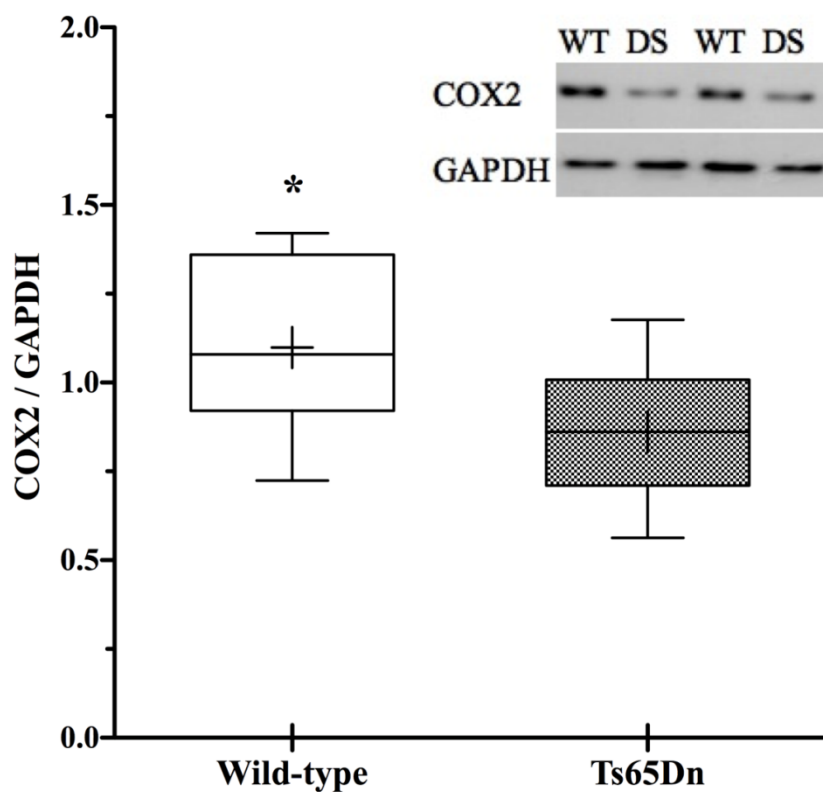
Figure 17. Soleus protein expression of COX2. COX2 protein bands expressed relative to GAPDH. Inset: Representative Western Blot images of COX2 and GAPDH. In this figure DS refers to Ts65Dn. N=10 animals/group. * Significantly different from Ts65Dn ($p < 0.05$).

Table 8. Expression of trisomic genes in soleus muscle.

Probe ID	Gene symbol	Fold change Ts65Dn/WT	Nominal p-value
Up-regulated			
10437055	single-minded homolog 2 (Drosophila) (Sim2)	1.82	0.000
10436830	interferon (alpha and beta) receptor 2 (Ifnar2)	2.06	0.000
10436892	intersectin 1 (SH3 domain protein 1A) (Itsn1)	1.84	0.001
10440600	chaperonin containing Tcp1, subunit 8 (theta) (Cct8)	1.56	0.001
10436951	RIKEN cDNA 1190017O12 gene (1190017O12Rik)	1.19	0.002
10440491	amyloid beta (A4) precursor protein (App)	2.48	0.002
10440593	RWD domain containing 2B (Rwdd2b)	1.70	0.002
10436708	ubiquitin specific peptidase 16 (Usp16)	1.49	0.003
10437080	tetratricopeptide repeat domain 3 (Ttc3)	2.22	0.003
10437023	microrchidia 3 (Morc3)	3.14	0.003
10441064	Down syndrome critical region gene 3 (Dscr3)	2.34	0.004

10441313	C2 calcium-dependent domain containing 2 (C2cd2)	2.22	0.004
10440849	Synaptojanin-1 gene:ENSMUSG00000022973	1.42	0.005
10440964	crystallin, zeta (quinone reductase)-like 1 (Cryzl1)	1.60	0.005
10440840	RIKEN cDNA 1110004E09 gene	1.64	0.005
10440929	phosphoribosylglycinamide formyltransferase (Gart)	1.50	0.007
10436873	Son DNA binding protein (Son)	1.91	0.008
10441115	bromodomain and WD repeat domain containing 1 (Brwd1)	2.63	0.008
10440926	DnaJ (Hsp40) homolog, subfamily C, member 28 (Dnajc28)	1.54	0.008
10437136	dual-specificity tyrosine-(Y)-phosphorylation regulated kinase 1a (Dyrk1a)	2.33	0.009
10437180	SH3-binding domain glutamic acid-rich protein (Sh3bgr)	1.30	0.010
10441003	runt related transcription factor 1 (Runx1)	1.33	0.011
10440977	ATP synthase, H+ transporting, mitochondrial F1 complex, O subunit (Atp5o)	1.20	0.015
10440993	regulator of calcineurin 1 (Rcan1)	1.78	0.015
10437174	tryptophan rich basic protein (Wrb)	1.96	0.019
10440534	a disintegrin-like and metallopeptidase (reprolysin type) with thrombospondin	1.81	0.025

	type 1 motif, 5 (aggrecanase-2) (Adamts5)		
10441093	avian erythroblastosis virus E-26 (v-ets) oncogene related (Erg)	1.29	0.031
10437160	E26 avian leukemia oncogene 2, 3' domain (Ets2)	2.13	0.031
10545528	phosphatidylinositol glycan anchor biosynthesis, class P (Pigp)	1.20	0.033
10436983	dopey family member 2 (Dopey2)	1.21	0.037
10441107	proteasome (prosome, macropain) assembly chaperone 1 (Psmg1)	1.56	0.037
10436698	N-6 adenine-specific DNA methyltransferase 1 (putative) (N6amt1)	1.53	0.041
10436967	carbonyl reductase 1 (Cbr1)	1.44	0.041
10436865	interferon gamma receptor 2 (Ifngr2)	1.41	0.043
10436678	GA repeat binding protein, alpha (Gabpa)	1.78	0.049
10436666	junction adhesion molecule 2 (Jam2)	1.63	0.059
10436841	interleukin 10 receptor, beta (Il10rb)	1.38	0.065
10440574	ring finger protein 160 (Rnf160)	1.43	0.068
10440881	RIKEN cDNA 1810007M14 gene (1810007M14Rik)	1.31	0.077
10436849	interferon (alpha and beta) receptor 1 (Ifnar1)	1.68	0.087

10440770	splicing factor, arginine/serine-rich 15 (Sfrs15)	1.22	0.090
10440471	mitochondrial ribosomal protein L39 (Mrpl39)	1.18	0.130
10436978	carbonyl reductase 3 (Cbr3)	1.31	0.134
10441038	holocarboxylase synthetase (biotin- [propriony-Coenzyme A-carboxylase (ATP-hydrolysing)] ligase) (Hlcs)	1.21	0.154
10440513	cysteine and tyrosine-rich protein 1 (Cyyr1)	1.33	0.223
10436945	solute carrier family 5 (inositol transporters), member 3 (Slc5a3)	1.17	0.329
10441161	high mobility group nucleosomal binding domain 1 (Hmgn1)	1.04	0.357
10440522	a disintegrin-like and metallopeptidase (reprolysin type) with thrombospondin type 1 motif, 1 (Adamts1)	1.05	0.357
10436941	mitochondrial ribosomal protein S6 (Mrps6)	1.07	0.360
10437224	myxovirus (influenza virus) resistance 2 (Mx2)	1.11	0.381
10436727	open reading frame 63 (ORF63)	1.17	0.385
10436783	superoxide dismutase 1, soluble (Sod1)	1.05	0.434
10440918	transmembrane protein 50B (Tmem50b)	1.21	0.632

10437205	Purkinje cell protein 4 (Pcp4)	1.05	0.756
10440794	RIKEN cDNA 2610039C10 gene (2610039C10Rik)	1.03	0.802
10436734	BTB and CNC homology 1 (Bach1)	1.01	0.953

Down-regulated

10441330	uncharacterized protein gene:ENSMUSG00000045331	1.38	0.001
10441233	immunoglobulin superfamily, member 5 (Igsf5)	1.47	0.006
10440621	UDP-Gal:betaGlcNAc beta 1,3-galactosyltransferase, polypeptide 5 (B3galt5)	1.29	0.008
10437073	integrin beta 2-like (Itgb2l)	1.29	0.009
10535647	oligodendrocyte transcription factor 1 (Olig1)	1.33	0.010
10436958	claudin 14 (Cldn14)	1.49	0.018
10437151	transmembrane protease, serine 2 (Tmprss2)	1.36	0.020
10440800	RIKEN cDNA 4930563D23 gene (4930563D23Rik)	1.34	0.021
10441280	oligodendrocyte transcription factor 2 (Olig2)	1.22	0.023
10440647	potassium inwardly-rectifying channel, subfamily J, member 6 (Kcnj6)	1.16	0.030
10440953	SET domain containing 4 (Setd4)	1.35	0.034

10440738	potassium voltage-gated channel, Isk-related subfamily, gene 2 (Kcne2)	1.41	0.034
10441167	melanocortin 2 receptor accessory protein (Mrap)	1.23	0.035
10440989	hormonally upregulated Neu-associated kinase (Hunk)	1.25	0.040
10441073	family with sequence similarity 3, member B (Fam3b)	1.34	0.040
10437040	receptor-interacting serine-threonine kinase 4 (Ripk4)	1.44	0.047
10436636	chromatin assembly factor 1, subunit B (p60) (Chaf1b)	1.17	0.070
10441231	ATP synthase, H+ transporting, mitochondrial F0 complex, subunit f, isoform 2 (Atp5j2)	1.06	0.076
10440643	neural cell adhesion molecule 2 (Ncam2)	1.18	0.080
10436823	T-cell lymphoma invasion and metastasis 1 (Tiam1)	1.13	0.106
10436804	PR domain containing 15 (Prdm15)	1.11	0.118
10436809	Down syndrome cell adhesion molecule (Dscam)	1.33	0.128
10436788	RIKEN cDNA 4932438H23 gene (4932438H23Rik)	1.25	0.153
10440903	Mus musculus miR-155 stem-loop	1.25	0.161
10440903	claudin 8 (Cldn8)	1.11	0.163

10437191	potassium voltage-gated channel, Isk-related subfamily, member 1 (Kcne1)	1.15	0.180
10441178	claudin 17 (Cldn17)	1.21	0.194
10441195	C21orf63 protein (C21orf63)	1.25	0.211
10436828	beta-site APP-cleaving enzyme 2 (Bace2)	1.18	0.231
10440985	potassium inwardly-rectifying channel, subfamily J, member 15 (Kcnj15)	1.10	0.235
10441244	Leber congenital amaurosis 5-like (Lca5l)	1.15	0.236
10441017	downstream neighbor of SON (Donson)	1.13	0.243
10441254	chloride intracellular channel 6 (Clic6)	1.10	0.300
10440655	hypothetical protein LOC207932 gene:ENSMUSG00000039929	1.10	0.332
10436947	glutamate receptor, ionotropic, kainate 1 (Grik1)	1.03	0.567
10441270	myxovirus (influenza virus) resistance 1 (Mx1)	1.03	0.748
10437195	ripply3 homolog (zebrafish) (Ripply3)	1.04	0.797
10441032	zinc finger protein 295 (Zfp295), transcript variant 1	1.02	0.897

Table 9. Differentially expressed genes in Ts65Dn soleus relative to wild-type.

Probe ID	Gene description/symbol	Function of encoded protein	Fold change
Up-regulated			
10440558	ring finger protein 160 (Rnf160)*	E3 ubiquitin ligase, neuronal	3.66
10597323	cyclic AMP-regulated phosphoprotein, 21 (Arpp21)	Nucleic acid binding	1.68
10472058	Rap1 interacting factor 1 homolog (yeast) (Rif1)	Protein binding, response to DNA damage stimulus	2.31
10571922	NIMA (never in mitosis gene a)-related expressed kinase 1 (Nek1)	Kinase, Response to DNA damage stimulus	2.37
10530692	kinase insert domain protein receptor (Kdr)	Vascular endothelial growth factor receptor, pro-angiogenic, VEGF signaling pathway	1.99
10514072	zinc finger, DHHC domain containing 21 (Zdhhc21)	Acyltransferase activity	3.01
10504692	tropomodulin 1 (Tmod1)	Actin/tropomyosin binding	1.89

10437055	single-minded homolog 2 (Drosophila) (Sim2)*	DNA binding, transcription regulator	1.81
10376163	Rap guanine nucleotide exchange factor (GEF) 6 (Rapgef6)	Cell adhesion	1.84
10436830	interferon (alpha and beta) receptor 2 (Ifnar2)*	Type I interferon receptor	2.06
10426751	transmembrane BAX inhibitor motif containing 6 (Tmbim6)	Negative regulation of apoptosis	1.55
10600836	moesin (Msn)	Actin binding, Regulation of actin cytoskeleton	1.63
10508759	replication protein A2 (Rpa2)	DNA binding, Nucleotide excision repair	1.52
10401382	numb gene homolog (Drosophila) (Numb)	Regulator of muscle differentiation by inhibiting Notch signaling pathway	1.63
10578157	tankyrase, TRF1-interacting ankyrin-related ADP-ribose polymerase (Tnks)	Peptidyl-threonine/serine phosphorylation	1.66
10373400	myosin, light polypeptide 6B (Myl6b)	Calcium ion binding, structural constituent of muscle	2.78
10495111	WD repeat domain 77 (Wdr77)	Ligand-dependent nuclear receptor transcription	2.20

		coactivator activity	
10440556	ring finger protein 160 (Rnf160)*	E3 ubiquitin ligase, neuronal	3.07
10520288	UDP-N-acetyl-alpha-D-galactosamine:polypeptide N-acetylgalactosaminyltransferase 11 (Galnt11)	Transferase activity, O-Glycan biosynthesis	1.43
10567355	G protein-coupled receptor, family C, group 5, member B (Gprc5b)	G-protein coupled receptor activity	2.16
10480329	DnaJ (Hsp40) homolog, subfamily C, member 1 (Dnajc1)	Chaperone binding	1.78
10358816	laminin, gamma 1 (Lamc1)	Major noncollagenous constituent of basement membranes	2.01
10385966	annexin A6 (Anxa6)	Calcium-dependent phospholipid binding, suggested roles in Ca^{2+} flux and inflammation	1.64
10503188	chromodomain helicase DNA binding protein 7 (Chd7)	DNA binding	2.27
10436892	intersectin 1 (SH3 domain protein 1A) (Itsn1)*	Protein binding, synaptic endocytosis	1.83

10440578	ring finger protein 160 (Rnf160)*	E3 ubiquitin ligase, neuronal	2.16
10571840	hydroxyprostaglandin dehydrogenase 15 (NAD) (Hpgd)	Prostaglandin metabolism	2.40
10435470	karyopherin (importin) alpha 1 (Kpna1)	Protein transporter	1.90
10530854	steroid 5 alpha-reductase 2-like 2 (Srd5a2l2)	Oxidoreductase activity	4.58
10495054	ras homolog gene family, member C (Rhoc)	GTP binding	2.02
10466800	phosphoglucomutase 5 (Pgm5)	Protein binding, associates with dystrophin	1.65
10525555	MLX interacting protein (Mlxip)	DNA binding, negative regulator of glucose uptake	1.76
10523468	BMP2 inducible kinase (Bmp2k)	Kinase	2.40
10366310	oxysterol binding protein-like 8 (Osbpl8)	Intracellular lipid receptor	3.45
10490826	zinc finger and BTB domain containing 10 isoform 1 gene (Zbtb10)	DNA binding	1.58
10388591	carboxypeptidase D (Cpd)	Carboxypeptidase	2.12
10471360	golgi autoantigen, golgin subfamily a, 2 (Golga2)	Protein complex binding	1.70

10526120	protein-tyrosine sulfotransferase 1 (Tpst1)	Protein-tyrosine sulfotransferase	1.77
10440491	amyloid beta (A4) precursor protein (App)*	Protein binding, neuromuscular synapse formation	2.41
10547657	complement component 3a receptor 1 (C3ar1)	C3a anaphylatoxin receptor, inflammation	2.37
10478447	serine/threonine kinase 4 (Stk4)	Protein serine/threonine kinase	1.76
10522024	TBC1 domain family, member 1 (Tbc1d1)	GTPase activator, regulator of glucose transport	1.93
Down-regulated			
10472688	trans-acting transcription factor 5 (Sp5)	DNA binding	1.59
10569163	cell cycle exit and neuronal differentiation 1 (Cend1)	Tissue regeneration, neuronal	1.41
10345101	collagen, type IX, alpha 1 (Col9a1)	Alpha chain of IX collagen, structural molecule	1.69
10542319	apolipoprotein L domain containing 1 (Apold1)	Lipid binding	1.71
10598493	proprotein convertase subtilisin/kexin type 1 inhibitor (Pcsk1n)	Endopeptidase inhibitor, Inhibitor of proprotein convertase subtilisin/kexin type 1 which is	1.62

		responsible for processing precursor proteins into biologically active products	
10432897	keratin 79 (Krt79)	Structural molecule	1.69
10477042	angiopoietin 4 (Angpt4)	Vascular endothelial growth factor receptor binding	1.45
10461867	vacuolar protein sorting 13A (yeast) (Vps13a)	Mutations cause Chorea-acanthocytosis which is an autosomal recessive hereditary disease, function is unknown	1.49
10383047	ectonucleotide pyrophosphatase / phosphodiesterase 7 (Enpp7)	Sphingomyelin phosphodiesterase	1.54
10376394	olfactory receptor 324 (Olfr324)	G-coupled receptor	1.56
10488558	syntaphilin (Snph)	Regulates mitochondrial docking in synaptic buttons of axons	1.54
10588720	RNA binding motif protein 6 (Rbm6)	DNA/RNA binding	1.42
10430324	transmembrane serine protease 6 (Tmprss6)	Iron regulation, suppressor of hepcidin	1.62

expression

10449000	mesothelin (Msln)	Cell adhesion	1.43
10470959	phytanoyl-CoA dioxygenase domain containing 1 (Phyhd1)	Oxidoreductase	1.45
10390909	keratin associated protein 9-3 (Krtap9-3)	Structural molecule	1.68
10589074	ariadne homolog 2 (Drosophila) (Arih2)	E3 ubiquitin-protein ligase	1.85
10434835	leprecan-like 1 (Leprel1)	Procollagen-proline 3-dioxygenase, hydroxylation of IV collagen	1.55
10554061	a disintegrin-like and metallopeptidase (reprolysin type) with thrombospondin type 1 motif, 17 (Adamts17)	Hydrolase	1.53
10392063	LIM domain containing 2 (Limd2)	Metal ion binding	1.56
10365015	zinc finger RNA binding protein 2 (Zfr2)	RNA binding	1.55
10552240	zinc finger protein 507 (Zfp507)	Zinc ion binding	1.69
10581388	lecithin cholesterol acyltransferase (Lcat)	Esterification of cholesterol,	1.40

		Glycerophospholipid metabolism pathway	
10364932	transmembrane protease, serine 9 (Tmprss9)	Peptidase, proteolysis	1.48
10485955	secretogranin V (Scg5)	Enzyme inhibitor, Neuropeptide signaling pathway	1.45
10442393	netrin 3 (Ntn3)	Transcription regulator, myoblast fusion, axon guidance	1.41
10563447	TP-binding cassette, sub-family C (CFTR/MRP), member 6 (Abcc6)	Transporter, mutations in this gene cause Pseudoxanthoma elasticum, calification, ABC transporters	1.59
10432907	keratin 78 (Krt78)	Intermediate filament	1.65
10551907	nephrosis 1 homolog, nephrin (human) (Nphs1)	Alpha-actinin binding, renal	1.66
10564290	Kruppel-like factor 13 (Klf13)	DNA binding	1.47
10425507	melanin-concentrating hormone receptor 1 (Mchr1)	Melanin-concentrating hormone receptor, Neuroactive ligand-receptor interaction	1.53
10500100	tumor necrosis factor, alpha-induced protein 8-like	Negative regulation of immune response	1.60

	2 (Tnfaip8l2)		
10386473	sterol regulatory element binding transcription factor 1 (Srebf1)	DNA binding, regulator of lipogenesis, Insulin signaling pathway	1.44
10594199	thrombospondin, type I, domain containing 4 (Thsd4)	Metalloendopeptidase	1.46
10458540	protocadherin 12 (Pcdh12)	Calcium ion binding	1.47
10421906	"PREDICTED: Mus musculus similar to ATP synthase, H+ transporting, mitochondrial F0 complex, subunit d (LOC676483)	Hydrogen ion transmembrane transporter, Oxidative phosphorylation	1.81
10601152	neuroligin 3 (Nlgn3)	Regulation of synaptic transmission, Cell adhesion molecules	1.41
10488771	N-terminal EF-hand calcium binding protein 3 (Necab3)	Calcium ion binding, regulator of amyloid precursor protein metabolism, substrate of Nek1	1.67
10460585	fos-like antigen 1 (Fosl1)	DNA binding, component of transcription factor complex AP-1, Wnt signaling pathway	1.43

10608721	steroid sulfatase (Sts)	Steryl-sulfatase	1.43
10524955	tescalcin (Tesc)	Calcium ion binding	1.53
10546452	a disintegrin-like and metallopeptidase (reprolysin type) with thrombospondin type 1 motif, 9 (Adamts9)	Endopeptidase	1.69
10428222	neurocalcin delta (Ncald)	Calcium ion binding	1.42
10585840	CD276 antigen precursor (Cd276)	Negative regulation of immune response, Cell adhesion molecules	1.52
10352971	RB1-inducible coiled-coil 1 (Rb1cc1)	Regulator of myoblast differentiation, Protein complex (ULK1-ATG13-RB1CC1 complex) is essential for mammalian autophagy	1.58
10454192	transthyretin (Ttr)	Hormone binding, transport of thyroid hormones and retinol	1.53
10559989	aurora kinase C (Aurkc)	Kinase	1.46
10351471	U2AF homology motif (UHM) kinase 1 (Uhmk1)	Kinase	1.48

10560575	avian reticuloendotheliosis viral (v-rel) oncogene related B (Relb)	DNA binding, Alternative NF-kB pathway	1.40
10409369	synuclein, beta (Sncb)	Synaptic integrity, axon terminus	1.41
10549594	tweety homolog 1 (Drosophila) (Ttyh1)	Chloride channel	1.47
10416099	adrenergic receptor, alpha 1a (Adra1a)	Alpha1-adrenergic receptor, mediates glucose uptake in L6 cells	1.45
10543466	G protein-coupled receptor 37 (Gpr37)	G-protein coupled receptor protein signaling pathway, Parkinson's disease	1.56
10377245	dehydrogenase/reductase (SDR family) member 7C (Dhrs7c)	Oxidoreductase	1.46
10418835	solute carrier family 18 (vesicular monoamine), member 3 (Slc18a3)	Mediator of acetylcholine transport into synaptic vesicles	1.61

* Gene is trisomic in Ts65Dn.

Table 10. Differentially expressed genes in Ts65Dn soleus relative to wild-type with no functional annotation.

Probe ID	Gene description/symbol	Fold change
Up-regulated		
10506668	Yip1 domain family, member 1 (Yipf1)	1.64
10496405	Predicted gene, EG329763 (EG329763)	2.73
10501676	hippocampus abundant gene transcript 1 (Hiat1)	1.76
10566870	transmembrane protein 41B (Tmem41b)	1.90
10350024	kelch-like 12 (Drosophila) (Klhl12)	1.79
10468275	polycomb group ring finger 6 (Pcgf6)	2.14
10354506	major facilitator superfamily domain containing 6 (Mfsd6)	1.81
10494445	ENSMUSG00000049288	2.33
10357954	protein phosphatase 1, regulatory (inhibitor) subunit 12B (Ppp1r12b)	1.41
10504668	ENSMUSG00000078708	3.13
10419416	RIKEN cDNA 3632451O06 gene (3632451O06Rik)	2.30
10558057	bromodomain and WD repeat domain containing 2 (Brwd2)	1.94

Down-regulated

10457836	ENSMUSG00000073619	1.81
10445891	similar to 3-phosphoglycerate dehydrogenase (LOC668506)	1.81
10538704	ENSMUSG00000064515	1.70
10509039	RIKEN cDNA 4930555I21 gene (4930555I21Rik)	1.41
10576088	mRNA for mKIAA1858 protein	1.54
10425109	leucine rich repeat and fibronectin type III, extracellular 2 (Elfn2)	1.53
10348570	espin-like (Espnl)	1.50
10604599	ENSMUSG00000081843	1.44
10459770	ENSMUSG00000076229	1.57
10524227	RIKEN cDNA 2410025L10 gene (2410025L10Rik), transcript variant 1	1.61
10519209	matrix-remodelling associated 8 (Mxra8)	1.40
10449654	ENSMUSG00000073427	1.55
10582221	RIKEN cDNA 1700018B08 gene (1700018B08Rik)	1.38
10379836	B6-derived CD11 +ve dendritic cells cDNA	1.52

10516238	RIKEN cDNA 1110065P20 gene (1110065P20Rik)	1.41
10468037	ENSMUSG00000035243	1.55
10380514	family with sequence similarity 117, memberA (Fam117a)	1.56
10598126	hedgehog interacting protein-like 2	1.72
10458709	gene model 94 (Gm94)	1.63
10348000	RIKEN cDNA 2810459M11 gene (2810459M11Rik)	1.45
10495592	NCBIM37:3:116527020:116550142:1	1.46
10477423	gene model 1006 (Gm1006)	1.50
10510880	ENSMUSG00000057751	1.76
10443852	ENSMUSG00000053467	1.54
10568318	cDNA sequence BC039632 (BC039632)	1.84
10551159	ribosomal protein L15 (LOC100047962)	1.59
10569311	ribosomal protein L27a-like (LOC270015)	1.72
10398211	hedgehog interacting protein-like 1 (Hhipl1)	1.59
10513112	erythrocyte protein band 4.1-like 4b (Epb4.1l4b)	1.52

10600781	predicted gene, EG245516 (EG245516)	1.50
10593101	similar to Glyceraldehyde-3-phosphate dehydrogenase (GAPDH) (LOC640094)	1.63
10522409	similar to ribosomal protein (LOC667154)	1.67
10457663	ENSMUSG00000082608	1.74
10405119	gene model 270, (NCBI) (Gm270)	1.42
10562394	ENSMUSG00000081863	1.63
10542270	NCBIM37:6:133259948:133262057:1	1.35
10356170	ENSMUSG00000080399	1.81
10448079	predicted gene, EG626573 (EG626573)	1.45
10535900	ENSMUSG00000084436	1.65
10568258	RIKEN cDNA 1700008J07 gene (1700008J07Rik)	1.50
10400892	glyceraldehyde-3-phosphate dehydrogenase (LOC666213)	1.63
10365727	ENSMUSG00000076238	1.70
10552260	ENSMUSG00000070060	1.66
10560474	expressed sequence C79127 (cDNA clone MGC:106176 IMAGE:4507828)	1.58

10442300	predicted gene, EG666030 (EG666030)	1.48
10593167	mRNA for transcription factor S-II-related proteins	1.67
10365335	NCBIM37:10:83364576:83486518:1	1.46

Table 11. Summary of conservative gene-by-gene analysis.

Gene description/symbol	Potential effect on Ts65Dn soleus
Genes with a role in metabolism	
TBC1 domain family, member 1 (Tbc1d1)	Stimulates glucose uptake
MLX interacting protein (Mlxip)	Stimulates glycolysis but suppresses glucose uptake
adrenergic receptor, alpha 1a (Adra1a)	Suppresses glucose uptake
trans-acting transcription factor 5 (Sp5)	Stimulates cytochrome c oxidase expression
sterol regulatory element binding transcription factor 1 (Srebf1)	Suppresses lipogenesis
tankyrase, TRF1-interacting ankyrin-related ADP-ribose polymerase (Tnks)	Suppresses lipid metabolism
melanin-concentrating hormone receptor 1 (Mchr1)	Increased energy expenditure
Genes with a role in neuromuscular transmission	
solute carrier family 18 (vesicular monoamine), member 3 (Slc18a3)	Suppresses synaptic vesicle formation
intersectin 1 (SH3 domain protein 1A) (Itsn1)	Regulates synaptic vesicle cycling
amyloid beta (A4) precursor protein (App)	Necessary for neuromuscular junction integrity

syntaphilin (Snph)	Regulates mitochondrial mobility in axons

Genes with a role in inflammation

CD276 antigen precursor (Cd276)	Decreased suppression of inflammation
tumor necrosis factor, alpha-induced protein 8-like 2 (Tnfaip8l2)	Decreased suppression of inflammation
complement component 3a receptor 1 (C3ar1)	Stimulates inflammation

Genes with a role in muscle differentiation/regeneration

netrin 3 (Ntn3)	Suppresses muscle differentiation
RB1-inducible coiled-coil 1 (Rb1cc1)	Suppresses muscle differentiation
nephrosis 1 homolog, nephrin (human) (Nphs1)	Suppresses muscle differentiation
numb gene homolog (Drosophila) (Numb)	Stimulates muscle differentiation and regeneration
avian reticuloendotheliosis viral (v-rel) oncogene related B (Relb)	Suppresses muscle differentiation
kinase insert domain protein receptor (Kdr)	Stimulates muscle regeneration

Genes with a role in proteolysis and damage stimulus

ring finger protein 160 (Rnf160)	Stimulates proteolysis
ariadne homolog 2 (Drosophila) (Arih2)	Suppresses proteolysis

serine/threonine kinase 4 (Stk4)	Stimulates proteolysis
replication protein A2 (Rpa2)	Stimulates DNA repair
Rap1 interacting factor 1 homolog (yeast) (Rif1)	Stimulates DNA repair
NIMA (never in mitosis gene a)-related expressed kinase 1 (Nek1)	Stimulates DNA repair
ectonucleotide pyrophosphatase / phosphodiesterase 7 (Enpp7)	Decreases oxidant production
fos-like antigen 1 (Fosl1)	Stimulates antioxidant gene expression
transmembrane BAX inhibitor motif containing 6 (Tmbim6)	Suppresses apoptosis

Genes with a role in skeletal muscle structure and function

tropomodulin 1 (Tmod1)	Enhances muscle force production
annexin A6 (Anxa6)	Enhances calcium regulation
secretogranin V (Scg5)	Stimulates ryanodine-sensitive calcium release
tescalcin (Tesc)	Stimulates maintenance of muscle pH
phosphoglucomutase 5 (Pgm5)	Enhances structural stability of muscle plasmalemma
moesin (Msn)	Enhances cytoskeletal stability
leprecan-like 1 (Leprel1)	Depressed collagen IV production for muscle basement

	membrane
laminin, gamma 1 (Lamc1)	Enhances sarcolemma stability
myosin, light polypeptide 6B (Myl6b)	Enhances cytoskeletal stability

Genes with a role in iron metabolism

transmembrane serine protease 6 (Tmprss6)	Stimulates iron uptake

Table 12. Terms identified from DAVID analysis. CL=cluster; ES=enrichment score; FE=fold enrichment; FDR=false discovery rate.

CL	ES	Category	Term	p-value	FE	FDR
1	6.5	Biological process	GO:0051603~proteolysis involved in cellular protein catabolic process	0.000	2.5	0.0
		Biological process	GO:0044257~cellular protein catabolic process	0.000	2.5	0.0
		Biological process	GO:0030163~protein catabolic process	0.000	2.4	0.0
		Keyword	ubl conjugation pathway	0.000	2.5	0.0
		Biological process	GO:0044265~cellular macromolecule catabolic process	0.000	2.3	0.0
		Biological process	GO:0043632~modification-dependent macromolecule catabolic process	0.000	2.4	0.0
		Biological process	GO:0019941~modification-dependent protein catabolic process	0.000	2.4	0.0
		Biological process	GO:0009057~macromolecule catabolic process	0.000	2.1	0.0
		Biological process	GO:0006508~proteolysis	0.000	1.6	0.6
2	4.3	Molecular function	GO:0008092~cytoskeletal protein binding	0.000	2.5	0.0
		Cellular component	GO:0015629~actin cytoskeleton	0.000	3.0	0.1
		Molecular function	GO:0003779~actin binding	0.000	2.4	0.4
		Keyword	actin-binding	0.001	2.5	0.7

3	4.1	Molecular function	GO:0008092~cytoskeletal protein binding	0.000	2.5	0.0
		Cellular component	GO:0005856~cytoskeleton	0.000	1.6	0.2
		Keyword	cytoskeleton	0.004	1.7	4.8
4	3.9	Molecular function	GO:0017076~purine nucleotide binding	0.000	1.6	0.0
		Molecular function	GO:0032553~ribonucleotide binding	0.000	1.5	0.0
		Molecular function	GO:0032555~purine ribonucleotide binding	0.000	1.5	0.0
		Molecular function	GO:0030554~adenyl nucleotide binding	0.000	1.6	0.0
		Molecular function	GO:0001883~purine nucleoside binding	0.000	1.6	0.0
		Keyword	serine/threonine-protein kinase	0.000	2.3	0.0
		Molecular function	GO:0001882~nucleoside binding	0.000	1.6	0.0
		Biological process	GO:0016310~phosphorylation	0.000	1.9	0.1
		Molecular function	GO:0004674~protein serine/threonine kinase activity	0.000	2.2	0.1
		Molecular function	GO:0005524~ATP binding	0.000	1.6	0.1
		Keyword	nucleotide-binding	0.000	1.5	0.1
		Molecular function	GO:0032559~adenyl ribonucleotide binding	0.000	1.5	0.1

				0.000	1.6	0.1
		Keyword	atp-binding	0.000	1.6	0.1
		Biological process	GO:0006468~protein amino acid phosphorylation	0.000	1.9	0.2
		Interpro	IPR008271:Serine/threonine protein kinase, active site	0.000	2.2	0.3
		Biological process	GO:0006793~phosphorus metabolic process	0.000	1.7	0.4
		Biological process	GO:0006796~phosphate metabolic process	0.000	1.7	0.4
		Keyword	transferase	0.000	1.5	0.4
		Interpro	IPR002290:Serine/threonine protein kinase	0.000	2.4	0.7
		Interpro	IPR017441:Protein kinase, ATP binding site	0.000	2.0	0.8
		Interpro	IPR000719:Protein kinase, core	0.001	1.9	0.9
		Interpro	IPR017442:Serine/threonine protein kinase-related	0.001	2.1	1.1
		Molecular function	GO:0004672~protein kinase activity	0.001	1.8	1.2
5	3.6	Cellular component	GO:0043232~intracellular non-membrane-bounded organelle	0.000	1.5	0.1
		Cellular component	GO:0043228~non-membrane-bounded organelle	0.000	1.5	0.1
		Cellular component	GO:0005856~cytoskeleton	0.000	1.6	0.2
		Cellular component	GO:0044430~cytoskeletal part	0.003	1.6	4.2

6	3.1	Biological process	GO:0009314~response to radiation	0.001	2.9	1.0
		Biological process	GO:0009416~response to light stimulus	0.001	3.4	1.2
		Biological process	GO:0009628~response to abiotic stimulus	0.002	2.2	2.7
7	3	Cellular component	GO:0005654~nucleoplasm	0.000	1.9	0.2
		Cellular component	GO:0031981~nuclear lumen	0.000	1.7	0.5
		Cellular component	GO:0044451~nucleoplasm part	0.000	1.9	0.6
		Cellular component	GO:0031974~membrane-enclosed lumen	0.002	1.5	2.5
		Cellular component	GO:0070013~intracellular organelle lumen	0.004	1.5	4.8
8	2.9	Biological process	GO:0009792~embryonic development ending in birth or egg hatching	0.000	2.1	0.2
		Biological process	GO:0043009~chordate embryonic development	0.000	2.1	0.4
9	2.9	Biological process	GO:0007010~cytoskeleton organization	0.000	2.2	0.4
		Biological process	GO:0030029~actin filament-based process	0.002	2.6	2.6
10	2.6	Interpro	IPR018502:Annexin repeat	0.001	11.9	0.9
		Interpro	IPR001464:Annexin	0.001	11.9	0.9
		Interpro	IPR018252:Annexin repeat, conserved site	0.001	11.9	0.9

		Keyword	annexin	0.001	11.7	0.9
		Keyword	phospholipid binding	0.001	11.7	0.9
		Keyword	calcium/phospholipid-binding	0.001	10.8	1.2
		Molecular function	GO:0005543~phospholipid binding	0.003	2.8	4.8
		Keyword	endonexin fold	0.004	28.0	5.0
11	2.5	Cellular component	GO:0030027~lamellipodium	0.000	4.8	0.3
		Cellular component	GO:0031252~cell leading edge	0.004	3.0	5.2
12	2.5	Biological process	GO:0033554~cellular response to stress	0.001	1.9	2.2
		Biological process	GO:0006281~DNA repair	0.002	2.3	4.2
13	2.3	Cellular component	GO:0031410~cytoplasmic vesicle	0.001	1.9	1.0
		Cellular component	GO:0031982~vesicle	0.001	1.9	1.4
14	2.3	Biological process	GO:0046907~intracellular transport	0.000	2.3	0.0
		Biological process	GO:0008104~protein localization	0.000	1.8	0.2
		Keyword	protein transport	0.000	2.1	0.2
		Biological process	GO:0015031~protein transport	0.000	1.9	0.2

		Biological process	GO:0045184~establishment of protein localization	0.000	1.8	0.3
		Biological process	GO:0006913~nucleocytoplasmic transport	0.001	3.5	1.0
		Biological process	GO:0051169~nuclear transport	0.001	3.4	1.2
15	2.2	Biological process	GO:0051146~striated muscle cell differentiation	0.000	3.8	0.5
		Biological process	GO:0014706~striated muscle tissue development	0.001	3.1	1.0
		Biological process	GO:0055002~striated muscle cell development	0.001	4.7	1.0
		Biological process	GO:0042692~muscle cell differentiation	0.001	3.1	1.6
		Biological process	GO:0060537~muscle tissue development	0.001	2.9	1.9
		Biological process	GO:0055001~muscle cell development	0.001	4.1	2.3
16	2.2	Biological process	GO:0007010~cytoskeleton organization	0.000	2.2	0.4
17	2.1	Molecular function	GO:0008047~enzyme activator activity	0.000	2.6	0.1
		Molecular function	GO:0030695~GTPase regulator activity	0.000	2.2	0.3
		Molecular function	GO:0060589~nucleoside-triphosphatase regulator activity	0.000	2.2	0.4
		Keyword	GTPase activation	0.001	2.9	1.6
		Molecular function	GO:0005096~GTPase activator activity	0.001	2.5	1.9

		Molecular function	GO:0005083~small GTPase regulator activity	0.002	2.3	3.6
18	2	Cellular component	GO:0046930~pore complex	0.000	4.6	0.2
		Cellular component	GO:0005635~nuclear envelope	0.001	3.0	0.7
		Cellular component	GO:0005643~nuclear pore	0.001	4.6	0.9
19	2	Interpro	IPR011989:Armadillo-like helical	0.002	2.9	3.2
20	1.9	Biological process	GO:0051146~striated muscle cell differentiation	0.000	3.8	0.5
		Biological process	GO:0055002~striated muscle cell development	0.001	4.7	1.0
		Biological process	GO:0055001~muscle cell development	0.001	4.1	2.3
21	1.7	Molecular function	GO:0017124~SH3 domain binding	0.002	3.6	2.7
22	1.7	Biological process	GO:0009152~purine ribonucleotide biosynthetic process	0.000	3.7	0.2
		Biological process	GO:0009260~ribonucleotide biosynthetic process	0.000	3.5	0.3
		Biological process	GO:0009150~purine ribonucleotide metabolic process	0.000	3.3	0.5
		Biological process	GO:0009165~nucleotide biosynthetic process	0.000	2.7	0.8
		Biological process	GO:0009259~ribonucleotide metabolic process	0.001	3.1	0.9
		Biological process	GO:0034654~nucleobase, nucleoside, nucleotide and nucleic acid	0.001	2.7	1.1

			biosynthetic process			
		Biological process	GO:0034404~nucleobase, nucleoside and nucleotide biosynthetic process	0.001	2.7	1.1
		Biological process	GO:0044271~nitrogen compound biosynthetic process	0.001	2.1	2.0
		Biological process	GO:0006164~purine nucleotide biosynthetic process	0.001	2.9	2.0
		Biological process	GO:0009206~purine ribonucleoside triphosphate biosynthetic process	0.002	3.3	2.9
		Biological process	GO:0009201~ribonucleoside triphosphate biosynthetic process	0.002	3.3	2.9
		Biological process	GO:0006163~purine nucleotide metabolic process	0.002	2.6	2.9
		Biological process	GO:0009145~purine nucleoside triphosphate biosynthetic process	0.002	3.3	3.1
		Biological process	GO:0009142~nucleoside triphosphate biosynthetic process	0.002	3.3	3.4
		Biological process	GO:0006754~ATP biosynthetic process	0.002	3.4	4.2
23	1.7	Kegg pathway	mmu05223:Non-small cell lung cancer	0.000	4.9	0.5
		Kegg pathway	mmu05215:Prostate cancer	0.001	3.6	1.0
		Kegg pathway	mmu05200:Pathways in cancer	0.003	2.0	3.1
24	1.6	Biological process	GO:0030334~regulation of cell migration	0.002	3.4	2.6

		Biological process	GO:0040012~regulation of locomotion	0.002	3.1	3.1
25	1.6	Biological process	GO:0007049~cell cycle	0.000	1.8	0.5
26	1.5	Interpro	IPR019775:WD40 repeat, conserved site	0.002	2.2	2.9
		Keyword	wd repeat	0.003	2.1	4.0
27	1.5	Molecular function	GO:0004221~ubiquitin thiolesterase activity	0.001	4.0	1.3
28	1.4	Molecular function	GO:0005543~phospholipid binding	0.003	2.8	4.8

Table 13. Differential expressed microRNAs in Ts65Dn soleus.

Name	Chromosome location	Up- or down-regulated?	Fold change
mmu-mir-99a	16	Down	1.9
mmu-mir-103-2	2	Up	1.7
mmu-mir-138-2	8	Down	1.5
mmu-mir-199a-1	9	Down	1.9
mmu-mir-181a-2	2	Down	1.6
mmu-mir-326	7	Down	1.9
mmu-mir-680-3	12	Down	2.0
mmu-mir-693	17	Down	1.4

Table 14. Effected pathways by microRNA identified using mirPATH.

KEGG pathway	KEGG pathway ID	Number of genes	-ln(p-value)
Wnt signaling pathway	mmu04310	39	20.76
Colorectal cancer	mmu05210	26	17.78
Acute myeloid leukemia	mmu05221	20	16.8
Long-term potentiation	mmu04720	21	16.09
Focal adhesion	mmu04510	44	15.81
mTOR signaling pathway	mmu04150	18	15.23
Axon guidance	mmu04360	32	14.3
Renal cell carcinoma	mmu05211	21	13.93
Glioma	mmu05214	19	12.79
Prostate cancer	mmu05215	24	12.66
ErbB signaling pathway	mmu04012	23	11.93
Insulin signaling pathway	mmu04910	32	11.87
Melanogenesis	mmu04916	25	11.62
Non-small cell lung cancer	mmu05223	15	8.99
Long-term depression	mmu04730	19	8.55
Chronic myeloid leukemia	mmu05220	19	8.55
Regulation of actin cytoskeleton	mmu04810	40	8.52
Type II diabetes mellitus	mmu04930	13	7.49
Endometrial cancer	mmu05213	14	7.28

|			
TGF-beta signaling pathway	mmu04350	20	6.91
GnRH signaling pathway	mmu04912	21	6.73
Ubiquitin mediated proteolysis	mmu04120	26	6.5
T cell receptor signaling pathway	mmu04660	20	5.97
Melanoma	mmu05218	16	5.67
Dorso-ventral axis formation	mmu04320	8	5.46
Pyrimidine metabolism	mmu00240	1	5.38
Pancreatic cancer	mmu05212	16	5.27
Phosphatidylinositol signaling system	mmu04070	15	4.51
Hedgehog signaling pathway	mmu04340	12	4.21
Arachidonic acid metabolism	mmu00590	1	4.17
Small cell lung cancer	mmu05222	17	4.03
Adherens junction	mmu04520	15	4.01
MAPK signaling pathway	mmu04010	40	3.97
Basal cell carcinoma	mmu05217	12	3.83
Cell cycle	mmu04110	20	3.8
p53 signaling pathway	mmu04115	13	3.4
Complement and coagulation cascades	mmu04610	2	3.19
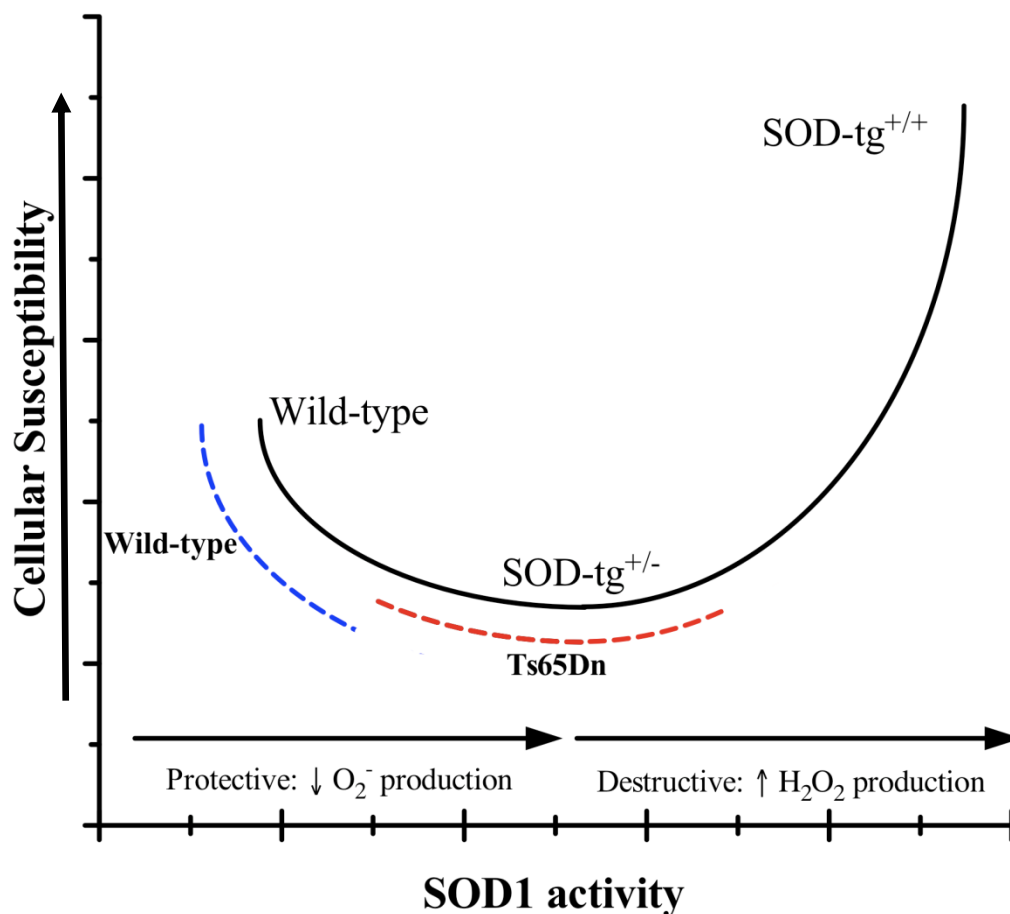
Figure 18. Model of the biphasic effect of SOD1 activity on oxidant production (cellular susceptibility to oxidative stress) proposed by Xing and colleagues is shown (132). The model proposes that increases in SOD1 activity are protective when the dismutation of superoxide radical predominates, but destructive when the production of hydrogen peroxide predominates. SOD1-tg$^{+/-}$ are hemizygous for human SOD1. SOD1-tg$^{+/+}$ are homozygous for human SOD1. We propose that WT muscles from our study (dashed blue line) are comparable to WT in the proposed model. Ts65Dn muscle (dashed red line) is comparable to SOD-tg$^{+/-}$.

CHAPTER IV. BIBLIOGRAPHY

1. Down JL (1995) Observations on an ethnic classification of idiots. 1866. *Ment. Retard.* 33(1):54-56.

2. Lejeune J, Gautier M, & Turpin R (1959) [Study of somatic chromosomes from 9 mongoloid children.]. *C. R. Hebd. Seances Acad. Sci.* 248(11):1721-1722.

3. Nikolaienko O, Nguyen C, Crinc LS, Cios KJ, & Gardiner K (2005) Human chromosome 21/Down syndrome gene function and pathway database. *Gene* 364:90-98.

4. Korenberg JR*, et al.* (1994) Down syndrome phenotypes: the consequences of chromosomal imbalance. *Proc. Natl. Acad. Sci. U. S. A.* 91(11):4997-5001.

5. Epstein CJ*, et al.* (1991) Protocols to establish genotype-phenotype correlations in Down syndrome. *Am. J. Hum. Genet.* 49(1):207-235.

6. Cowley PM*, et al.* (2010) Physical fitness predicts functional tasks in individuals with Down syndrome. *Med. Sci. Sports Exerc.* 42(2):388-393.

7. Pitetti KH & Boneh S (1995) Cardiovascular fitness as related to leg strength in adults with mental retardation. *Med. Sci. Sports Exerc.* 27(3):423-428.

8. Carmeli E, Kessel S, Bar-Chad S, & Merrick J (2004) A comparison between older persons with down syndrome and a control group: clinical characteristics, functional status and sensorimotor function. *Downs Syndr Res Pract* 9(1):17-24.

9. Carmeli E, Barchad S, Lenger R, & Coleman R (2002) Muscle power, locomotor performance and flexibility in aging mentally-retarded adults with and without Down's syndrome. *J Musculoskelet Neuronal Interact* 2(5):457-462.

10. Fernhall B & Pitetti KH (2001) Limitations to work capacity in individuals with intellectual disabilities. *Clin Exerc Physiol* 3:176-185.

11. Fernhall B*, et al.* (1996) Cardiorespiratory capacity of individuals with mental retardation including Down syndrome. *Med. Sci. Sports Exerc.* 28(3):366-371.

12. Angelopoulou N*, et al.* (2000) Bone mineral density and muscle strength in young men with mental retardation (with and without Down syndrome). *Calcif. Tissue Int.* 66(3):176-180.

13. Angelopoulou N, Tsimaras V, Christoulas K, Kokaridas D, & Mandroukas K (1999) Isokinetic knee muscle strength of individuals with mental retardation, a comparative study. *Percept. Mot. Skills* 88(3 Pt 1):849-855.

14. Carmeli E, Kessel S, Coleman R, & Ayalon M (2002) Effects of a treadmill walking program on muscle strength and balance in elderly people with Down syndrome. *J. Gerontol. A. Biol. Sci. Med. Sci.* 57(2):M106-110.

15. Cioni M*, et al.* (1994) Strength deficit of knee extensor muscles of individuals with Down syndrome from childhood to adolescence. *Am. J. Ment. Retard.* 99(2):166-174.

16. Croce RV, Pitetti KH, Horvat M, & Miller J (1996) Peak torque, average power, and hamstrings/quadriceps ratios in nondisabled adults and adults with mental retardation. *Arch. Phys. Med. Rehabil.* 77(4):369-372.

17. Horvat M, Pitetti KH, & Croce R (1997) Isokinetic torque, average power, and flexion/extension ratios in nondisabled adults and adults with mental retardation. *J. Orthop. Sports Phys. Ther.* 25(6):395-399.

18. Mercer VS & Lewis CL (2001) Hip Abductor and Knee Extensor Muscle Strength of Children with and without Down Syndrome. *Pediatr Phys Ther* 13(1):18-26.

19. Morris AF, Vaughan SE, & Vaccaro P (1982) Measurements of neuromuscular tone and strength in Down's syndrome children. *J. Ment. Defic. Res.* 26(Pt 1):41-46.

20. Pitetti KH, Climstein M, Mays MJ, & Barrett PJ (1992) Isokinetic arm and leg strength of adults with Down syndrome: a comparative study. *Arch. Phys. Med. Rehabil.* 73(9):847-850.

21. Stanish HI & Draheim CC (2005) Walking habits of adults with mental retardation. *Ment. Retard.* 43(6):421-427.

22. Stancliffe RJ*, et al.* (2011) Overweight and obesity among adults with intellectual disabilities who use intellectual disability/developmental disability services in 20 u.s. States. *American journal on intellectual and developmental disabilities* 116(6):401-418.

23. Hawli Y, Nasrallah M, & El-Hajj Fuleihan G (2009) Endocrine and musculoskeletal abnormalities in patients with Down syndrome. *Nat. Rev. Endocrinol.* 5(6):327-334.

24.   Vincent HK, Vincent KR, & Lamb KM (2010) Obesity and mobility disability in the older adult. *Obes. Rev.* 11(8):568-579.

25.   Eyman RK & Call TL (1991) Life expectancy of persons with Down syndrome. *Am. J. Ment. Retard.* 95(6):603-612.

26.   Coppus AM*, et al.* (2008) Survival in elderly persons with Down syndrome. *J. Am. Geriatr. Soc.* 56(12):2311-2316.

27.   Croce RV & Horvat M (1992) Effects of reinforcement based exercise on fitness and work productivity in adults with mental retardation. *Adap Phys Act Quart* 9:148-178.

28.   Nordgren B & Backstrom L (1971) Correlations between muscular strength and industrial work performance in mentally retarded persons. *Acta Paediatr. Scand. Suppl.* 217:122-126.

29.   Stephens DL, Collins MD, & Dodder RA (2005) A longitudinal study of employment and skill acquisition among individuals with developmental disabilities. *Res. Dev. Disabil.* 26(5):469-486.

30.   Wehmeyer ML & Bolding N (2001) Enhanced self-determination of adults with intellectual disability as an outcome of moving to community-based work or living environments. *J. Intellect. Disabil. Res.* 45(Pt 5):371-383.

31.   Halliwell B & Gutteridge JM (2007) *Free Radicals in Biology and Medicine* (Oxford University Press, New York) 4th Ed.

32.   Kedziora J & Bartosz G (1988) Down's syndrome: a pathology involving the lack of balance of reactive oxygen species. *Free Radic. Biol. Med.* 4(5):317-330.

33.   Sies H (1997) Oxidative stress: oxidants and antioxidants. *Exp. Physiol.* 82(2):291-295.

34.   Jones DP (2006) Redefining oxidative stress. *Antioxid. Redox. Signal.* 8(9-10):1865-1879.

35.   Reid MB, Shoji T, Moody MR, & Entman ML (1992) Reactive oxygen in skeletal muscle. II. Extracellular release of free radicals. *J. Appl. Physiol.* 73(5):1805-1809.

36.   Reid MB*, et al.* (1992) Reactive oxygen in skeletal muscle. I. Intracellular oxidant kinetics and fatigue in vitro. *J. Appl. Physiol.* 73(5):1797-1804.

37. Jackson MJ, Edwards RH, & Symons MC (1985) Electron spin resonance studies of intact mammalian skeletal muscle. *Biochim. Biophys. Acta* 847(2):185-190.

38. Reid MB (2001) Invited Review: redox modulation of skeletal muscle contraction: what we know and what we don't. *J. Appl. Physiol.* 90(2):724-731.

39. Reid MB, Khawli FA, & Moody MR (1993) Reactive oxygen in skeletal muscle. III. Contractility of unfatigued muscle. *J. Appl. Physiol.* 75(3):1081-1087.

40. Moylan JS & Reid MB (2007) Oxidative stress, chronic disease, and muscle wasting. *Muscle Nerve* 35(4):411-429.

41. Powers SK & Jackson MJ (2008) Exercise-induced oxidative stress: cellular mechanisms and impact on muscle force production. *Physiol. Rev.* 88(4):1243-1276.

42. Busciglio J & Yankner BA (1995) Apoptosis and increased generation of reactive oxygen species in Down's syndrome neurons in vitro. *Nature* 378(6559):776-779.

43. Jovanovic SV, Clements D, & MacLeod K (1998) Biomarkers of oxidative stress are significantly elevated in Down syndrome. *Free Radic. Biol. Med.* 25(9):1044-1048.

44. Odetti P*, et al.* (1998) Early glycoxidation damage in brains from Down's syndrome. *Biochem. Biophys. Res. Commun.* 243(3):849-851.

45. Zitnanova I*, et al.* (2006) Markers of oxidative stress in children with Down syndrome. *Clin. Chem. Lab. Med.* 44(3):306-310.

46. Moore CS & Roper RJ (2007) The power of comparative and developmental studies for mouse models of Down syndrome. *Mamm. Genome* 18(6-7):431-443.

47. Salehi A, Faizi M, Belichenko PV, & Mobley WC (2007) Using mouse models to explore genotype-phenotype relationship in Down syndrome. *Ment. Retard. Dev. Disabil. Res. Rev.* 13(3):207-214.

48. Moore CS (2006) Postnatal lethality and cardiac anomalies in the Ts65Dn Down syndrome mouse model. *Mamm. Genome* 17(10):1005-1012.

49. Richtsmeier JT, Baxter LL, & Reeves RH (2000) Parallels of craniofacial maldevelopment in Down syndrome and Ts65Dn mice. *Dev. Dyn.* 217(2):137-145.

50.   Reeves RH, *et al.* (1995) A mouse model for Down syndrome exhibits learning and behaviour deficits. *Nat. Genet.* 11(2):177-184.

51.   Costa AC, Walsh K, & Davisson MT (1999) Motor dysfunction in a mouse model for Down syndrome. *Physiol. Behav.* 68(1-2):211-220.

52.   Yarom R, Sagher U, Havivi Y, Peled IJ, & Wexler MR (1986) Myofibers in tongues of Down's syndrome. *J. Neurol. Sci.* 73(3):279-287.

53.   Kahlem P, *et al.* (2004) Transcript level alterations reflect gene dosage effects across multiple tissues in a mouse model of down syndrome. *Genome Res.* 14(7):1258-1267.

54.   Chrast R, *et al.* (2000) The mouse brain transcriptome by SAGE: differences in gene expression between P30 brains of the partial trisomy 16 mouse model of Down syndrome (Ts65Dn) and normals. *Genome Res.* 10(12):2006-2021.

55.   Brooksbank BW & Balazs R (1984) Superoxide dismutase, glutathione peroxidase and lipoperoxidation in Down's syndrome fetal brain. *Brain Res.* 318(1):37-44.

56.   Lorenzo LP, *et al.* (2011) Defective Hematopoietic Stem Cell and Lymphoid Progenitor Development in the Ts65Dn Mouse Model of Down Syndrome: Potential Role of Oxidative Stress. *Antioxid. Redox. Signal.* 15(8):2083-2094.

57.   Shichiri M, *et al.* (2011) alpha-Tocopherol suppresses lipid peroxidation and behavioral and cognitive impairments in the Ts65Dn mouse model of Down syndrome. *Free Radic. Biol. Med.* 50(12):1801-1811.

58.   Cefalu JA, *et al.* (1998) Jejunal function and plasma amino acid concentrations in the segmental trisomic Ts65Dn mouse. *Growth. Dev. Aging* 62(1-2):47-59.

59.   Larsson L, Grimby G, & Karlsson J (1979) Muscle strength and speed of movement in relation to age and muscle morphology. *J. Appl. Physiol.* 46(3):451-456.

60.   Overend TJ, Cunningham DA, Kramer JF, Lefcoe MS, & Paterson DH (1992) Knee extensor and knee flexor strength: cross-sectional area ratios in young and elderly men. *J. Gerontol.* 47(6):M204-210.

61.   Cowley PM, *et al.* (The effect of progressive resistance training on leg strength, aerobic capacity and functional tasks of daily living in persons with Down syndrome. *Disabil. Rehabil.*

62.   Carmeli E, Ayalon M, Barchad S, Sheklow SL, & Reznick AZ (2002) Isokinetic leg strength of institutionalized older adults with mental retardation with and without Down's syndrome. *J. Strength Cond. Res.* 16(2):316-320.

63.   Droge W (2002) Free radicals in the physiological control of cell function. *Physiol. Rev.* 82(1):47-95.

64.   Jackson MJ, Pye D, & Palomero J (2007) The production of reactive oxygen and nitrogen species by skeletal muscle. *J. Appl. Physiol.* 102(4):1664-1670.

65.   Stamler JS & Meissner G (2001) Physiology of nitric oxide in skeletal muscle. *Physiol. Rev.* 81(1):209-237.

66.   McClung JM, Judge AR, Talbert EE, & Powers SK (2009) Calpain-1 is required for hydrogen peroxide-induced myotube atrophy. *Am J Physiol Cell Physiol* 296(2):C363-371.

67.   Falk DJ*, et al.* (2006) Mechanical ventilation promotes redox status alterations in the diaphragm. *J. Appl. Physiol.* 101(4):1017-1024.

68.   Brugge K, Nichols S, Saitoh T, & Trauner D (1999) Correlations of glutathione peroxidase activity with memory impairment in adults with Down syndrome. *Biol. Psychiatry* 46(12):1682-1689.

69.   Crosti N, Bajer J, Gentile M, Resta G, & Serra A (1989) Catalase and glutathione peroxidase activity in cells with trisomy 21. *Clin. Genet.* 36(2):107-116.

70.   Gerli G*, et al.* (1990) Erythrocyte antioxidant system in Down syndrome. *Am. J. Med. Genet. Suppl.* 7:272-273.

71.   Gulesserian T, Seidl R, Hardmeier R, Cairns N, & Lubec G (2001) Superoxide dismutase SOD1, encoded on chromosome 21, but not SOD2 is overexpressed in brains of patients with Down syndrome. *J. Investig. Med.* 49(1):41-46.

72.   Kurobe N, Suzuki F, Okajima K, & Kato K (1990) Sensitive enzyme immunoassay for human Cu/Zn superoxide dismutase. *Clin. Chim. Acta* 187(1):11-20.

73.   Muchova J*, et al.* (2001) Influence of age on activities of antioxidant enzymes and lipid peroxidation products in erythrocytes and neutrophils of Down syndrome patients. *Free Radic. Biol. Med.* 31(4):499-508.

74.   Pastor MC, *et al.* (1998) Antioxidant enzymes and fatty acid status in erythrocytes of Down's syndrome patients. *Clin. Chem.* 44(5):924-929.

75.   Pastore A, *et al.* (2003) Glutathione metabolism and antioxidant enzymes in children with Down syndrome. *J. Pediatr.* 142(5):583-585.

76.   Percy ME, *et al.* (1990) Red cell superoxide dismutase, glutathione peroxidase and catalase in Down syndrome patients with and without manifestations of Alzheimer disease. *Am. J. Med. Genet.* 35(4):459-467.

77.   De La Torre R, *et al.* (1996) Overexpression of copper-zinc superoxide dismutase in trisomy 21. *Experientia* 52(9):871-873.

78.   Ordonez FJ, Rosety-Plaza M, & Rosety-Rodriguez M (2006) Glucose-6-phosphatedehydrogenase is also increased in erythrocytes from adolescents with Down syndrome. *Downs Syndr Res Pract* 11(2):84-87.

79.   Nunomura A, *et al.* (2000) Neuronal oxidative stress precedes amyloid-beta deposition in Down syndrome. *J. Neuropathol. Exp. Neurol.* 59(11):1011-1017.

80.   Pinto M, Neves J, Palha M, & Bicho M (2002) Oxidative stress in Portuguese children with Down syndrome. *Downs Syndr Res Pract* 8(2):79-82.

81.   Flore P, *et al.* (2008) Oxidative stress and metabolism at rest and during exercise in persons with Down syndrome. *Eur. J. Cardiovasc. Prev. Rehabil.* 15(1):35-42.

82.   Massaccesi L, *et al.* (2006) Erythrocyte glycohydrolases in subjects with trisomy 21: could Down's syndrome be a model of accelerated ageing? *Mech. Ageing Dev.* 127(4):324-331.

83.   Casado A, Lopez-Fernandez ME, & Ruiz R (2007) Lipid peroxidation in Down syndrome caused by regular trisomy 21, trisomy 21 by Robertsonian translocation and mosaic trisomy 21. *Clin. Chem. Lab. Med.* 45(1):59-62.

84.   Pratico D, *et al.* (2000) Down's syndrome is associated with increased 8,12-iso-iPF2alpha-VI levels: evidence for enhanced lipid peroxidation in vivo. *Ann. Neurol.* 48(5):795-798.

85.   Carratelli M, *et al.* (2001) Reactive oxygen metabolites and prooxidant status in children with Down's syndrome. *Int. J. Clin. Pharmacol. Res.* 21(2):79-84.

86.   Pallardo FV, *et al.* (2006) Multiple evidence for an early age pro-oxidant state in Down Syndrome patients. *Biogerontology* 7(4):211-220.

160

87. Zana M, *et al.* (2006) Age-dependent oxidative stress-induced DNA damage in Down's lymphocytes. *Biochem. Biophys. Res. Commun.* 345(2):726-733.

88. Kandel ER, Schwartz JH, & Jessel TM (2000) *Principles of Neural Science* (McGraw-Hill, USA) Fourth Ed.

89. MacIntosh BR, Gardiner PF, & McComas AJ (2006) *Skeletal Muscle: Form and Function* (Human Kinetics, Champaign, IL) Second Ed.

90. Balon TW & Nadler JL (1994) Nitric oxide release is present from incubated skeletal muscle preparations. *J. Appl. Physiol.* 77(6):2519-2521.

91. Close GL, Ashton T, McArdle A, & Jackson MJ (2005) Microdialysis studies of extracellular reactive oxygen species in skeletal muscle: factors influencing the reduction of cytochrome c and hydroxylation of salicylate. *Free Radic. Biol. Med.* 39(11):1460-1467.

92. Pattwell DM, McArdle A, Morgan JE, Patridge TA, & Jackson MJ (2004) Release of reactive oxygen and nitrogen species from contracting skeletal muscle cells. *Free Radic. Biol. Med.* 37(7):1064-1072.

93. Andrade FH, Reid MB, Allen DG, & Westerblad H (1998) Effect of hydrogen peroxide and dithiothreitol on contractile function of single skeletal muscle fibres from the mouse. *J. Physiol.* 509 (Pt 2):565-575.

94. Andrade FH, Reid MB, & Westerblad H (2001) Contractile response of skeletal muscle to low peroxide concentrations: myofibrillar calcium sensitivity as a likely target for redox-modulation. *FASEB J.* 15(2):309-311.

95. Kobzik L, Reid MB, Bredt DS, & Stamler JS (1994) Nitric oxide in skeletal muscle. *Nature* 372(6506):546-548.

96. Supinski G, *et al.* (1999) Peroxynitrite induces contractile dysfunction and lipid peroxidation in the diaphragm. *J. Appl. Physiol.* 87(2):783-791.

97. Allen DG, Lamb GD, & Westerblad H (2008) Skeletal muscle fatigue: cellular mechanisms. *Physiol. Rev.* 88(1):287-332.

98. Khawli FA & Reid MB (1994) N-acetylcysteine depresses contractile function and inhibits fatigue of diaphragm in vitro. *J. Appl. Physiol.* 77(1):317-324.

99. Matuszczak Y, *et al.* (2005) Effects of N-acetylcysteine on glutathione oxidation and fatigue during handgrip exercise. *Muscle Nerve* 32(5):633-638.

100. Reid MB, Stokic DS, Koch SM, Khawli FA, & Leis AA (1994) N-acetylcysteine inhibits muscle fatigue in humans. *J. Clin. Invest.* 94(6):2468-2474.

101. Supinski G, Nethery D, Stofan D, & DiMarco A (1997) Effect of free radical scavengers on diaphragmatic fatigue. *Am. J. Respir. Crit. Care Med.* 155(2):622-629.

102. Ferreira LF & Reid MB (2008) Muscle-derived ROS and thiol regulation in muscle fatigue. *J. Appl. Physiol.* 104(3):853-860.

103. Reid MB (2008) Free radicals and muscle fatigue: Of ROS, canaries, and the IOC. *Free Radic. Biol. Med.* 44(2):169-179.

104. Supinski GS & Callahan LA (2007) Free radical-mediated skeletal muscle dysfunction in inflammatory conditions. *J. Appl. Physiol.* 102(5):2056-2063.

105. Powers SK, Kavazis AN, & DeRuisseau KC (2005) Mechanisms of disuse muscle atrophy: role of oxidative stress. *Am. J. Physiol. Regul. Integr. Comp. Physiol.* 288(2):R337-344.

106. Jones DP (2008) Radical-free biology of oxidative stress. *Am J Physiol Cell Physiol* 295(4):C849-868.

107. Kourie JI (1998) Interaction of reactive oxygen species with ion transport mechanisms. *Am. J. Physiol.* 275(1 Pt 1):C1-24.

108. Sun J, Xu L, Eu JP, Stamler JS, & Meissner G (2001) Classes of thiols that influence the activity of the skeletal muscle calcium release channel. *J. Biol. Chem.* 276(19):15625-15630.

109. Ishii T, *et al.* (1998) Inhibition of skeletal muscle sarcoplasmic reticulum Ca2+-ATPase by nitric oxide. *FEBS Lett.* 440(1-2):218-222.

110. Viner RI, Williams TD, & Schoneich C (2000) Nitric oxide-dependent modification of the sarcoplasmic reticulum Ca-ATPase: localization of cysteine target sites. *Free Radic. Biol. Med.* 29(6):489-496.

111. Xu KY, Zweier JL, & Becker LC (1997) Hydroxyl radical inhibits sarcoplasmic reticulum Ca(2+)-ATPase function by direct attack on the ATP binding site. *Circ. Res.* 80(1):76-81.

112. Putkey JA, Dotson DG, & Mouawad P (1993) Formation of inter- and intramolecular disulfide bonds can activate cardiac troponin C. *J. Biol. Chem.* 268(10):6827-6830.

113. Williams DL, Jr. & Swenson CA (1982) Disulfide bridges in tropomyosin. Effect on ATPase activity of actomyosin. *Eur. J. Biochem.* 127(3):495-499.

114. Ajtai K & Burghardt TP (1989) Fluorescent modification and orientation of myosin sulfhydryl 2 in skeletal muscle fibers. *Biochemistry (Mosc.)* 28(5):2204-2210.

115. Konczol F, Lorinczy D, & Belagyi J (1998) Effect of oxygen free radicals on myosin in muscle fibres. *FEBS Lett.* 427(3):341-344.

116. Canton M, Neverova I, Menabo R, Van Eyk J, & Di Lisa F (2004) Evidence of myofibrillar protein oxidation induced by postischemic reperfusion in isolated rat hearts. *Am. J. Physiol. Heart Circ. Physiol.* 286(3):H870-877.

117. DalleDonne I, Milzani A, & Colombo R (1995) H2O2-treated actin: assembly and polymer interactions with cross-linking proteins. *Biophys. J.* 69(6):2710-2719.

118. Muller FL*, et al.* (2006) Absence of CuZn superoxide dismutase leads to elevated oxidative stress and acceleration of age-dependent skeletal muscle atrophy. *Free Radic. Biol. Med.* 40(11):1993-2004.

119. Jang YC*, et al.* (2010) Increased superoxide in vivo accelerates age-associated muscle atrophy through mitochondrial dysfunction and neuromuscular junction degeneration. *FASEB J.* 24(5):1376-1390.

120. Flood DG*, et al.* (1999) Hindlimb motor neurons require Cu/Zn superoxide dismutase for maintenance of neuromuscular junctions. *Am. J. Pathol.* 155(2):663-672.

121. Shefner JM*, et al.* (1999) Mice lacking cytosolic copper/zinc superoxide dismutase display a distinctive motor axonopathy. *Neurology* 53(6):1239-1246.

122. Larkin LM*, et al.* (Skeletal muscle weakness due to deficiency of Cu,Zn superoxide dismutase is associated with loss of functional innervation. *Am. J. Physiol. Regul. Integr. Comp. Physiol.*

123. Kostrominova TY (2010) Advanced age-related denervation and fiber-type grouping in skeletal muscle of SOD1 knockout mice. *Free Radic. Biol. Med.* 49(10):1582-1593.

124.   Vasilaki A*, et al.* (2010) The age-related failure of adaptive responses to contractile activity in skeletal muscle is mimicked in young mice by deletion of Cu,Zn superoxide dismutase. *Aging Cell* 9(6):979-990.

125.   Rando TA, Crowley RS, Carlson EJ, Epstein CJ, & Mohapatra PK (1998) Overexpression of copper/zinc superoxide dismutase: a novel cause of murine muscular dystrophy. *Ann. Neurol.* 44(3):381-386.

126.   McClung JM*, et al.* (2010) Overexpression of antioxidant enzymes in diaphragm muscle does not alter contraction-induced fatigue or recovery. *Exp. Physiol.* 95(1):222-231.

127.   Peled-Kamar M*, et al.* (1997) Oxidative stress mediates impairment of muscle function in transgenic mice with elevated level of wild-type Cu/Zn superoxide dismutase. *Proc. Natl. Acad. Sci. U. S. A.* 94(8):3883-3887.

128.   Avraham KB, Schickler M, Sapoznikov D, Yarom R, & Groner Y (1988) Down's syndrome: abnormal neuromuscular junction in tongue of transgenic mice with elevated levels of human Cu/Zn-superoxide dismutase. *Cell* 54(6):823-829.

129.   Avraham KB, Sugarman H, Rotshenker S, & Groner Y (1991) Down's syndrome: morphological remodelling and increased complexity in the neuromuscular junction of transgenic CuZn-superoxide dismutase mice. *J. Neurocytol.* 20(3):208-215.

130.   Yarom R*, et al.* (1988) Premature aging changes in neuromuscular junctions of transgenic mice with an extra human CuZnSOD gene: a model for tongue pathology in Down's syndrome. *J. Neurol. Sci.* 88(1-3):41-53.

131.   Groner Y*, et al.* (1990) Down syndrome clinical symptoms are manifested in transfected cells and transgenic mice overexpressing the human Cu/Zn-superoxide dismutase gene. *J. Physiol. (Paris)* 84(1):53-77.

132.   Xing J, Yu Y, & Rando TA (2002) The modulation of cellular susceptibility to oxidative stress: protective and destructive actions of Cu,Zn-superoxide dismutase. *Neurobiol. Dis.* 10(3):234-246.

133.   Wong M & Martin LJ (2010) Skeletal muscle-restricted expression of human SOD1 causes motor neuron degeneration in transgenic mice. *Hum. Mol. Genet.* 19(11):2284-2302.

134.   Rosen DR*, et al.* (1993) Mutations in Cu/Zn superoxide dismutase gene are associated with familial amyotrophic lateral sclerosis. *Nature* 362(6415):59-62.

135. Barber SC & Shaw PJ (2010) Oxidative stress in ALS: key role in motor neuron injury and therapeutic target. *Free Radic. Biol. Med.* 48(5):629-641.

136. Dobrowolny G, *et al.* (2008) Skeletal muscle is a primary target of SOD1G93A-mediated toxicity. *Cell Metab.* 8(5):425-436.

137. Hattori M, *et al.* (2000) The DNA sequence of human chromosome 21. *Nature* 405(6784):311-319.

138. Ait Yahya-Graison E, *et al.* (2007) Classification of human chromosome 21 gene-expression variations in Down syndrome: impact on disease phenotypes. *Am. J. Hum. Genet.* 81(3):475-491.

139. Prandini P, *et al.* (2007) Natural gene-expression variation in down syndrome modulates the outcome of gene-dosage imbalance. *Am. J. Hum. Genet.* 81(2):252-263.

140. Lockstone HE, *et al.* (2007) Gene expression profiling in the adult Down syndrome brain. *Genomics* 90(6):647-660.

141. Mao R, *et al.* (2005) Primary and secondary transcriptional effects in the developing human Down syndrome brain and heart. *Genome Biol.* 6(13):R107.

142. Freeman SB, *et al.* (2008) Ethnicity, sex, and the incidence of congenital heart defects: a report from the National Down Syndrome Project. *Genet. Med.* 10(3):173-180.

143. Roper RJ & Reeves RH (2006) Understanding the basis for Down syndrome phenotypes. *PLoS Genet.* 2(3):e50.

144. Gardiner K, Fortna A, Bechtel L, & Davisson MT (2003) Mouse models of Down syndrome: how useful can they be? Comparison of the gene content of human chromosome 21 with orthologous mouse genomic regions. *Gene* 318:137-147.

145. Patterson D & Costa AC (2005) Down syndrome and genetics - a case of linked histories. *Nat. Rev. Genet.* 6(2):137-147.

146. Davisson MT, Schmidt C, & Akeson EC (1990) Segmental trisomy of murine chromosome 16: a new model system for studying Down syndrome. *Prog. Clin. Biol. Res.* 360:263-280.

147. Davisson MT, *et al.* (1993) Segmental trisomy as a mouse model for Down syndrome. *Prog. Clin. Biol. Res.* 384:117-133.

148. Baxter LL, Moran TH, Richtsmeier JT, Troncoso J, & Reeves RH (2000) Discovery and genetic localization of Down syndrome cerebellar phenotypes using the Ts65Dn mouse. *Hum. Mol. Genet.* 9(2):195-202.

149. Belichenko PV*, et al.* (2004) Synaptic structural abnormalities in the Ts65Dn mouse model of Down Syndrome. *J. Comp. Neurol.* 480(3):281-298.

150. Klein SL*, et al.* (1996) Characterization of sensorimotor performance, reproductive and aggressive behaviors in segmental trisomic 16 (Ts65Dn) mice. *Physiol. Behav.* 60(4):1159-1164.

151. Salehi A*, et al.* (2006) Increased App expression in a mouse model of Down's syndrome disrupts NGF transport and causes cholinergic neuron degeneration. *Neuron* 51(1):29-42.

152. Holtzman DM*, et al.* (1996) Developmental abnormalities and age-related neurodegeneration in a mouse model of Down syndrome. *Proc. Natl. Acad. Sci. U. S. A.* 93(23):13333-13338.

153. Williams AD, Mjaatvedt CH, & Moore CS (2008) Characterization of the cardiac phenotype in neonatal Ts65Dn mice. *Dev. Dyn.* 237(2):426-435.

154. Roper RJ, St John HK, Philip J, Lawler A, & Reeves RH (2006) Perinatal loss of Ts65Dn Down syndrome mice. *Genetics* 172(1):437-443.

155. Villar AJ*, et al.* (2005) Identification and characterization of a new Down syndrome model, Ts[Rb(12.1716)]2Cje, resulting from a spontaneous Robertsonian fusion between T(171)65Dn and mouse chromosome 12. *Mamm. Genome* 16(2):79-90.

156. Sago H*, et al.* (2000) Genetic dissection of region associated with behavioral abnormalities in mouse models for Down syndrome. *Pediatr. Res.* 48(5):606-613.

157. Olson LE*, et al.* (2004) Down syndrome mouse models Ts65Dn, Ts1Cje, and Ms1Cje/Ts65Dn exhibit variable severity of cerebellar phenotypes. *Dev. Dyn.* 230(3):581-589.

158. Li Z*, et al.* (2007) Duplication of the entire 22.9 Mb human chromosome 21 syntenic region on mouse chromosome 16 causes cardiovascular and gastrointestinal abnormalities. *Hum. Mol. Genet.* 16(11):1359-1366.

159. O'Doherty A*, et al.* (2005) An aneuploid mouse strain carrying human chromosome 21 with Down syndrome phenotypes. *Science* 309(5743):2033-2037.

160.   Reeves RH (2006) Down syndrome mouse models are looking up. *Trends Mol. Med.* 12(6):237-240.

161.   Lyle R, Gehrig C, Neergaard-Henrichsen C, Deutsch S, & Antonarakis SE (2004) Gene expression from the aneuploid chromosome in a trisomy mouse model of down syndrome. *Genome Res.* 14(7):1268-1274.

162.   Shichiri M*, et al.* (2011) alpha-Tocopherol suppresses lipid peroxidation and behavioral and cognitive impairments in the Ts65Dn mouse model of Down syndrome. *Free Radic. Biol. Med.* 50(12):1801-1811.

163.   Rachidi M & Lopes C (2008) Mental retardation and associated neurological dysfunctions in Down syndrome: a consequence of dysregulation in critical chromosome 21 genes and associated molecular pathways. *Eur. J. Paediatr. Neurol.* 12(3):168-182.

164.   McCully KK & Faulkner JA (1983) Length-tension relationship of mammalian diaphragm muscles. *J. Appl. Physiol.* 54(6):1681-1686.

165.   Arbogast S*, et al.* (2007) Bowman-Birk inhibitor concentrate prevents atrophy, weakness, and oxidative stress in soleus muscle of hindlimb-unloaded mice. *J. Appl. Physiol.* 102(3):956-964.

166.   Close RI (1972) Dynamic properties of mammalian skeletal muscles. *Physiol. Rev.* 52(1):129-197.

167.   Brooks SV & Faulkner JA (1988) Contractile properties of skeletal muscles from young, adult and aged mice. *J. Physiol.* 404:71-82.

168.   Jones DA (1996) High-and low-frequency fatigue revisited. *Acta Physiol. Scand.* 156(3):265-270.

169.   Segal SS & Faulkner JA (1985) Temperature-dependent physiological stability of rat skeletal muscle in vitro. *Am. J. Physiol.* 248(3 Pt 1):C265-270.

170.   Edwards JN, Macdonald WA, van der Poel C, & Stephenson DG (2007) O2(*-) production at 37 degrees C plays a critical role in depressing tetanic force of isolated rat and mouse skeletal muscle. *Am J Physiol Cell Physiol* 293(2):C650-660.

171.   Moopanar TR & Allen DG (2005) Reactive oxygen species reduce myofibrillar Ca2+ sensitivity in fatiguing mouse skeletal muscle at 37 degrees C. *J. Physiol.* 564(Pt 1):189-199.

172. Zhang SJ, Bruton JD, Katz A, & Westerblad H (2006) Limited oxygen diffusion accelerates fatigue development in mouse skeletal muscle. *J. Physiol.* 572(Pt 2):551-559.

173. Agbulut O, Li Z, Mouly V, & Butler-Browne GS (1996) Analysis of skeletal and cardiac muscle from desmin knock-out and normal mice by high resolution separation of myosin heavy-chain isoforms. *Biol. Cell.* 88(3):131-135.

174. Plant DR, Gregorevic P, Williams DA, & Lynch GS (2001) Redox modulation of maximum force production of fast-and slow-twitch skeletal muscles of rats and mice. *J. Appl. Physiol.* 90(3):832-838.

175. van Lunteren E & Leahy P (2007) Gene expression microarrays and respiratory muscles. *Respir. Physiol. Neurobiol.* 156(2):103-115.

176. Stekel D (2003) *Microarray Bioinformatics* (Cambridge University Press, New York City) p 263.

177. Affymetrix (2007) Whole-transcript Expression Analysis. (Santa Clara).

178. Affymetrix (GeneChip® Gene 1.0 ST Array System for Human, Mouse and Rat. (Santa Clara).

179. Affymetrix (2004) GeneChip® Expression Analysis: Data Analysis Fundamentals. (Santa Clara).

180. Bekoff A & Betz WJ (1977) Physiological properties of dissociated muscle fibres obtained from innervated and denervated adult rat muscle. *J. Physiol.* 271(1):25-40.

181. Bischoff R (1986) Proliferation of muscle satellite cells on intact myofibers in culture. *Dev. Biol.* 115(1):129-139.

182. Canato M*, et al.* (2010) Mechanical and electrophysiological properties of the sarcolemma of muscle fibers in two murine models of muscle dystrophy: col6a1-/- and mdx. *J Biomed Biotechnol* 2010:981945.

183. Bruton JD*, et al.* (2010) Increased fatigue resistance linked to Ca2+-stimulated mitochondrial biogenesis in muscle fibres of cold-acclimated mice. *J. Physiol.* 588(Pt 21):4275-4288.

184. Calderon JC, Bolanos P, Torres SH, Rodriguez-Arroyo G, & Caputo C (2009) Different fibre populations distinguished by their calcium transient characteristics

in enzymatically dissociated murine flexor digitorum brevis and soleus muscles. *J. Muscle Res. Cell Motil.* 30(3-4):125-137.

185. Ravenscroft G*, et al.* (2007) Dissociated flexor digitorum brevis myofiber culture system--a more mature muscle culture system. *Cell Motil. Cytoskeleton* 64(10):727-738.

186. Liu Y, Carroll SL, Klein MG, & Schneider MF (1997) Calcium transients and calcium homeostasis in adult mouse fast-twitch skeletal muscle fibers in culture. *Am. J. Physiol.* 272(6 Pt 1):C1919-1927.

187. Palomero J, Pye D, Kabayo T, Spiller DG, & Jackson MJ (2008) In situ detection and measurement of intracellular reactive oxygen species in single isolated mature skeletal muscle fibers by real time fluorescence microscopy. *Antioxid. Redox. Signal.* 10(8):1463-1474.

188. Chen X, Zhong Z, Xu Z, Chen L, & Wang Y (2010) 2',7'-Dichlorodihydrofluorescein as a fluorescent probe for reactive oxygen species measurement: Forty years of application and controversy. *Free Radic. Res.* 44(6):587-604.

189. Murrant CL & Reid MB (2001) Detection of reactive oxygen and reactive nitrogen species in skeletal muscle. *Microsc. Res. Tech.* 55(4):236-248.

190. Arbogast S & Reid MB (2004) Oxidant activity in skeletal muscle fibers is influenced by temperature, CO2 level, and muscle-derived nitric oxide. *Am. J. Physiol. Regul. Integr. Comp. Physiol.* 287(4):R698-705.

191. Murrant CL, Andrade FH, & Reid MB (1999) Exogenous reactive oxygen and nitric oxide alter intracellular oxidant status of skeletal muscle fibres. *Acta Physiol. Scand.* 166(2):111-121.

192. Parker SE*, et al.* (Updated National Birth Prevalence estimates for selected birth defects in the United States, 2004-2006. *Birt. Defects Res. A. Clin. Mol. Teratol.* 88(12):1008-1016.

193. Sinet PM (1982) Metabolism of oxygen derivatives in down's syndrome. *Ann. N. Y. Acad. Sci.* 396:83-94.

194. Gollnick PD, Armstrong RB, Saubert CWt, Piehl K, & Saltin B (1972) Enzyme activity and fiber composition in skeletal muscle of untrained and trained men. *J. Appl. Physiol.* 33(3):312-319.

195. Agbulut O, Noirez P, Beaumont F, & Butler-Browne G (2003) Myosin heavy chain isoforms in postnatal muscle development of mice. *Biol. Cell.* 95(6):399-406.

196. Bradford MM (1976) A rapid and sensitive method for the quantitation of microgram quantities of protein utilizing the principle of protein-dye binding. *Anal. Biochem.* 72:248-254.

197. Rasband WS (1997-2011) ImageJ (U. S. National Institutes of Health, Bethesda), 1.43u.

198. Mizunoya W, Wakamatsu J, Tatsumi R, & Ikeuchi Y (2008) Protocol for high-resolution separation of rodent myosin heavy chain isoforms in a mini-gel electrophoresis system. *Anal. Biochem.* 377(1):111-113.

199. Talmadge RJ & Roy RR (1993) Electrophoretic separation of rat skeletal muscle myosin heavy-chain isoforms. *J. Appl. Physiol.* 75(5):2337-2340.

200. Kohn TA & Myburgh KH (2006) Electrophoretic separation of human skeletal muscle myosin heavy chain isoforms: the importance of reducing agents. *J. Physiol. Sci.* 56(5):355-360.

201. Tusher VG, Tibshirani R, & Chu G (2001) Significance analysis of microarrays applied to the ionizing radiation response. *Proc. Natl. Acad. Sci. U. S. A.* 98(9):5116-5121.

202. Saeed AI*, et al.* (2003) TM4: a free, open-source system for microarray data management and analysis. *Biotechniques* 34(2):374-378.

203. Ashburner M*, et al.* (2000) Gene ontology: tool for the unification of biology. The Gene Ontology Consortium. *Nat. Genet.* 25(1):25-29.

204. Huang da W, Sherman BT, & Lempicki RA (2009) Systematic and integrative analysis of large gene lists using DAVID bioinformatics resources. *Nat. Protoc.* 4(1):44-57.

205. Guller I & Russell AP (2010) MicroRNAs in skeletal muscle: their role and regulation in development, disease and function. *J. Physiol.* 588(Pt 21):4075-4087.

206. Chen JF, Callis TE, & Wang DZ (2009) microRNAs and muscle disorders. *J. Cell Sci.* 122(Pt 1):13-20.

207. Papadopoulos GL, Alexiou P, Maragkakis M, Reczko M, & Hatzigeorgiou AG (2009) DIANA-mirPath: Integrating human and mouse microRNAs in pathways. *Bioinformatics* 25(15):1991-1993.

208. Lewis BP, Burge CB, & Bartel DP (2005) Conserved seed pairing, often flanked by adenosines, indicates that thousands of human genes are microRNA targets. *Cell* 120(1):15-20.

209. Papadopoulos GL, Reczko M, Simossis VA, Sethupathy P, & Hatzigeorgiou AG (2009) The database of experimentally supported targets: a functional update of TarBase. *Nucleic Acids Res.* 37(Database issue):D155-158.

210. Shefer G & Yablonka-Reuveni Z (2005) Isolation and culture of skeletal muscle myofibers as a means to analyze satellite cells. *Methods Mol. Biol.* 290:281-304.

211. Schwartz LM, Gao Z, Brown C, Parelkar SS, & Glenn H (2009) Cell death in myoblasts and muscles. *Methods Mol. Biol.* 559:313-332.

212. Schiaffino S & Reggiani C (1994) Myosin isoforms in mammalian skeletal muscle. *J. Appl. Physiol.* 77(2):493-501.

213. Allen DL, Roy RR, & Edgerton VR (1999) Myonuclear domains in muscle adaptation and disease. *Muscle Nerve* 22(10):1350-1360.

214. Busciglio J*, et al.* (2002) Altered metabolism of the amyloid beta precursor protein is associated with mitochondrial dysfunction in Down's syndrome. *Neuron* 33(5):677-688.

215. Cooper CE, Nicholls P, & Freedman JA (1991) Cytochrome c oxidase: structure, function, and membrane topology of the polypeptide subunits. *Biochem. Cell Biol.* 69(9):586-607.

216. Samelman TR, Shiry LJ, & Cameron DF (2000) Endurance training increases the expression of mitochondrial and nuclear encoded cytochrome c oxidase subunits and heat shock proteins in rat skeletal muscle. *Eur. J. Appl. Physiol.* 83(1):22-27.

217. Sans CL, Satterwhite DJ, Stoltzman CA, Breen KT, & Ayer DE (2006) MondoA-Mlx heterodimers are candidate sensors of cellular energy status: mitochondrial localization and direct regulation of glycolysis. *Mol. Cell. Biol.* 26(13):4863-4871.

218. Fujimura N*, et al.* (2007) Wnt-mediated down-regulation of Sp1 target genes by a transcriptional repressor Sp5. *J. Biol. Chem.* 282(2):1225-1237.

219. Connor MK, Irrcher I, & Hood DA (2001) Contractile activity-induced transcriptional activation of cytochrome C involves Sp1 and is proportional to mitochondrial ATP synthesis in C2C12 muscle cells. *J. Biol. Chem.* 276(19):15898-15904.

220. Stoltzman CA*, et al.* (2008) Glucose sensing by MondoA:Mlx complexes: a role for hexokinases and direct regulation of thioredoxin-interacting protein expression. *Proc. Natl. Acad. Sci. U. S. A.* 105(19):6912-6917.

221. Hutchinson DS & Bengtsson T (2005) alpha1A-adrenoceptors activate glucose uptake in L6 muscle cells through a phospholipase C-, phosphatidylinositol-3 kinase-, and atypical protein kinase C-dependent pathway. *Endocrinology* 146(2):901-912.

222. Sakamoto K & Holman GD (2008) Emerging role for AS160/TBC1D4 and TBC1D1 in the regulation of GLUT4 traffic. *Am. J. Physiol. Endocrinol. Metab.* 295(1):E29-37.

223. Ferre P & Foufelle F (2007) SREBP-1c transcription factor and lipid homeostasis: clinical perspective. *Horm. Res.* 68(2):72-82.

224. Kamei Y*, et al.* (2008) Regulation of SREBP1c gene expression in skeletal muscle: role of retinoid X receptor/liver X receptor and forkhead-O1 transcription factor. *Endocrinology* 149(5):2293-2305.

225. Yeh TY*, et al.* (2009) Hypermetabolism, hyperphagia, and reduced adiposity in tankyrase-deficient mice. *Diabetes* 58(11):2476-2485.

226. Ito M*, et al.* (2003) Characterization of MCH-mediated obesity in mice. *Am. J. Physiol. Endocrinol. Metab.* 284(5):E940-945.

227. Shimada M, Tritos NA, Lowell BB, Flier JS, & Maratos-Flier E (1998) Mice lacking melanin-concentrating hormone are hypophagic and lean. *Nature* 396(6712):670-674.

228. Erickson JD*, et al.* (1994) Functional identification of a vesicular acetylcholine transporter and its expression from a "cholinergic" gene locus. *J. Biol. Chem.* 269(35):21929-21932.

229. Pechstein A, Shupliakov O, & Haucke V (Intersectin 1: a versatile actor in the synaptic vesicle cycle. *Biochem. Soc. Trans.* 38(Pt 1):181-186.

230. Choi JH, *et al.* (2009) Age-dependent dysregulation of brain amyloid precursor protein in the Ts65Dn Down syndrome mouse model. *J. Neurochem.* 110(6):1818-1827.

231. Head E & Lott IT (2004) Down syndrome and beta-amyloid deposition. *Curr. Opin. Neurol.* 17(2):95-100.

232. Wang P, *et al.* (2005) Defective neuromuscular synapses in mice lacking amyloid precursor protein (APP) and APP-Like protein 2. *J. Neurosci.* 25(5):1219-1225.

233. Shtifman A, *et al.* (Amyloid-beta protein impairs Ca(2+) release and contractility in skeletal muscle. *Neurobiol. Aging* 31(12):2080-2090.

234. McFerrin J, Engel WK, & Askanas V (1998) Impaired innervation of cultured human muscle overexpressing betaAPP experimentally and genetically: relevance to inclusion-body myopathies. *Neuroreport* 9(14):3201-3205.

235. Lee DS, Tomita S, Kirino Y, & Suzuki T (2000) Regulation of X11L-dependent amyloid precursor protein metabolism by XB51, a novel X11L-binding protein. *J. Biol. Chem.* 275(30):23134-23138.

236. Hamilton JA & Benson MD (2001) Transthyretin: a review from a structural perspective. *Cell. Mol. Life Sci.* 58(10):1491-1521.

237. Buxbaum JN & Reixach N (2009) Transthyretin: the servant of many masters. *Cell. Mol. Life Sci.* 66(19):3095-3101.

238. Cai Q & Sheng ZH (2009) Mitochondrial transport and docking in axons. *Exp. Neurol.* 218(2):257-267.

239. Waschbisch A, *et al.* (2008) Human muscle cells express the costimulatory molecule B7-H3, which modulates muscle-immune interactions. *Arthritis Rheum.* 58(11):3600-3608.

240. Zhang G, *et al.* (Tissue-specific expression of TIPE2 provides insights into its function. *Mol. Immunol.* 47(15):2435-2442.

241. Sun H, *et al.* (2008) TIPE2, a negative regulator of innate and adaptive immunity that maintains immune homeostasis. *Cell* 133(3):415-426.

242. Mamane Y, *et al.* (2009) The C3a anaphylatoxin receptor is a key mediator of insulin resistance and functions by modulating adipose tissue macrophage infiltration and activation. *Diabetes* 58(9):2006-2017.

243. Kang JS*, et al.* (2004) Netrins and neogenin promote myotube formation. *J. Cell Biol.* 167(3):493-504.

244. Watanabe R*, et al.* (2005) Rb1cc1 is critical for myoblast differentiation through Rb1 regulation. *Virchows Arch.* 447(3):643-648.

245. Sohn RL*, et al.* (2009) A role for nephrin, a renal protein, in vertebrate skeletal muscle cell fusion. *Proc. Natl. Acad. Sci. U. S. A.* 106(23):9274-9279.

246. Bakkar N & Guttridge DC (NF-kappaB signaling: a tale of two pathways in skeletal myogenesis. *Physiol. Rev.* 90(2):495-511.

247. Buas MF & Kadesch T (Regulation of skeletal myogenesis by Notch. *Exp. Cell Res.* 316(18):3028-3033.

248. Wagatsuma A, Tamaki H, & Ogita F (2006) Sequential expression of vascular endothelial growth factor, Flt-1, and KDR/Flk-1 in regenerating mouse skeletal muscle. *Physiol. Res.* 55(6):633-640.

249. Chu J*, et al.* (2009) A mouse forward genetics screen identifies LISTERIN as an E3 ubiquitin ligase involved in neurodegeneration. *Proc. Natl. Acad. Sci. U. S. A.* 106(7):2097-2103.

250. Marteijn JA*, et al.* (2005) The E3 ubiquitin-protein ligase Triad1 inhibits clonogenic growth of primary myeloid progenitor cells. *Blood* 106(13):4114-4123.

251. Yuan Z*, et al.* (2009) Regulation of neuronal cell death by MST1-FOXO1 signaling. *J. Biol. Chem.* 284(17):11285-11292.

252. Kandarian SC & Jackman RW (2006) Intracellular signaling during skeletal muscle atrophy. *Muscle Nerve* 33(2):155-165.

253. Prendergast AM, Cruet-Hennequart S, Shaw G, Barry FP, & Carty MP (2011) Activation of DNA damage response pathways in human mesenchymal stem cells exposed to cisplatin or gamma-irradiation. *Cell Cycle* 10(21).

254. Buonomo SB, Wu Y, Ferguson D, & de Lange T (2009) Mammalian Rif1 contributes to replication stress survival and homology-directed repair. *J. Cell Biol.* 187(3):385-398.

255.	Chen Y, Chen PL, Chen CF, Jiang X, & Riley DJ (2008) Never-in-mitosis related kinase 1 functions in DNA damage response and checkpoint control. *Cell Cycle* 7(20):3194-3201.

256.	Chen Y, Gaczynska M, Osmulski P, Polci R, & Riley DJ (Phosphorylation by Nek1 regulates opening and closing of voltage dependent anion channel 1. *Biochem. Biophys. Res. Commun.* 394(3):798-803.

257.	Duan RD (2006) Alkaline sphingomyelinase: an old enzyme with novel implications. *Biochim. Biophys. Acta* 1761(3):281-291.

258.	Ferreira LF, *et al.* (Sphingomyelinase stimulates oxidant signaling to weaken skeletal muscle and promote fatigue. *Am J Physiol Cell Physiol* 299(3):C552-560.

259.	Jaiswal AK (2004) Nrf2 signaling in coordinated activation of antioxidant gene expression. *Free Radic. Biol. Med.* 36(10):1199-1207.

260.	Lee GH, *et al.* (2007) Bax inhibitor-1 regulates endoplasmic reticulum stress-associated reactive oxygen species and heme oxygenase-1 expression. *J. Biol. Chem.* 282(30):21618-21628.

261.	Gokhin DS, *et al.* (Tropomodulin isoforms regulate thin filament pointed-end capping and skeletal muscle physiology. *J. Cell Biol.* 189(1):95-109.

262.	Kaetzel MA & Dedman JR (2004) Annexin VI regulation of cardiac function. *Biochem. Biophys. Res. Commun.* 322(4):1171-1177.

263.	Schmitz-Peiffer C, Browne CL, Walker JH, & Biden TJ (1998) Activated protein kinase C alpha associates with annexin VI from skeletal muscle. *Biochem. J.* 330 (Pt 2):675-681.

264.	Anyatonwu GI, Estrada M, Tian X, Somlo S, & Ehrlich BE (2007) Regulation of ryanodine receptor-dependent calcium signaling by polycystin-2. *Proc. Natl. Acad. Sci. U. S. A.* 104(15):6454-6459.

265.	Li X, Liu Y, Kay CM, Muller-Esterl W, & Fliegel L (2003) The Na+/H+ exchanger cytoplasmic tail: structure, function, and interactions with tescalcin. *Biochemistry (Mosc.)* 42(24):7448-7456.

266.	Juel C (1997) Lactate-proton cotransport in skeletal muscle. *Physiol. Rev.* 77(2):321-358.

267. Moiseeva EP, Belkin AM, Spurr NK, Koteliansky VE, & Critchley DR (1996) A novel dystrophin/utrophin-associated protein is an enzymatically inactive member of the phosphoglucomutase superfamily. *Eur. J. Biochem.* 235(1-2):103-113.

268. Ziegler WH, Gingras AR, Critchley DR, & Emsley J (2008) Integrin connections to the cytoskeleton through talin and vinculin. *Biochem. Soc. Trans.* 36(Pt 2):235-239.

269. Jarnum S, *et al.* (2004) LEPREL1, a novel ER and Golgi resident member of the Leprecan family. *Biochem. Biophys. Res. Commun.* 317(2):342-351.

270. Tiainen P, Pasanen A, Sormunen R, & Myllyharju J (2008) Characterization of recombinant human prolyl 3-hydroxylase isoenzyme 2, an enzyme modifying the basement membrane collagen IV. *J. Biol. Chem.* 283(28):19432-19439.

271. Light N & Champion AE (1984) Characterization of muscle epimysium, perimysium and endomysium collagens. *Biochem. J.* 219(3):1017-1026.

272. Rooney JE, Gurpur PB, & Burkin DJ (2009) Laminin-111 protein therapy prevents muscle disease in the mdx mouse model for Duchenne muscular dystrophy. *Proc. Natl. Acad. Sci. U. S. A.* 106(19):7991-7996.

273. Muckenthaler MU (2008) Fine tuning of hepcidin expression by positive and negative regulators. *Cell Metab.* 8(1):1-3.

274. De Domenico I, McVey Ward D, & Kaplan J (2008) Regulation of iron acquisition and storage: consequences for iron-linked disorders. *Nat. Rev. Mol. Cell Biol.* 9(1):72-81.

275. Gerke V & Moss SE (2002) Annexins: from structure to function. *Physiol. Rev.* 82(2):331-371.

276. Lennon NJ, *et al.* (2003) Dysferlin interacts with annexins A1 and A2 and mediates sarcolemmal wound-healing. *J. Biol. Chem.* 278(50):50466-50473.

277. Necchi D, Lomoio S, & Scherini E (Dysfunction of the ubiquitin-proteasome system in the cerebellum of aging Ts65Dn mice. *Exp. Neurol.*

278. Jung T & Grune T (2008) The proteasome and its role in the degradation of oxidized proteins. *IUBMB Life* 60(11):743-752.

279. Marques C, *et al.* (2004) Ubiquitin-dependent lysosomal degradation of the HNE-modified proteins in lens epithelial cells. *FASEB J.* 18(12):1424-1426.

280. Yarom R, *et al.* (1987) Elevated concentrations of elements and abnormalities of neuromuscular junctions in tongue muscles of Down's syndrome. *J. Neurol. Sci.* 79(3):315-326.

281. Abdul-Ghani MA, *et al.* (2008) Deleterious action of FA metabolites on ATP synthesis: possible link between lipotoxicity, mitochondrial dysfunction, and insulin resistance. *Am. J. Physiol. Endocrinol. Metab.* 295(3):E678-685.

282. Shortreed KE, *et al.* (2009) Muscle-specific adaptations, impaired oxidative capacity and maintenance of contractile function characterize diet-induced obese mouse skeletal muscle. *PLoS ONE* 4(10):e7293.

283. Flagg TP, Enkvetchakul D, Koster JC, & Nichols CG (2010) Muscle KATP channels: recent insights to energy sensing and myoprotection. *Physiol. Rev.* 90(3):799-829.

284. Gong B, Miki T, Seino S, & Renaud JM (2000) A K(ATP) channel deficiency affects resting tension, not contractile force, during fatigue in skeletal muscle. *Am J Physiol Cell Physiol* 279(5):C1351-1358.

285. Gramolini A & Renaud JM (1997) Blocking ATP-sensitive K+ channel during metabolic inhibition impairs muscle contractility. *Am. J. Physiol.* 272(6 Pt 1):C1936-1946.

286. Chan S, *et al.* (2008) A gene for speed: contractile properties of isolated whole EDL muscle from an alpha-actinin-3 knockout mouse. *Am J Physiol Cell Physiol* 295(4):C897-904.

CHAPTER V. APPENDICES

SYRACUSE UNIVERSITY
INSTITUTIONAL ANIMAL CARE & USE COMMITTEE
OFFICE OF RESEARCH INTEGRITY PROTECTIONS
621 SKYTOP ROAD | SYRACUSE, NEW YORK 13244
TELEPHONE: (315) 443-1690
FAX: (315) 443-2382
E-mail: mphenn@syr.edu

MEMORANDUM

TO: Dr. Keith DeRuisseau

FROM: Michael Henn, IACUC/LAR

DATE: July 24, 2007

RE: New Protocol for Animal Use

Your protocol for animal use, entitled **Skeletal Muscle Function in a Mouse Model of Down Syndrome** was reviewed by the Institutional Care and Use Committee on 6/19/2007 and assigned the IACUC #07-014. Full approval was granted from 6/19/2007 to 6/19/2010, subject to continuous annual review.

PLEASE NOTE: By its very nature, research involving animals often requires significant change in plans, procedures and/or personnel. If this should occur, you need to inform the committee promptly by requesting an amendment to the protocol. This amendment will be reviewed by the IACUC and you may begin use of the new procedure only after IACUC approval. It is also your responsibility to submit a Training Documentation Form for each new person who intends to work with animals on your project.

PLEASE NOTE; The Association for Assessment and Accreditation of Laboratory Animal Care (AAALAC) now requires an Occupational Health and Safety Program (OHSP) for all AAALAC accredited institutions. As part of Syracuse University's Occupational Health and Safety Program, the IACUC has now incorporated an Environmental Health Office (EHO) review of your protocol. Please review and sign the attached review sheet, make a copy to post in your lab and send the signed original within 30-days to Office of Research Integrity Protections 621 Skytop Road. If you have any questions, please contact Tim Coughlin, Industrial Hygiene Manager 443-2447.

Refer to the IACUC Protocol number 07-014, on all related correspondence and purchase requisitions. Please direct all to the following address:

Office of Research Integrity Protections
Attn. Michael Henn, Room 254 ISR
621 Skytop Road, Syracuse, N.Y. 13244

SYRACUSE UNIVERSITY
INSTITUTIONAL ANIMAL CARE & USE COMMITTEE
OFFICE OF RESEARCH INTERGRITY PROTECTIONS
621 SKYTOP ROAD | SYRACUSE, NEW YORK 13244
TELEPHONE: (315) 443-1690
FAX: (315) 443-2382
E-mail: mphenn@syr.edu

MEMORANDUM

TO: Dr. Keith DeRuisseau

FROM: Michael Henn, IACUC/LAR

DATE: January25, 2010

RE: New Protocol for Animal Use

Your protocol for animal use, **Assessment of Oxidative Stress in Skeletal Muscle Fibers from Down Syndrome Mice** was initially reviewed by the Institutional Care and Use Committee on 10/28/2009 and assigned the IACUC #10-002. Full approval was granted from 1/21/2010 to 1/20/2013, subject to continuous annual review.

PLEASE NOTE: By its very nature, research involving animals often requires significant change in plans, procedures and/or personnel. If this should occur, please inform the committee promptly by requesting an amendment to the protocol. The amendment will be reviewed by the IACUC and you may begin use of the new procedure only after IACUC approval. It is also your responsibility to submit a Training Documentation form for each additional person who intends to work with animals on your project.

PLEASE NOTE; The Association for Assessment and Accreditation of Laboratory Animal Care International (AAALAC) now requires an Occupational Health and Safety Program (OHSP) for all AAALAC accredited institutions. As part of Syracuse University's Occupational Health and Safety Program, the IACUC has now incorporated an Environmental Health Office (EHO) review of your protocol. **Please review and sign the attached review sheet, print a copy to post in your lab and then return the signed original within 30-days to my attention at ISR, 621 Skytop Road**. If you have any questions regarding the EHO review, please contact Tim Coughlin, Industrial Hygiene Manager at 443-2447.

Please refer to your assigned IACUC Protocol number on all related correspondence and purchase requisitions. Direct all to the following address:

Michael Henn
Office of Research Integrity and Protections
ISR, Room 254
621 Skytop Road, Syracuse, N.Y. 13244

CHAPTER VI. BIOGRAPHICAL DATA

CURRICULUM VITA

Patrick M. Cowley, Ph.D., C.S.C.S.

273 Reed Avenue, Syracuse, NY, 13207, (315) 436-9161; email: pmcowley@syr.edu

EDUCATION

Syracuse University, Syracuse, NY
Ph.D. in Exercise Science and Science Education   2011

Ithaca College, Ithaca, NY
M.S. in Exercise and Sport Sciences   2005

Ithaca College, Ithaca, NY
B.A. in Biology, Minor in Applied Exercise Science   2002

CERTIFICATIONS

National Strength and Conditioning Association
Certified Strength and Conditioning Specialist®   2004

RESEARCH

EXPERIENCE

Syracuse University, Syracuse, NY
Doctoral Research   2009-2011

- Research Projects:
    - "Skeletal Muscle Function in a Mouse Model of Down Syndrome"
    - "Assessment of Oxidative Stress in Skeletal Muscle Fibers from Down Syndrome Mice"

Research Assistant   2005-2011

- Research Project: "Iron Accumulation in Aging Skeletal Muscle" P.I. Dr. Keith C. DeRuisseau, Spring 2010 and Fall 2011.

- Research Project: "Effects of Sensory Level Electrical Stimulation on Muscle Cross-sectional Area, Strength and Metabolite Production in Children with Cerebral Palsy" P.I. Lynne Logan, 2007-2009.

- Research Project: "Study of Secondary Conditions and Effects of Aquatic Intervention on Adult Cerebral Palsy" P.I. Dr. Deborah Thorpe, July 2008.

- Research Project: "Muscle Strength, Physical Work Capacity and Functional Performance in Individuals with Down Syndrome" Co-P.I. Drs. Bo Fernhall, 2005-2007.

COMPETENCIES

Laboratory Bench Skills:

- Handling and care of rodents (injections, harvesting tissue, and euthanasia)
- In vitro assessment of skeletal muscle contractility
- Isolation and culture of single adult myofibers from rodent muscle
- Reactive oxygen and nitrogen species detection assays
    - 2',7'-dichlorodihydrofluorescein and Amplex Red assays
- Tissue homogenization, protein quantification, and Western blot
- RNA isolation, cDNA synthesis, and RT-PCR
- Embedding, cryo-sectioning, and processing of tissue sections and/or single myofibers
    - Hematoxylin and eosin, Periodic Acid-Schiff, iron staining
    - TUNEL, CuZnSOD, and myosin heavy chain immunofluorescence
- Separation of myosin heavy chain isoforms by electrophoresis
- Microarray data analysis
    - Gene set analysis using MultiExperiment Viewer
    - Pathway analysis using Database for Annotation, Visualization and Integrated Discovery (DAVID), Ingenuity Pathway Analysis (IPA), Gene Set Enrichment Analysis (GSEA), and miRNA target and pathway analysis
- Cell culture training
    - Sterile techniques
    - Proliferating, sub-culturing, harvesting, and cryo-preservation of C2C12 cell line

Laboratory Clinical Skills:

- Isometric and isokinetic strength testing
- Electrophysiological measurements
    - Electromyography recordings, Hoffman reflex, nerve conduction, and compound muscle fiber action potential
- Evoked force measurements from the triceps surae and quadriceps
    - Twitch force and interpolated twitch technique
- Resistance training interventions
- Assessment of physical function (chair rise, stair climbing, gait speed)
- Peak aerobic capacity (VO_2) testing
- MRI data analysis

Special skills:

- Extensive formal training in biostatistics (24 credit hours of graduate coursework)
- Participant recruitment of special populations

PUBLICATIONS

Peer-Reviewed:

1. **Cowley PM**, Ploutz-Snyder LL, Baynard T, Heffernan K, Jae SY, Hsu S, Lee M, Pitetti K, Reiman M, Fernhall B. The effect of progressive resistance training on leg strength, aerobic capacity and functional tasks of daily living in persons with Down syndrome. *Disability and Rehabilitation.* In press.

2. Behm DG, Drinkwater EJ, Willardson JM, **Cowley PM**. The role of instability rehabilitative resistance training for the core musculature. Invited review article for "Special topics" issue on "Sports Medicine". *Strength and Conditioning Journal,* 33: 72-81, 2011.

3. Behm DG, Drinkwater EJ, Willardson JM, **Cowley PM**. Canadian Society for Exercise Physiology position stand: The use of instability to train the core in athletic and non-athletic conditioning. *Applied Physiology, Nutrition and Metabolism,* 35: 109-112, 2010. 2010.

4. Behm DG, Drinkwater EJ, Willardson JM, **Cowley PM**. The use of instability to train the core musculature. *Applied Physiology, Nutrition and Metabolism,* 35: 91-108, 2010.

5. **Cowley PM**, Ploutz-Snyder LL, Baynard T, Heffernan K, Jae SY, Hsu S, Lee M, Pitetti K, Reiman M, Fernhall B. Physical fitness predicts functional tasks in individuals with Down syndrome. *Medicine and Science in Sports and Exercise*, 42: 388-393, 2010.

6. **Cowley PM**, Fitzgerald S, Sottung K, Swensen T. Age, weight, and the front abdominal power test as predictors of isokinetic trunk strength and work in young men and women. *Journal of Strength and Conditioning Research*, 23: 915-925, 2009.

7. **Cowley PM**, Clark BC, Ploutz-Snyder LL. Kinesthetic motor imagery and spinal excitability excitability: The effect of contraction intensity and spatial localization. *Clinical Neurophysiology*, 119: 1849-1856, 2008.

8. **Cowley PM**, Swensen T. Development and reliability of two core stability field tests. *Journal of Strength and Conditioning Research*, 22: 619-624, 2008.

9. **Cowley PM**, Swensen T, Sforzo GA. Efficacy of instability resistance training. *International Journal of Sports Medicine* 10: 829-835, 2007.

Published Abstracts:

1. **Cowley PM**, DeRuisseau KC. Soleus muscle of Down syndrome (DS) mice exhibits elevated markers of oxidative and nitrosative stress. *FASEB J*, 24: 989.4, 2010.

2. **Cowley PM**, DeRuisseau KC. Soleus muscle from Down syndrome (Ds) mice does not exhibit impaired contractile function or resistant to fatigue. *FASEB J*, 23: 601.12, 2009.

3. DiStasio, TJ, DeRuisseau LR, **Cowley PM**, Recca DM, DeRuisseau KC. Impact of caffeine administration on skeletal muscle oxidative stress and antioxidant status. *FASEB J*, 23: 601.11, 2009.

4. **Cowley PM**, Baynard T, Ploutz-Snyder L, Jae SY, Heffernan K, Hsu S, Fernhall B, Reiman M, Chapman S, Pitetti K. Knee extensor strength and aerobic capacity predict functional ambulatory ability in individuals with Down syndrome. *Medicine and Science in Sports and Exercise*, 40: S540, 2008.

5. Fernhall B, Jae SY, Heffernan K, Hsu S, Ploutz-Snyder L, **Cowley P**, Baynard T, Reiman M, Chapman S, Pitetti K. Aerobic capacity is related to muscle strength in individuals with Down syndrome. *Medicine and Science in Sports and Exercise*, 39: S245, 2007.

6. Clark B, **Cowley P**, Conatser R, Ploutz-Snyder L. Role of biarticular muscles in regulating task failure and muscle synergies. *Medicine and Science in Sports and Exercise*, 39: S268, 2007.

7. **Cowley P**, Baynard T, Fernhall B, Ploutz-Snyder L. The effect of resistance training in individuals with Down syndrome. *Medicine and Science in Sports and Exercise*, 39: S98-99, 2007.

8. **Cowley P**, Clark B, Ploutz-Snyder L. Kinesthetic motor imagery acutely increases spinal excitability. *Medicine and Science in Sports and Exercise* 38: S446, 2006.

9. Swensen T, **Cowley P**, Sforzo G. The effects of resistance training with a stability ball. *Medicine and Science in Sports and Exercise* 37: S186, 2005.

PRESENTATIONS

National:

1. Soleus muscle from Down syndrome (Ds) mice does not exhibit impaired contractile function or resistant to fatigue. Poster presentation at *Experimental Biology*, New Orleans, LA. April 2009.

2. Knee extensor strength and aerobic capacity predict functional ambulatory ability in individuals with Down syndrome. Poster presentation at *American College of Sports Medicine Annual Meeting*, Indianapolis, IN. June 2008.

3. The effect of resistance training in individuals with Down syndrome. Oral presentation at *American College of Sports Medicine Annual Meeting*, New Orleans, LA. June 2007.

4. Kinesthetic motor imagery acutely increases spinal excitability. Poster presentation at *American College of Sports Medicine Annual Meeting*, Denver, CO. June 2006.

Local:

1. Measurement of Oxidant Production in Single Skeletal Muscle Fibers from Down Syndrome (DS) Mice. Oral presentation at the *Mid-Atlantic American College of Sports Medicine Annual Meeting*, Harrisburg, PA. November 2011.

2. Production of Reactive Oxygen Species and Morphology of Single Skeletal Muscle Fibers from Down Syndrome Mice. Poster presentation at *Muscle and Metabolism*

Symposium, Pennsylvania Muscle Institute, University of Pennsylvania, Philadelphia, PA. October 2011.

3. Modeling Down syndrome in mice. Oral presentation at the *Department of Exercise Science Seminar Series*, Syracuse University, Syracuse, NY. April 2008.

4. Muscle strength, functional performance, and physical work capacity in individuals with Down syndrome. Oral presentation at *Department of Exercise Science Seminar Series*, Syracuse University, Syracuse, NY. March 2006.

5. The effect of resistance training in individuals with Down syndrome. Oral presentation at *Mid-Atlantic American College of Sports Medicine Annual Meeting*, Harrisburg, PA. November 2006.

6. The effect of short-term instability resistance training on muscular strength, endurance, and core strength. Oral presentation at *Mid-Atlantic American College of Sports Medicine Annual Meeting*, Bushkill, PA. October 2004.

7. Substrate preference and rate of attachment of the limpet, *lottia limatula*. Oral presentation at *Ithaca College Junior Research Symposium*, Ithaca, NY. May 2001.

GRANTS FUNDED

1. *Neuromuscular Characteristics of Individuals with Down Syndrome*, Funded by Syracuse University SOE Creative Research Grant, PI: Patrick M. Cowley, $610, 2006.

TEACHING

Syracuse University, Syracuse, NY
Graduate:

PPE 795: Skeletal Muscle Physiology, Laboratory in Spring 2007 and 2009-11
PPE 515: Graded Exercise Testing and Interpretation, Laboratory in Spring 2006

Undergraduate:

PPE 483: Scientific Principles of Conditioning, Lecture in Spring 2009
PPE 408: Analysis of Human Motion, Lecture and Laboratory in Fall 2008
PPE 497: Exercise Physiology, Laboratory in Fall 2007 and 2009
HEA 332: Personal Health and Safety, Lecture (co-taught) in Fall 2006 and Spring 2007

State University of New York Institute of Technology, Utica, NY
Undergraduate:

BIO 215: Anatomy and Physiology I, Laboratory in Fall 2008

SERVICE

Manuscript Reviewer (Invited):

- Medicine and Science in Sports and Exercise
- Disability and Rehabilitation

- Journal of Clinical Neurophysiology
- Intellectual & Developmental Disabilities
- Therapeutics and Clinical Risk Management
- Journal of Clinical Medicine and Research

Professional Organizations

- The American Physiological Society, 2006-Present
- American College of Sports Medicine, 2006-Present
- *Beta Beta Beta*, National Biological Honor Society, Honorary, 2001-Present

HONORS AND AWARDS

- Finalist for the *MARC-ACSM Doctoral Student Investigator Award*, Mid-Atlantic American College of Sports Medicine Annual Meeting, 2011.
- American Physiological Society *Carolyn tum Suden/Francis A. Hellebrandt Professional Opportunity Award*, Experimental Biology, 2009.
- Named '*Teaching Associate*' in the Syracuse University Future Professoriate Program, 2006-2007.

RELATED PROFESSIONAL EXPERIENCE

Manager of Musculoskeletal Laboratory   2006-2008
Syracuse University, Syracuse, NY
   - Provided technical support to students working in the laboratory.

Assistant Team Leader   2004–2005
JM Murray Center Inc., Cortland, NY
   - Provided day-habilitation services to persons with developmental disability.